BNL 646 (S-56)
(General, Miscellaneous, and Progress
Reports - TID 4500, 16th Ed.)

Progress Report
Nuclear Engineering Department

May 1 - August 31, 1960

CLARKE WILLIAMS, Chairman

F.T. MILES, Assistant to Chairman

BROOKHAVEN NATIONAL LABORATORY
Associated Universities, Inc.
Upton, New York

II

DISCLAIMER

PRINTED IN USA
PRICE $1.75

Available from the
Office of Technical Services,
Department of Commerce
Washington 25, D.C.

May 1961 850 copies

SUMMARY

REACTOR PHYSICS (04-04-06-09-0, 05-01-02-02, 04-01-16-00-1, 04-04-01-00-0)

Reactor Theory

Work is reported on reactor physic studies of the BBRR, on PWR reactor physics evaluations, and on Pu-fuelled reactors. Further work on the detailed comparison of theory and experiment for water lattices was carried out. The equal charge displacement rule has been applied to calculations of fission product poisoning.

In the area of general reactor physics, results are reported on the effect of temperature on Xe instability, on flux trap reactors, on analysis of the Snell experiment, on neutron thermalization, and the effect of anisotropic scattering for various cases. The importance of the spatial distribution of neutron sources on the asymptotic neutron spectrum was demonstrated. Monte Carlo calculations of the fast effect in U and Be systems were completed.

Experimental Reactor Physics

Work was continued on the water lattices, Dy^{164} and Eu^{151} cross section measurements, pulsed neutron experiments, and the BBRR critical experiments.

In the water lattices 3% oxide 0.5 in. o.d. rod exponential experiments and analysis of the data, miniature slab measurements, in the 3:1 and 4:1 lattices, and preparations for the slab critical experiments were carried out.

The activation cross section of Dy^{164} in the energy region 0.06 to 2.0 ev was measured. Measurements of the total cross sections of Dy^{164} and Eu^{151} were also made.

Pulsed neutron measurements of GBF graphite and Bi continued.

Fifty-two different experimental runs were carried out on BBRR during this period. Among these were runs to determine the thermal neutron lifetime, to check the useful range of the "analog reactivity meter," and to measure the thermal neutron importance function in the reflector.

CHEMISTRY AND CHEMICAL ENGINEERING (04-01-17-10-1, 04-04-02-00-1, 04-04-03-00-0, 05-02-01, 04-04-05-01-0, 05-02-02, 08-04, 04-04-04-02-0, 04-04-05-02-0)

Reactor Chemistry and Chemical Technology

Radiation experiments on aromatic fluorocarbons have been started.

A new technique for measuring the absorption spectra of very strongly absorbing materials is being developed for particular application to fused salts in the ultraviolet. Films of a micron or less are sandwiched between silica flats. Spectra have so far been obtained on $PbCl_2$ and KI.

Thermodynamic properties of liquid Na-Bi alloys in the high-sodium region have been obtained by a vapor pressure technique.

A satisfactory Re-graphite thermocouple has been constructed and operated up to 2300°C. The inversion of the temperature emf curve at about 1650°C limits the usefulness of the thermocouple in the range below 1550°C or above 1800°C.

Experiments were performed to determine whether Xe or I diffuse through reactor cladding. Xe did not diffuse through 2S Al (0.015 and 0.020 in. thick) up to 510°C or through 304 SS (0.020 in. thick) up to 650°C. I was not found to diffuse through 0.035 in. thick 2S Al up to 500°C.

Preliminary postirradiation meltdown studies were performed to simulate a reactor temperature excursion leading to a fuel element meltdown. Specifically, the fission products I and Xe were investigated as to the effect of meltdown temperature, time of meltdown, and the resulting distribution of these fission products in the experimental apparatus.

An investigation has been completed (BNL 633) in which it has been established that the predominant mechanism by which Xe is sorbed into graphite at high temperatures is that of pore entrainment and thus dependent on the porosity of the graphite. Work has been initiated on the adsorption of I on graphite at high temperatures.

Experiments indicate that I is sorbed to an extent considerably greater than would be expected on the basis of only containment of I in the pores as was the case with Xe.

Liquid Metal Heat Transfer Studies

As part of an analytical study of heat transfer to liquid metals flowing in concentric annuli, results have been obtained for the case of heat transfer through the outer wall only. They are based on the conditions of constant heat flux, fully-established turbulent flow, and no effect of temperature on physical properties.

Fluoride Volatility Process

Fuel material consisting of uranium carbide in graphite has been successfully treated with the Nitrofluor reagent, NO_2-HF mixture. The solid disintegrated to a powder and the U went into the liquid phase, from which it was recovered in nearly 100% yield.

Experiments on modification of the Nitrofluor process for Naval type fuel by omitting the decantation from the complex zirconium fluoride precipitate revealed a difficulty in the subsequent fluorination step; the volatilization of the U was incomplete. Pu also was much less completely volatilized in the presence of ZrF_4 than in its absence. In the absence of Zr, microgram quantities of Pu have been recovered by fluorination in 82% yield.

The liquidus line of the freezing-point *vs* composition diagram of the system NO_2-HF has been determined in the region 0 to 45 mole % HF.

Heavy gamma irradiation was found not to impair the subsequent ability of NO_2-HF to dissolve Zircaloy.

Infrared absorption spectra indicate the existence of strong interaction, if not compound formation, between NO_2 and HF in mixtures of the vapors.

Radiochemical Technology

A decontamination factor of 1.1×10^6 was demonstrated for Cs^{137} removal from a high salt content waste stream.

Development work is continuing on aqueous processes for Zircaloy and SS-clad UO_2 fuels.

Observance of a long induction period before the reaction of UO_2 with a calcium amalgam persists.

Equipment is being assembled and tested for high temperature physical property measurements.

Preliminary results are presented in the N_2-O_2 system and the NH_3-H_2O system.

A research irradiator is being constructed. A low-level source for dose distribution studies in finite targets was prepared.

Chloride-Fluoride Volatility Process Studies

Investigation of the Zr-HCl reaction in an Al_2O_3 fluidized bed was continued. Several experiments were carried out in which a Zircaloy-clad fuel coupon was reacted with HCl to completion in an Al_2O_3 bed, after which the bed was contacted with F_2. Results are given for an experiment in which SS was reacted with Cl_2 in a static bed.

Ultimate Waste Disposal

One of the major problems in the development of the ion exchange process has been the interference due to the relatively large concentration of nonradioactive ions in the waste. Recently methods have been studied for suppressing such bulk ion interference in the processing of Purex type waste by absorption on mineral ion exchange materials.

A program was started to study the formation of phosphate glasses as a means of incorporating the fission products in stable media. Of primary interest here is the development of a process in which the entire conversion from the raw aqueous waste to the final glass product would be carried out in an all-liquid system.

HOT LABORATORY (05-02-02, 05-02-05)

Dowex-50-W, a new product being manufactured as a replacement for Dowex-50, has been shown to perform similarly to Dowex-50 with respect to the elution of Y^{90} in a Brookhaven Y^{90} generator. The Sr^{90} contamination is even lower in the eluate from the new resin than from the old.

Experiments not yet completed indicate that calcium phthalocyanine (Ca-Pc) is not as unreactive as the original experiments indicated. It appears to be at least partially decomposed by fuming sulfuric acid although no correlation has been found yet with strength of acid or length of contact time. The infrared absorption spectra have been found useful in identifying Ca-Pc, H_2Pc, thenoyltrifluoroacetone (TTA), and Ca-TTA.

Satisfactory reproducibility has been firmly established for 1) a flame photometric procedure for determining Ca in mixtures of water-cyclohexanone-TTA, and 2) the extraction of Ca from such mixtures by water and by hydrochloric acid. This procedure was used to demonstrate a Szilard-Chalmers enrichment factor of 1.40 ± 0.24 when Ca-TTA was irradiated, dissolved in cyclohexanone, and extracted with water. Although this enrichment factor is much too low to be of practical importance, this work is continuing in the hope of improving it. Attempts to effect a Szilard-Chalmers reaction by the irradiation of paper impregnated with Ca-TTA have not yet given positive results.

Very rough preliminary measurements indicate a cross section of around 10 ± 30 mb for the $Ti^{50}(n,\alpha)Ca^{47}$ reaction with 14-Mev neutrons.

Two full-scale preparations of Cu^{67} were made via the $Ni^{64}(\alpha,p)Cu^{67}$ reaction using enriched Ni^{64}. Thick target yields of 2 mC/mah were obtained, and the 61-hr half-life of Cu^{67} has been confirmed.

The $Sb^{121}(\alpha,n)I^{124}$ reaction has been used to produce about ¼ mC I^{124} with a yield of about 100 mC/mah. Attempts are under way to produce an Sb target large enough to furnish 10 mC I^{124}.

The production of pure Sc^{47} from CaO was shown to be feasible.

In assaying Ar^{38} for isotopic content via mass spectrograph, it was found that the normal Ar contamination occluded *inside* glass itself is sufficient to vitiate the analysis when the sample is introduced into the spectrograph by melting the glass capillary tube containing it. Attempts to contain samples of Ar^{38} in Cu tubing, the ends of which were crimped shut, failed to produce gas-tight seals. Calibrated glass vials with microbreak seals are being tried.

An electroplate having a thickness of a few microns is required as a protective cover over an alpha-emitting needle which is being fabricated. A technique involving the use of the electron microscope was developed for measuring the thickness of such a plate to within a fraction of a micron.

The preparation of several Curies of very pure Kr^{83m} to be used as a plasma in testing the Stellarator, is being undertaken for Project Matterhorn. Experiments thus far indicate that the literature value for the cross section for the $Se^{82}(n,\gamma)Se^{83}$ reaction is probably correct and that a yield of 50% Kr^{83m} can be expected to emanate from molten, irradiated Se even when quiescent.

Development of a procedure for milking the positron-emitting Ga^{68} from its long-lived Ge^{68} parent was begun. The use of slightly basic Dowex-1 resin and either glycerol or glucose as complexing agents to retain the Ge but pass the Ga appears promising.

Calculations and preliminary tests indicate that the use of fully enriched Mg^{26} instead of natural Mg in the production of Mg^{28} is both feasible and economical, nothwithstanding the high price of \$3000/g of Mg^{26}. As would be expected, the enriched material gives a much more valuable end product having a considerably higher specific activity.

A direct comparison is being made of the $\geqq 13$ Mev neutron flux produced by thermal neutron irradiation of Li^6D and of U^{235}.

Experiments were begun to test a proposal for continuously measuring B concentration in blood and a modification of this proposal which will allow the continuous production of very short-lived radioisotopes and the use of such isotopes for localized irradiation of selected sites *in vivo*.

The reaction between tri-n-octylamine (R_3N) and 2-thenoyl-trifluoroacetone (HT) has been investigated and found to be

$$R_3N + HT \rightleftharpoons R_3N \cdot HT$$

with a formation constant of $(1.43 \pm 0.10) \times 10^3$. The study used a spectrophotometric method and covered a 5000-fold range in amine concentration.

Radioactive tracers have established the validity of an ashing procedure for the spectrographic determination of Mg in blood. Cu has been found to be a suitable internal standard for this purpose, and with it a Mn concentration of 0.0033 μg/ml has been measured in dog plasma. Differences in the rates of volatilization of Mn and Co prevented the use of the latter as an internal standard.

The flame photometric estimation of fluoride in solutions of Zircaloy has proved infeasible because Zr suppresses the Ca-F emission band to unacceptable levels.

An investigation of the feasibility of molten sulphate as a medium for electrochemical studies has begun. The density of Li_2SO_4-K_2SO_4 eutectic at 625°C was found to be 2.12 ± 0.01 g/ml. Titration of Cl^- released when the sulphate was passed through the chloride form of Dowex-1, readily gave accurate assays of the eutectic. The electrode reactions at the cathode are being studied in detail. The measured Nernst equation factor for the Ag^+-Ag electrode agrees with the theoretical value,

and this electrode was found to be a suitable reference electrode at Ag ion concentrations greater than 0.01 molal. Potentials of the Pd^{2+}-Pd and Cu^{+}-Cu electrodes have been found to be +0.541 and −0.206 v, respectively, *vs* the Ag^{+}-Ag electrode.

A low-melting $LiNO_3$-KNO_3 eutectic affords the possibility of using Hg electrodes for electrochemical studies. The apparatus for such studies has been assembled, and preliminary experiments have indicated that the half-wave potential for Pb and Cd are identical, a remarkably interesting phenomenon which will be investigated further.

Investigation of the Bi-pool electrode has demonstrated that Bi metal and LiCl-KCl eutectic can be purified so that oxide contamination is no longer a problem. It has been shown that Cd-Bi alloys can be made in pure form. The Zn-Bi system has been studied, and the diffusion coefficient of Zn in Bi has been found to be 5.2×10^{-5} cm^2 sec^{-1} at 450°C. The diffusion coefficient of Li in Bi at the same temperature was found to be 2.1×10^{-5} cm^2 sec^{-1}, and the activity coefficient was found to be 4×10^{-7}.

The stability, resolution, and reproducibility of the new incremental polarograph are excellent. As little as 5×10^{-7} *M* Cd^{2+} gives a significant response. Incremental polarograms showing good resolution between Fe and U, each 10^{-5} *M* in 10^{-2} *M* Bi, have been obtained using EDTA.

The applicability of contact radiography in identifying active electrode sites at which electron transfer processes may selectively occur is being studied. Long-range objectives include the elucidation of the mechanism of electrode reactions and the refinement of voltammetry of solid electrodes into an accurate non-empirical method of quantitative analysis. Well-defined contact radiograms were produced by Tl^{204} tracer in deposits which had an average thickness ranging from 10 to 1500 A. Contact autoradiographs of Tl^{204} electrodeposited on Pt indicate a remarkable inhomogeniety in the thickness of the electrodeposit, which averaged 15 atomic monolayers. An experiment which was identical except for the absence of electrolytic current showed TlOH adsorbed uniformly over the Pt. A tentative interpretation involves three sequential processes.

Optimum conditions for activation analysis of Au in biological tissue have been determined in connection with a study of the localization of Au-thioglucose in brain tissue.

Exploratory studies of organic disulphide compounds indicate that disulphide-sulfhydryl reduction in compounds like cystine and glutathione disulphide can be carried out coulometrically with 100% current efficiency.

Prices of all processed isotopes in routine production have been reviewed and adjusted in order to put this production on a self-supporting basis. A catalog describing these isotopes has been published. In general, the demand for these isotopes has held up better than in similar periods in previous years in spite of vacations. A shipment of 21-hr Mg^{28} was made to France, the most distant point thus far for this isotope. Shipments of 2.3-hr I^{132} have been made to points as far away as Australia.

The Waste Concentration Plant was shut down for approximately 1 month while leaks were located in an auxiliary steam coil and a new coil fabricated and installed.

METALLURGY
(04-04-01-00-0, 04-04-02-00-1, 05-03-02, 05-03-03)

Nearly all thermal convection loops containing U-Bi have been shut down; emphasis has been shifted to loops containing Hg and Na. Steel thermal convection loops containing inhibited Hg under pressure have operated at ΔT for over 1500 hr without detectable corrosion or precipitation. The first boiling Hg loop is ready for startup. A Na purification apparatus has been designed. At high velocities, corrosion and cavitation-like attack by inhibited Bi are much more severe on 2¼ Cr – 1 Mo steel than on 1¼ Cr – ½ Mo steel.

Measurements of the emf between steels immersed in Bi as a function of Cr content show a pronounced electropositive maximum at ~5% Cr, which may or may not be associated with the selective attack so often found on this material. Solubilities of Mg and Sm in Bi have been redetermined; the relationship between the heat of solution and the solvent-to-solute radius ratio (suggested by Strauss, White, and Brown of NRL) does not appear to hold for Bi solubility curves.

Stripped films formed on steels by reaction with Zr-Bi melts possibly contain carbides and nitrides (of Si, Cr, Fe) along with the ZrN. Ion bombardment of a steel surface, followed by Bi-vapor deposition on the surface, does not appear to improve uniformity and reproducibility of Zr-bearing surface films on steels after contact with Zr-Bi melts.

The rate of formation of Zr film appears to be diffusion-controlled, while the rate-controlling step in formation of ZrC films is not clear from the available data.

The Radiation Loop has operated in-pile for 1817 hr, of which 1552 hr have been at ΔT condition, without difficulty.

Modification of the Hot Cell to permit cryogenic testing of irradiated specimens is proceeding.

A revised graphite monitoring and Radiation Damage Program for the graphite in the BNL reactor has been made.

Pore volume studies with natural graphite powder have shown that the volume available to Hg penetration is inversely proportional to the compacting pressure; also, the percentage of the pore volume shifts to the lower-diameter pores as pressure increases. Hg that has penetrated the pores under pressure is only partially released upon release of pressure. The amount released varies with the source of the graphite and is probably related to the structure and shape of the pores. Experimental apparatus for measurement of the density distribution of graphite powders and the volume of pore space inaccessible to penetrating liquids have been constructed. Approximately ⅓ of the total pore volume of AGOT graphite outgassed 1 hr at 500°C is inaccessible (i.e., occurs as closed pores).

A program to measure the rate of release of gaseous fission products from uranium carbide powders has been initiated; equipment to produce these powders under controlled conditions is being constructed.

Blisters that appear on the surface of the fuel elements for the graphite reactor during storage probably result from inclusions in the U-Al alloy meat which penetrate the clad during rolling. The slow oxidation of the inclusion [probably UAl_4 or $UC_{(2)}$] during storage produces the observed swelling.

Heat treatment improves the properties of the steel used in the telescope plates of the Greenbank Observatory by refinement of the grain size.

Fission fragment damage to thin evaporated films results in tracks visible under transmission electron microscopy. In thin films ($<$100Å) the matrix is vaporized; in thicker films it is melted and recrystallized; and in films $>$250Å no visible tracks are produced. Attempts are now being made to produce single-crystal films for these studies.

A high temperature vacuum furnace has been built to produce the high purity Fe required for the radiation effects studies. Development work on Mo brazing of graphite continued; the material flowing into the joints ($>$0.008 in. clearance is required) is a Mo-C alloy. An apparatus has been built to determine the effects of cycling temperature gradients on the fuel elements for the BBRR.

Capsule experiments show that migration of Th and U through slurries of their intermetallic compounds in Bi is due to the temperature coefficient of solubility and to convection currents in the slurry. Increasing the volume concentration of solids in the hot end may retard this migration by reducing the convection currents. A graphite frit appeared to act as a barrier for migration of U but not of Th through the slurry to the coldest end of the capsule.

Experiments in the escape of fission product gases from irradiated U-Bi slurry alloys have not yielded positive evidence for the rate of Xe release; a revised experiment to eliminate background radiation from the slurry is being set up.

MECHANICAL ENGINEERING (05-01-02-02, 04-04-03-00-0, 04-04-01-00-0, 08-04, 05-02-01, 04-04-04-02-0)

The Lummus Company changed its nuclear adjunct from Curtiss-Wright to Combustion Engineering in June on the Brookhaven Beam Research Reactor project. The preliminary design report has been completed. Also, a site report has been submitted to the AEC.

The new 7-ft spherical containment vessel has been designed for the critical experiments, and a contract has been awarded. It is intended to use the existing pump, piping, etc., and couple directly to the spherical tank by means of flanged joints. The design for the control rod plate locations and accessory equipment is in progress.

Modifications have been made to the tank for the BBRR Fuel Handling Mockup. Shutters and an indexing carriage and respective supporting structures were designed, fabricated, and installed and testing is in progress. A new handling tool and cooling bonnet are being designed. Six dummy fuel elements have been modified.

All equipment for the BBRR Fuel Element Test Loop have been delivered. The framework has been completed and fabrication of piping spool pieces is proceeding.

Erection of the Mercury Test Loop – Mark IV framework and piping has been completed and all components have been installed. Final testing of the system is in progress.

Pipe and fittings for the NaK Heat Transfer Loop have been received. All other equipment is on order except the oxide control system. A reference design for the test section has been completed.

A conceptual design has been completed for a Laminar Fluidized Bed Reactor. An evaluation of the economics of this system was made.

A preliminary flow sheet and cost estimate has been made for a High Temperature Critical Facility.

All three fans for the Brookhaven No. 1 Research Reactor have now been installed and have been on the line for about two months. Early indications show that the power savings will amount to about $10,000/month.

AMF Atomics has completed the cell layouts and equipment specifications for the High Level Radiation Development Laboratory and have forwarded the drawings to Burns and Roe, the Architect-Engineer. Work is progressing on review of equipment specifications and drawings by BNL and the invitation to bid for various equipment should be forthcoming shortly. A model of the cells is being constructed by BNL shops.

New control rod mechanisms and supporting framework were designed, fabricated, and installed for the Facility for Criticality Measurements of Slab Lattices. The 4 to 1 ratio slab lattice critical experiment will be run shortly. The fabrication of the 3 to 1 ratio slab lattice has been completed and is awaiting assembly. Component parts for the 2 to 1 ratio and 1½ to 1 ratio slab criticals are under fabrication.

A measurement platform for the UO_2 Rod Lattice Assembly has been designed, fabricated, and installed.

The in-pile hole mockup assembly for the Dry Irradiation Facility – Mark IV has been fabricated and installed in the basement of the Graphite Reactor Building. Final components for the furnaces are being fabricated. The assembly will be tested in the mockup prior to installation in the graphite reactor. Installation in the graphite reactor is scheduled for October 1960.

The production cost estimate of the Nitrofluor Process has been completed.

A cost estimate and plant design was prepared for a reprocessing facility utilizing the method of halogenation and fluorination of fuel elements in a fluidized bed. The estimate compared favorably with present day plants.

The Irradiation Facility is to be used by MIT to establish dose rates and other basic data for the irradiation of foods and other materials. Two more units are slated to go to two west coast universities.

REACTOR EVALUATION
(04-01-01-09-1, 04-01-16-00-1)

The review of the status of direct conversion programs was completed during this period and a report was submitted to the AEC. The full potential of these systems for use in civilian nuclear power plants cannot be assumed at this time due to the early stage of development. Theoretical work and exploratory experiments have been initiated on a pulsed fission plasma device. The chemonuclear studies are now directed toward the investigation of the radiation polymerization of ethylene. Evaluation of the suspended fuel concepts continues and during the period a report entitled "Laminar Fluidized Bed Reactor" was issued. Evaluation assignments and special projects for the AEC were continued during the period.

CONTENTS

SUMMARY iii
REACTOR PHYSICS DIVISION (04-04-06-09-0, 05-01-02-02, 04-01-16-00-1, 04-04-01-00-0)* 1
Reactor Theory 1
Experimental Reactor Physics 3
CHEMISTRY AND CHEMICAL ENGINEERING DIVISION (04-01-17-10-1, 04-04-02-00-1, 04-04-03-00-0, 05-02-01, 04-04-05-01-0, 05-02-02, 08-04, 04-04-04-02-0, 04-04-05-02-0) 6
Reactor Chemistry and Chemical Technology 6
Liquid Metal Heat Transfer Studies 13
Fluoride Volatility Process 14
Radiochemical Technology 16
Chloride-Fluoride Volatility Process Studies 18
Ultimate Waste Disposal 21
HOT LABORATORY DIVISION (05-02-02, 05-02-05) 25
Radioisotopes Development 25
Radiochemical Analysis 28
Hot Laboratory Operations 33
METALLURGY DIVISION (04-04-01-00-0, 04-04-02-00-1, 05-03-02, 05-03-03) 36
Corrosion Studies and Engineering Tests 36
Corrosion Fundamentals 39
Radiation Effects 46
Graphite Studies 49
Metallography 54
General Metallurgical Studies 56
Fuel and Blanket Development 59
MECHANICAL ENGINEERING DIVISION (05-01-02-02, 04-04-03-00-0, 04-04-01-00-0, 08-04, 05-02-01, 04-04-04-02-0) 63
Brookhaven Beam Research Reactor 63
Mercury Test Loop – Mark IV 63
NaK Heat Transfer Loop 63
Laminar Fluidized Bed Reactor 63
High Temperature Critical Facility 63
New Fans for Brookhaven No. 1 Research Reactor 64
High Level Radiation Development Laboratory 64
Facility for Criticality Measurements of Slab Lattices 64
UO_2 Rod Lattice Assembly 64
Low Mass Critical Assembly 64
Dry Irradiation Facility – Mark IV 64
Nitrofluor Process 64
Fluidized Bed Reprocessing Plant 64
Research Irradiation Project 64
REACTOR EVALUATION AND ADVANCED DESIGN (04-01-01-09-1, 04-01-16-00-1) 66

*AEC budget activity numbers.

Reactor Physics Division

Reactor Theory

J. CHERNICK

Brookhaven Beam Research Reactor

Work has continued in support of the BBRR design group. Calculations of the effect of voids in the heavy water on reactivity were completed as an aid to kinetics studies. P. MICHAEL

REACTOR PHYSICS DESIGN STUDIES

PWR Physics Program Evaluation

Program reviews were continued during this period for the New York Office of the AEC. Consultation on physics problems of the U^{235}-Th-fuelled Consolidated Edison reactor was continued for the Hazards Evaluation Branch of the AEC.

J. CHERNICK, M. LEVINE

Plutonium-Fuelled Thermal Reactors

Preliminary calculations of Pu-fuelled reactors with Be and D_2O moderation were made by the use of two group diffusion theory. A two region spherical configuration was considered with a Pu moderator core and a blanket of depleted U and moderator. This was done as a prelude to multigroup machine calculations, in order to obtain the range of the variables involved such as the critical radius, blanket thickness, volume ratios in core and blanket, etc.

Multigroup cross sections for U^{238} in the resonance range were computed for a few cases of interest to be used later in machine calculations.

G. SRIKANTIAH

Plutonium-Bismuth Fast Breeder Reactor

Physics calculations were initiated for a Pu-Bi fast breeder reactor. The primary work in this report period consisted of the compilation of cross sections and the determination of the appropriate methods of calculation. The Atomics International AIM code is used for criticality and flux calculations and preliminary calculations have been carried out. P. MICHAEL

LMFRE

In response to a request made by the Metallurgy Division, a rough estimate was made of the fission fragment flux at the inner surface of the reactor core vessel, and the external piping in a typical LMFRE scheme. The calculations were based on the 5-Mw experiment described in BAW-1052.

N. CORNGOLD

CRITICALITY STUDIES

Calculations based on purely microscopic cross section data have been made for the BNL and WAPD critical and exponential experiments on uranium-water and uranium-oxide-water lattices described at the 2nd Geneva Conference. The purpose of this work is to see how well the various results of the experiments can be calculated using the present microscopic data and computational methods.

The calculations use the MUFT-IV program together with results from Monte Carlo calculations of fast fission factors and resonance escape probability. M. LEVINE, Y. FUKAI, R. RECHTSCHAFFEN

Analytic Dancoff Calculations

An approximate formulation of the Dancoff effect has been undertaken with the aim of representing analytically the shadowing effect between pairs of resonance absorbing rods in a lattice and the interference due to other rods which partly block the line of sight between the pairs of rods being considered.

The results are supplemented by comparing analytic calculations with Monte Carlo calculations of collision probabilities in the lattices.

Y. FUKAI

Fission Product Poisoning

The equal charge displacement rule has been applied to the calculation of reactor poisoning for fission products for which yields have not been measured. This has yielded estimates for gross barns per fission poisoning of both thermal and resonance poisons. M. LEVINE

Reactor Kinetics

Work is continuing on the problem of the effect of temperature on Xe instability. More exact calculations including the delayed neutrons and the Newton's law of cooling model for temperature have been investigated to determine the range of applicability of the basic model. It has been found that in the range of interest of the physical parameters the simple model is quite accurate. Machine studies have been started on the exact solution of the equations. J. CHERNICK, G. LELLOUCHE

Flux Trap Reactors

A study has been completed on the performance of idealized flux trap reactors under various parameter changes. Central (or trap) regions of light and heavy water were considered, in which the fuel regions contained heavy water moderated with varying amounts of D_2O. The study indicates that H_2O is the better trap material and that if maximum power density is the limiting factor the better moderated cores give higher fluxes. This study is detailed in a memorandum by E. Pilat dated September 2, 1960. P. MICHAEL, E. PILAT

Analysis of the Snell Experiment

The Snell Experiment, which is an exponential experiment in natural U, is being analyzed with emphasis on the calculation of the ratio of average fission cross sections of U^{235} and U^{238}. Several sources of cross sections have been used and the strong dependence on inelastic cross sections has been noted. P. MICHAEL

THERMALIZATION OF NEUTRONS

The uses of difference-equation techniques in studying the time-dependent thermalization of neutrons have been considered. These techniques were applied to the heavy-gas model, where they gave an easy determination of the lower decay constants, and of the coefficients in the expansion of the flux in terms of Laguerre polynominals. The extension of these techniques to more realistic models of the thermalization process is being sought. N. CORNGOLD

Corngold's asymptotic series solution to the Boltzmann equation to include diffusive effects has been extended. The modified equation has been used to analyze some unpublished experimental results of R. Beyster (GA).

L. ZAMICK, N. CORNGOLD

A study of the thermal flux distributions in slab lattices was started with the use of INTRAN code. The lattices consist of slightly enriched U plates in water and are being studied experimentally at BNL. Preliminary results indicate that a bound proton scattering kernel for water and the assumption of isotropic scattering can be successfully used to predict foil activation distributions in the lattices. H. HONECK

Space Dependent Thermalization

A paper entitled "Thermal Neutron Flux Distributions in Space and Energy" was prepared for publication in *Nuclear Sci. and Eng.* (November 1960). An oral paper on this work was given at the June meeting of the ANS. The results demonstrate the importance of the spatial distribution of neutron sources on the asymptotic neutron spectrum. P. MICHAEL

Transport Kernels

An IBM 704 subroutine was written which will follow the trajectory of a neutron through a rectangular or hexagonal lattice. This routine will be used to compute transport kernels for the INTRAN code which will exactly describe the boundary conditions in these lattices. H. HONECK, G. STOLLER

Generalization of Singular Integral Methods for an Anisotropic Scattering Medium

The singular integral method recently suggested by CASE for solving neutron diffusion problems in an isotropic scattering medium is generalized for a linearly anisotropic medium. The formulation of the anisotropic problem is the same as that of the isotropic scattering problem except for small correction terms. These correction terms are proportional to the absorption probability. In the case of a nonabsorbing medium, it is shown that the anisotropic scatterings affect only the asymptotic flux distribution and not the transient flux distribution. H. TAKAHASHI

Milne Problem in Nonabsorbing Medium with a Linearly Anisotropic Scattering

The work with the above title has been completed and written in a BNL memorandum dated August 11, 1960. H. TAKAHASHI

The Effect of Anisotropic Scattering on Neutron Thermalization

A code for the problem with the above title is being programmed. When the two coupled second

order differential equations for isotropic flux and current are reduced to the corresponding difference equation, a four point method has to be used because the current is proportional to the square of the velocity in the lower limit.

More careful consideration of the condition at $v=0$ is needed than in the corresponding isotropic case. H. TAKAHASHI

Anisotropic of the Neutron Spectrum in Heterogeneous Systems

Neutron thermalization in a heterogeneous system has recently been studied by many authors. The present author and H.C. Honeck studied this problem theoretically by use of first flight collision probabilities. Campbell, et al. and Mostovoi, et al. have measured the neutron flux emerging from a hole in a U-H_2O lattice system. The anisotropy of the neutron spectrum was demonstrated by Campbell's experiment. Thus, it is important to consider the effect of anisotropy of the neutron spectrum in the emergent beam from a heterogeneous system. This study was performed by use of the integral transport equation of the slab lattice. It is found that the anisotropy of neutron spectrum is proportional to the absorption in the fuel and that it persists even in the limit of vanishingly small fuel and moderator regions. H. TAKAHASHI

The Fast Effect in U-Be Systems

Monte Carlo calculations of the fast effect in U and Be systems were completed during this period. A paper on this subject was presented at the June meeting of the ANS [*Trans. Am. Nuclear Soc.* 3, 1, 270 (1960)]. H. RIEF

Experimental Reactor Physics

H. KOUTS

WATER LATTICES

During this report period oxide rod exponential experiments and data analysis were carried out. The preparation for slab lattice critical approaches and experiments, and oxide miniature rod lattices was continued. Miniature measurements on the 3 and 4:1 slab lattices were completed.

The 3% oxide 0.5 in. o.d. rod clean-exponentials were completed and poison exponentials were begun. The clean data were analyzed and both anisotropy and variation of reflector savings with radius were observed (see Table 1). The analysis of the poison lattices has not yet been carried out.

Preparation for the slab lattice critical experiments has continued. The 3:1 and 2:1 lattices were almost completely fabricated; the 1.5:1 and 1:1 lattices were about half fabricated. The console and instrumentation were completed and the hazards report prepared.

The oxide pellets are being manufactured for use in the oxide miniature measurements. The design of all related equipment was completed. Measurements should commence during the next report period.

The miniature slab measurements, δ_{25}, δ_{28}, ρ_{28}, and disadvantage factors, have been completed in the 4:1 and 3:1 slab lattices. The analysis of the data is in progress. H. WINDSOR

ACTIVATION CROSS SECTION OF Dy^{164}

The relative activation cross section of Dy^{164} in the energy region 0.06 to 2.0 ev has been measured by exposing a Dy_2O_3 foil in the arm of a crystal neutron spectrometer [using the Bragg reflections from the $(10\bar{1}1)$ planes of a Be crystal] and counting the resulting 139-min β^- activity from Dy^{165}. The absolute cross section was obtained at 0.06 ev by comparing the β^- activities of the Dy_2O_3 foil and a Au foil after both had been exposed together at 0.06 ev. Table 2 lists the results. The uncertainties are those of the relative measurement. In addition there is an uncertainty of ± 120 b in the absolute cross section at 0.06 ev. From the lack of constancy of $\sigma_{act}^{164}\sqrt{E}$ it is apparent that for energies >0.1 ev the cross section is falling off more rapidly than a $1/v$ function. This is in agreement with the behavior of the Cd ratio of Dy, which was measured by activating bare and Cd-covered Dy-Al foils in the forward ("white") beam of the spectrometer. The Cd ratio for Dy was 328 ± 3, whereas that for a thin BF_3 counter was 102 ± 2; the ratio $(\text{C.R.}-1)_{Dy}/(\text{C.R.}-1)_B$, where C.R. = Cd ratio, was therefore 3.24 ± 0.07. A calculation of this ratio, using the measured cross sections in the region 0.06 to 2.0 ev, a $1/v$ dependence at energies <0.06, and a reasonable extrapolation at energies >2.0 ev (the extrapolation does not strongly affect the results) gives 3.19 ± 0.1. This value is independent of the absolute value of the cross section, but it has been assumed that up to the effective Cd cutoff the flux distribution is Maxwellian and beyond that it falls off as $1/E$.

The value of

$$\int_{0.4}^{\infty} \sigma_{act}^{164}\,(dE/E)$$

is about 420 b.

The above measurement, when combined with that of R. Tornau [*Z. Physik* **159**, 101 (1960)], gives for the individual activation cross sections to the 1.3-min isomeric state and to the 139-min state of Dy^{165} the values 1140 and 606 b, respectively, at 0.06 ev.

If the activation cross sections are assumed to be $1/v$ in the region between 0.0253 and 0.06 ev then the above measurements correspond to 2200 m/sec cross sections of 2690±190, 1756, and 933 b, respectively, for total activation, activation of the 1.3-min state, and activation of the 139-min state.

The departure of the Dy^{164} activation cross section from $1/v$ behavior affects the interpretation of flux measurements made with Dy foils, but although detailed calculations have not yet been made it is expected that the effects of the observed departure will be small.

The results obtained are in agreement with the cross sections of Dy^{164} presented in the references cited in BNL 325; however the cross sections quoted in BNL 325 are incorrectly stated.

E. Weinstock

MEASUREMENTS OF Dy^{164} AND Eu^{151} TOTAL NEUTRON CROSS SECTIONS

In view of the recent interest in Dy^{164} as a neutron detector in reactor physics measurements, the total cross section of this isotope has been measured between 0.02 and 2.00 ev, using isotopically enriched samples. Preliminary results indicate that the total cross section of Dy^{164} decreases with energy considerably faster than the $1/v$ law; there is also evidence for the presence of a broad resonance, or possibly two overlapping resonances, in the vicinity of 0.12 ev.

The total neutron cross section of Eu^{151} has been measured in the energy level from 0.08 to 1.00 ev, by the use of samples of high isotopic purity. The double resonance which occurs at 0.321 and 0.460 ev has been analyzed by fitting the experimental values to the sum of two one-level Breit-Wigner expressions, after the usual corrections. The results of the analysis are $E_{o_1}=0.0321\pm0.001$ ev, $\sigma_{o_1}=4250\pm60$ b, $\Gamma_1=0.0796\pm0.002$ ev; $E_{o_2}=0.460\pm0.001$ ev, $\sigma_{o_2}=24910\pm200$ b, and $\Gamma_2=0.088\pm0.002$ ev, where the symbols have the usual meanings.

S. Tassan

BBRR CRITICAL EXPERIMENTS

During the period May 1, 1960 to August 31, 1960 there were 52 different experiments run in the BBRR critical experiment facility. The results of these experiments are reported in BBRR Critical Experiment Reports Nos. 15 through 19. Copies of these reports were sent to appropriate members of the project staff for use in the design studies. While most of the runs were made to determine reactivities of specific engineering materials some runs were devoted to more general reactor physics problems.

A series of runs was devoted to the measurement of the thermal neutron lifetime. This lifetime was measured by both the Rossi-α technique and by the use of a neutron pulser. In both cases the time decay characteristics of the reactor were measured at various shutdown configurations. Of the two

Table 1

3% Oxide 0.5 in. o.d. Rod Exponential Measurements*

V_{H_2O}/V_{UO_2}	λ_o, cm	α, $cm^{-1}(\times10^3)$	M	$B_{m\parallel}$, $cm^{-2}(\times10^4)$	$B^2_{m\perp}$, $cm^{-2}(\times10^4)$
1	7.335±0.058	1.7±2.4	0.943±0.016	52.92±1.11	56.14±0.38
1.5	6.878±0.069	2.0±1.7	0.919±0.015	59.52±1.11	64.78±0.42
2	6.725±0.036	3.6±1.6	0.944±0.016	66.32±1.28	70.26±0.43
3	6.594±0.104	3.6±1.1	0.957±0.023	67.34±1.70	70.35±0.69
4	6.344±0.079	3.0±0.5	0.974±0.014	59.95±0.9	61.52±0.40

$M=(M^2_\perp/M^2_\parallel)(1/L^2)=(M^2_\perp/M^2_\parallel)\left(2.4048/[r+\lambda_o+\alpha(r-R_o)^2]\right)^2-B^2_{m\parallel}$, where λ_o and R_o are those measured at $L=40$ cm.

*28-mil, 304 SS clad compacted elements, with an oxide density of 9.3 g/cm^3.

Table 2

Total Activation Cross Section of Dy^{164} as a function of Neutron Energy*

E, ev	σ_{act}^{164}, b	$\sigma_{act}^{164}\sqrt{E}$, b$-(ev)^{1/2}$
0.06	1750±50	429
0.1	1340±40	425
0.2	831±25	371
0.4	439±22	277
0.6	307±15	238
0.8	232±12	208
1.0	191±19	191
2.0	94± 9	132

*Quoted uncertainties are those of the relative measurements. In addition there is an uncertainty of ±120 b in the normalization at 0.06 ev.

techniques the pulsed source gave by far the more accurate measurement. Combining the data for several runs gives a lifetime of 672 ± 13 μsec. A detailed report of the measurement is given in BBRR Critical Experiment Report No. 17.

As part of the above series a number of runs was devoted to checking the useful range of the "Analog Reactivity Meter." This check was made by a comparison of the "meter" reading with the multiplication curve technique. The result of this check was to show that for this reactor the two techniques agreed up to $-$\$15 in reactivity.

Another series of runs was made to measure the thermal neutron importance function in the reflector. Here the thermal importance is defined as the reactivity value of a thermal poison divided by the flux. The thermal flux was measured by the usual In foil techniques and the positional dependence of the reactivity of a Cd slug was measured on the "reactivity meter." Figure 1 shows a plot of the importance function or adjoint flux in core 14.

Besides the engineering reactivity runs a series of runs was devoted to measuring the gamma heating at various positions in the reactor. These runs are reported in Report No. 20. Figure 2 shows a part of the results of these runs.

K. Downes

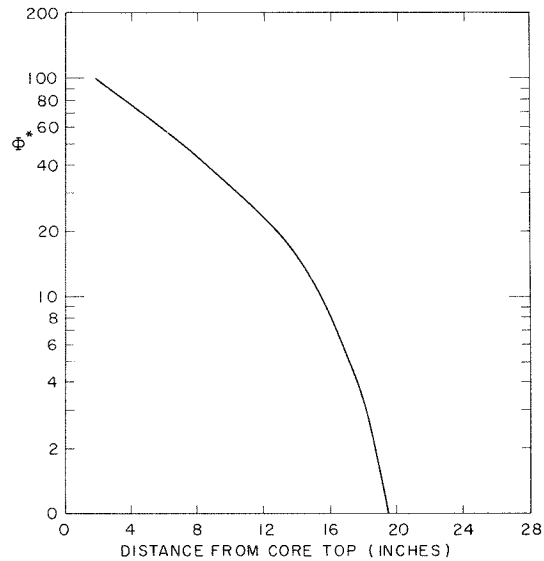

Figure 1. Adjoint flux in top reflector of core 14.

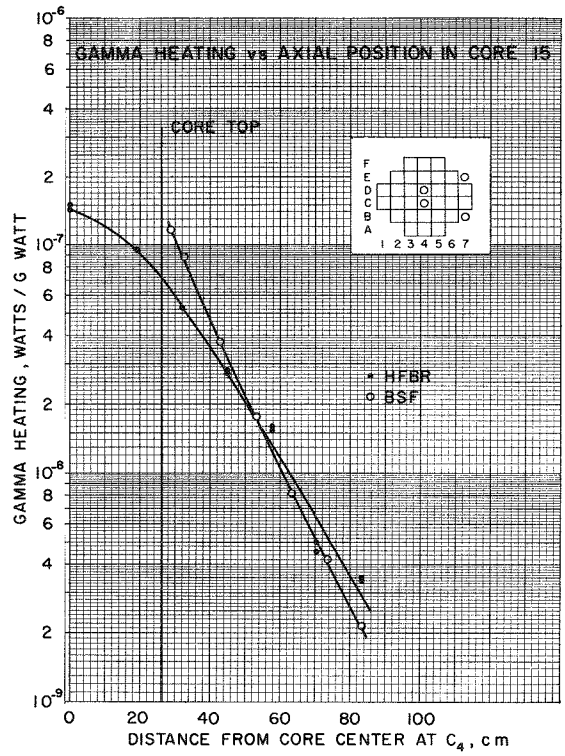

Figure 2.

Chemistry and Chemical Engineering Division

O.E. DWYER

Reactor Chemistry and Chemical Technology

R. WISWALL

FLUOROCARBON STUDIES

This program was undertaken to measure the stability to heat and ionizing radiation of a number of fluorocarbons which might, if stable, find application in nuclear technology. Most of the effort of the current report period has been devoted to the development of analytical methods, with emphasis on the gas-liquid chromatography of fluorocarbons, the determination of free fluorine, and the elemental analysis for C, H, and F in highly fluorinated organic compounds. Irradiation experiments were carried out on cyclohexane in order to gain experience in the techniques of exposure and analysis. The behavior of this compound under irradiation has been investigated by other workers, and satisfactory agreement with their results has been obtained. Hexafluorobenzene has also been exposed to radiation, but analyses have not yet been completed.

In the synthetic part of the program, fluorinations were suspended pending the completion of a new fluorine facility. However, auxiliary apparatus has been assembled, gas-chromatographic columns suitable for preparative runs, and a Podbielniak spinning-band fractional distillation column. D.MACKENZIE, F.BLOCH, W. RIEL, A. SCHOFIELD

SPECTROPHOTOMETRIC STUDIES OF FUSED SALTS

Fused salt spectra generally consist of a region of complete transmission, and one of near-opacity. In order to examine the latter, very thin films (believed to be roughly a micron thick) were prepared between two optically flat quartz plates, and the spectrum measured.

Lead chloride (purified by treating the molten salt with hydrogen chloride) was examined in this manner and the spectrum at room temperature obtained (Figure 3). The spectrum agrees essentially with that of Hilsch and Pohl [*Z. Physik* **48**, 390 (1928)]. Subsequent preparations gave similar, but not identical, spectra. After the examination of the spectrum at higher temperatures, it was found that the peak at 2700Å shifted to red (2800 Å at 400°C). Above this temperature, the peak flattened considerably as the melting point (501°C) was approached.

Potassium iodide (dried and loaded into the cell under hydrogen to prevent the formation of KOH) showed a peak at 2200 Å similar to that reported by Hilsch and Pohl [*Z. Physik* **59**, 816 (1930)]. The peak shifted to about 2250 Å at 290°C, and was obliterated at higher temperatures, possibly due to the shifting, with increased temperature, of a strong peak at 1875 Å. (This peak is reported by Hilsch and Pohl but is below the range of our instrument.) J. BOOKLESS

THERMODYNAMICS OF Na-Bi ALLOYS

The thermodynamic properties of Na-Bi alloys rich in Na ($x_{Na} > 0.76$) have been obtained by measuring the boiling points of the alloys at various pressures and compositions. The apparatus is shown in Figure 4 and follows the plan of Makansi, Muendel, and Selke.* It consists of a stainless steel container welded onto a stainless steel reflux column one meter high. A Chromel-Alumel thermocouple contained in a thin stainless steel tube as shown measured the boiling points. A Nichrome furnace surrounded the Na container and the reflux column. Generally only the portion surrounding the Na container was heated.

A Wilson seal at the top of the reflux tube enabled one to vary the height of the thermocouple so that it would be just above the surface of the alloys. Molten Na metal was loaded into the apparatus by filtering it through a Pyrex fritted filter by the application of a pressure of purified Ar

*M. Makansi, C. Muendel, and W. Selke, *J. Phys. Chem.* **49**, 40 (1955).

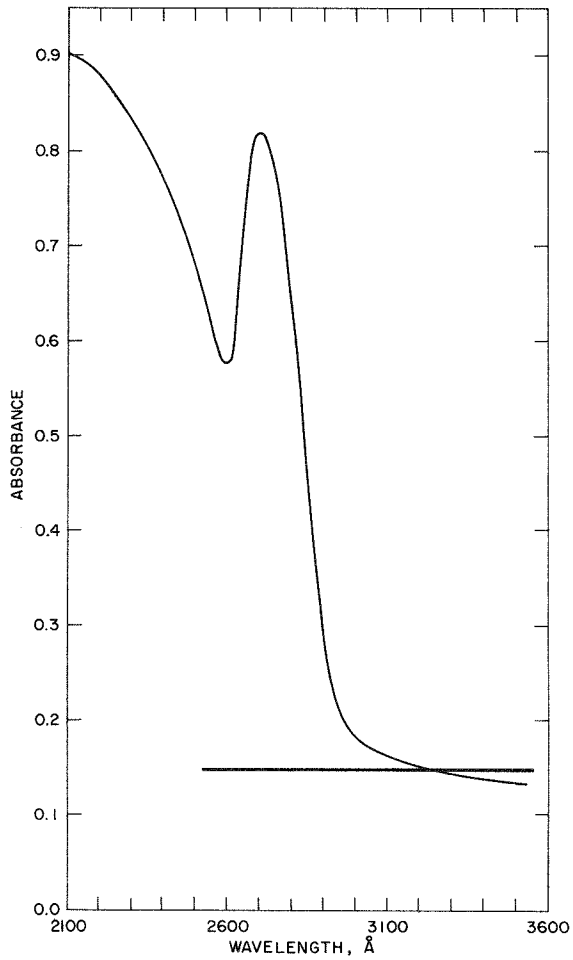

Figure 3. Absorption spectrum of $PbCl_2$.

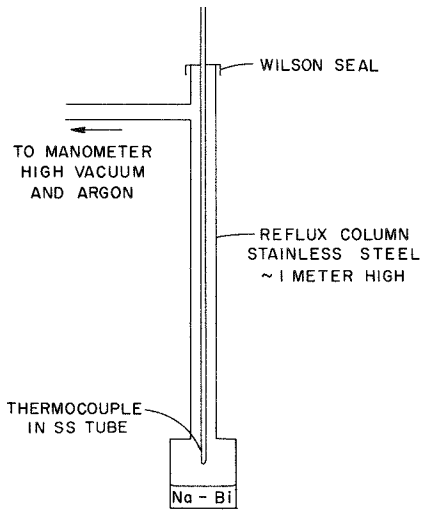

Figure 4. Apparatus for determining boiling points of Na-Bi alloys.

above the frit. During the loading operation all precautions were taken so that no Na would come into contact with the air and be oxidized. The system was connected to a manometer and source of purified Ar through the side arm.

Boiling points of pure Na were measured and agreed well with previous measurements (*loc. cit.*). Bi was then added and further measurements were taken. By repeated additions of Bi, values of the boiling points for alloys of several compositions were obtained. These results are plotted in Figure 5.

In order to calculate the activity of Na in the alloy, two assumptions were made: 1) only the Na had any appreciable vapor above the alloy, and 2) the ratio of Na to Na_2 atoms in the vapor did not change with a change in composition of the alloy.

With these assumptions the activity was calculated by the use of the equation

$$a_{Na}=P_{Na}/P_{Na}^{\circ},$$

where P_{Na}° is the vapor pressure of pure Na and P_{Na} is the vapor pressure of Na above the alloys. The activity values were converted to emf's and are shown in Figure 6 along with previous values obtained with the cell Na(l) | glass | Na-Bi(l).

J. EGAN, J. BRACKER

THERMOCOUPLES FOR MEASUREMENT OF HIGH TEMPERATURES

Tungsten-Rhenium Thermocouple (Graphite Junction)

Runs were made in both the resistance heated furnace used before and in the new induction heater unit shown in Figure 7. Considerable difficulty was encountered in obtaining proper operation of the latter equipment and the presence of an RF voltage at the potentiometer was noted in all runs whether or not a capacitor-resistor filter circuit was employed in the thermocouple lead wires.

The results of three runs are shown in Figure 8. One induction heater run and the resistance heater run agreed quite well although both differed by as much as 80°C from the calibration curve published by Lachman; the latter data, however, were obtained in the absence of any C. The highest temperatures (2370°C) were obtained only with the induction heater and show that a maximum in thermocouple output is reached at

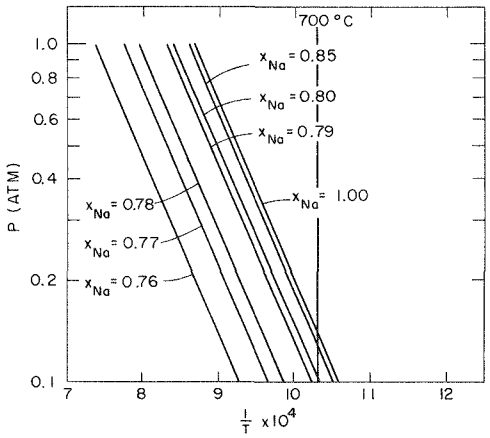

Figure 5. Vapor pressure of Na-Bi alloys.

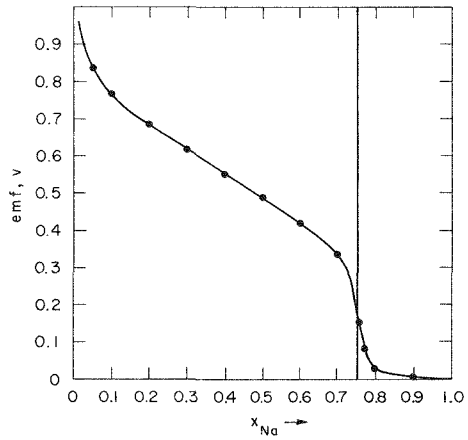

Figure 6. Emf of the cell Na(l) | glass | Na-Bi | (l) at 700°C. Values for $x_{Na} > 0.76$ are calculated from vapor pressure data.

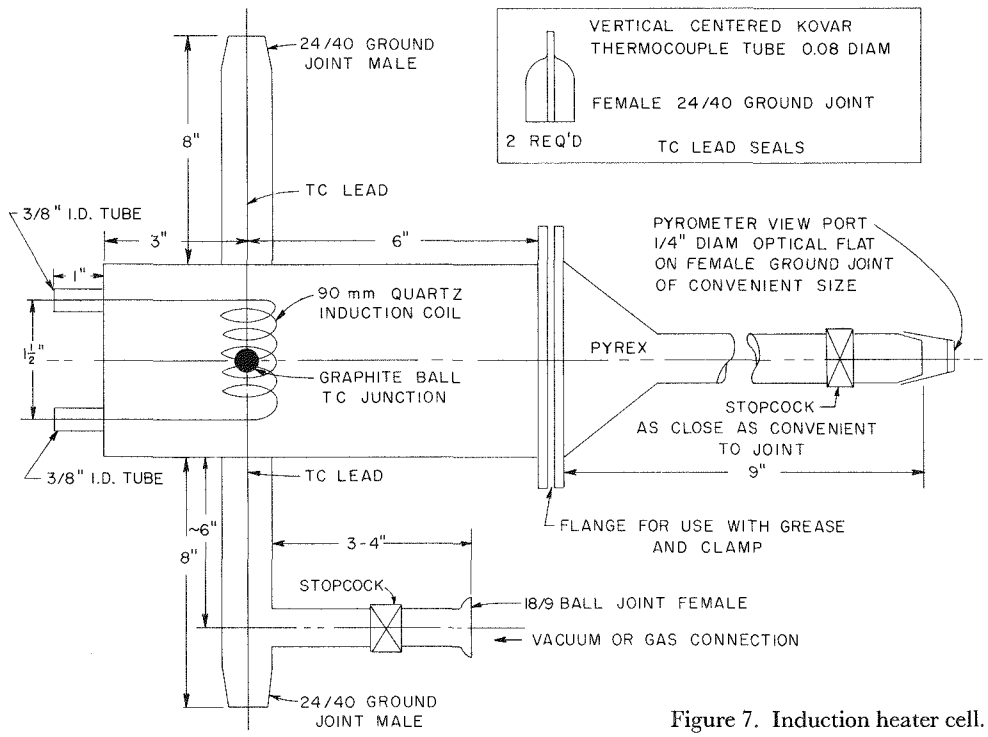

Figure 7. Induction heater cell.

about 2160°C. No such maximum is seen in Lachman's data although these data give a curve which is quite flat at 2200°C.

The second induction heater run does not show any maximum but is about 1 mv lower than the other two runs at 2150°C. Thus some question exists as to the actual behavior of this type of thermocouple in the presence of carbon at these temperatures. Since the junctions in the two induction heater runs were made by tying the two separate wires to a graphite ball and not to each other, it is possible that the junction may have moved during heating enough to give poor contact and hence a low reading. It is also possible that some reaction takes place which changes the emf of the thermocouple. The second possibility can-

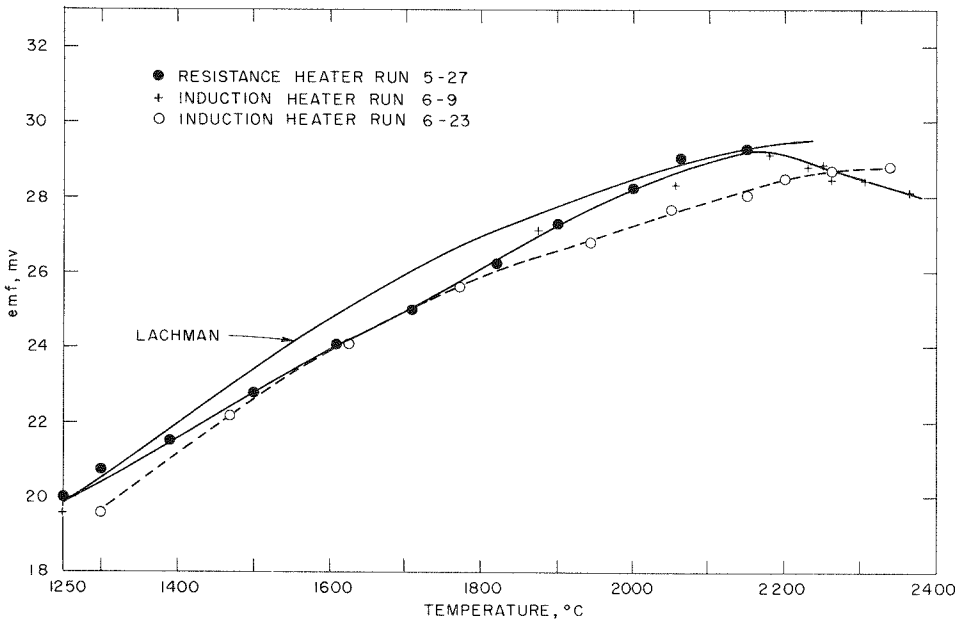

Figure 8. Tungsten-rhenium thermocouple, graphite junction.

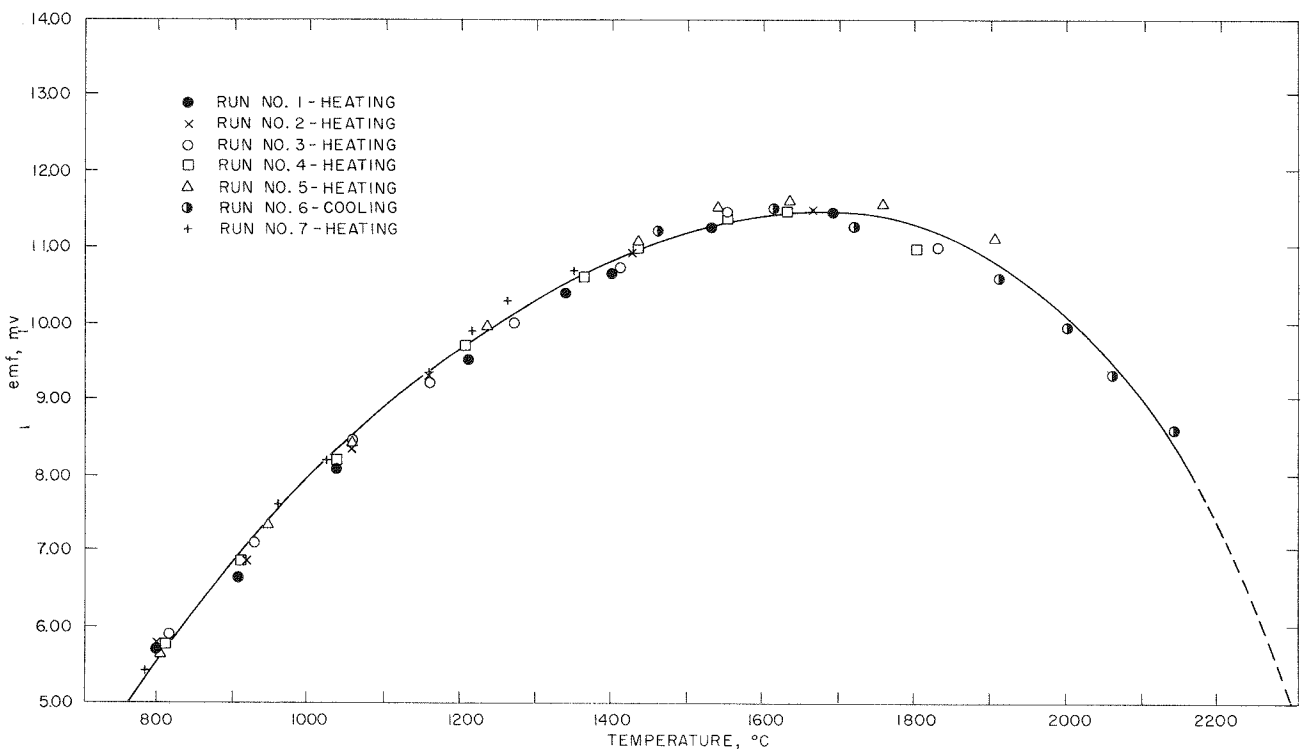

Figure 9. Rhenium-graphite thermocouple.

not be properly evaluated until the question of a proper contact at the junction is satisfactorily solved.

Graphite-Rhenium Thermocouple

Experiments were performed using the induction heater apparatus shown in Figure 7. The junction of the thermocouple was made by winding the Re wire through a graphite ball which in turn was supported by a ⅛-in.-diam graphite rod, the other electrode of the thermocouple.

Seven runs were completed with a graphite-Re thermocouple. The results are shown in Figure 9. Examination of these results shows that:

1) The thermocouple is stable, i.e., it has withstood seven heating and cooling cycles within one month without any change in the emf-temperature relationship. The slight deviations of the experimental points from the average curve attributed to the precision of the optical pyrometer readings of the temperature and not to any changes in the characteristics of the thermocouple. The deviations are random and do not show the systematic shifts noticed in work with other thermocouples.

2) The stability of the thermocouple is interpreted as an indication of the absence of carbide formation or any other interactions between Re and graphite.

3) The thermoelectric power of the thermocouple is 8 μv/°C in the range 765° to 1550°C. While this is about half of the thermoelectric power of W-Gr, it is adequate, since standard potentiometers can be read to 5 μv.

4) The inversion of the temperature-emf curve at about 1650°C limits the usefulness of this thermocouple to the range below 1550°C, or above 1800°C. The flatness of the curve between these two points makes the thermocouple useless in the range bracketed by them. There seems to be nothing to prevent the use of this thermocouple on the descending part of the curve to a temperature of 2400°C. W. Kenney, A. Eshaya

RELEASE OF FISSION PRODUCTS FROM FUEL ELEMENTS

Diffusion Studies

Results obtained in the experiments on the diffusion of Xe through several materials of interest as possible cladding for organic moderated reactors were reported in BNL 624. In summary, it was found that Xe did not diffuse through 2S Al of 0.015 and 0.020 in. thickness up to 510°C which was the highest temperature studied. Similarly, no diffusion was found in experiments with PIQUA cladding (0.030 in. Al backed by 0.0005 in. Ni diffusion barrier) to a temperature of 369°C, which was the upper limit of the temperature range investigated. There was no diffusion through type 304 SS of 0.020 in. thickness at 510°C. A run conducted at 610°C for 120 min indicated some Xe activity which raised the possibility that the lower limit of Xe diffusion through 304 SS was reached. Another experiment performed at 650°C for 390 min however showed no Xe diffusion, and it is concluded that an imperfection in the diffusion barrier for the 610°C run led to this erroneous conclusion.

With the completion of the work on Xe diffusion, attention was focused on similar diffusion measurements with I. Three independent experimental techniques were employed. The first, a sealed capsule, provided a sensitive method of determining accurate diffusivities at low I partial pressures using radioactive tracer I. A second experiment was designed to measure the solubility of I in Al spheres and diffusivities by unsteady state measurements. The third technique utilizing an Al-U tube as the diffusion barrier, provided a method of measuring permeabilities using radioactive tracer I at partial pressure much higher than possible using the first technique.

The results of the capsule experiments show that I does not diffuse through a 0.035-in. Al barrier maintained at temperatures between 315° and 500°C for durations as long as 7000 min. Formation of microscopic cracks was observed in the machined Al diffusion surface of two capsules maintained at 500°C for long periods of time.

The results of the solubility experiments also show that I does not diffuse and also does not dissolve in Al in quantities larger than 1.2×10^{15} atom/g Al at 1 atm pressure, which is the lower limit of detection. Al was found in the I deposit at the end of an equilibration. A small amount of Al surface pitting was visible. This, together with the capsule failure noted above, would indicate that although I will not permeate an Al fuel element cladding, it could penetrate by chemical reaction, i.e., by what is essentially a corrosion mechanism, if sufficient quantities of I are present to continue the reaction.

Further confirmation of the absence of I diffusion is provided by the third set of experiments.

In these, the I driving force was varied between the vapor pressures of I at specific temperatures, i.e., 5.6 to 50.4 mm. Al specimen temperatures were maintained in the temperature range 461° to 483°C for durations as long as 260 min.

It is concluded from these studies that I does not diffuse through 2S Al in the temperature range from 315° to 500°C.

Detailed descriptions of the experimental apparatus and results are reported in BNL 644.

A. CASTLEMAN

Meltdown Studies

The equipment for the studies of fission product release during meltdown has been assembled and satisfactorily tested. In these studies emphasis will be placed on the quantities of several typical fission product nuclides released and also the chemical and physical form of the release. It was decided not to spend much time on the release of Xe and Kr but to concentrate the efforts on I.

Since most of the metal matrix consists of U, chances are good for the formation of U-I compounds. Mo, which is also present in comparatively large concentrations in the U-Mo alloy, could also react with I to form I compounds. Similarly one could list I compounds with Th, Cs, Ce, Ba, La, Nd, Sr, Te, etc. There is, however, the very definite possibility that statistical kinetic considerations are the determining factor. Thus an atom of I surrounded by U atoms may react to form a U-I compound before it ever gets a chance to form a compound with Cs, Ce, Ba, or any other fission product nuclides. In addition, one has to take into account the decomposition of many of these compounds at the high temperatures of the meltdowns.

As a first step in the experimental program, it was decided to establish the conditions under which I is released from irradiated U-Mo alloy. A sample of U-Mo was placed in one leg of the meltdown cell while the other leg was filled with activated carbon. The cell was sealed under vacuum and irradiated in the BNL reactor. A sealed cell was decided upon in order to avoid any losses or contamination by air.

For the melting step of the experiment, the sample was heated by induction while the activated carbon was immersed in liquid nitrogen. The sample was then brought up very rapidly to the desired temperature, held at that temperature for a predetermined period of time, and then allowed to cool. After cooling, the two legs were separated by a torch in such a way as to prevent any escape of fission products from the cell. The two parts were then treated separately for their analysis.

Six samples were run with meltdown times from 2 to 30 min, and temperatures from 1050° to 1450°C. Xe^{133} and Xe^{135} were released during the short meltdowns and at the lower and higher temperatures. With meltdowns of 2, 3, and 3.5 min no other nuclides were observed. With a meltdown of 5 min at 1140°C, I^{131}, I^{132}, and I^{133} were released in addition to Xe^{133} and Xe^{135}. With a meltdown of 30 min at 1450°C, Te^{131m}, Te^{131}, and Te^{132} were released in addition to the I and Xe. It was found that the quantity of Xe and I released increased with temperature and also increased with time. All of the released Xe was found in the activated carbon; most of the I released was found on the quartz wall near the melted U-Mo alloy, and all of the released Te was found on the quartz wall near the melted U-Mo alloy. One cannot account for the distribution of I on the basis of normal condensation of I. The evidence points to the presence of either particulates which settle rapidly on the nearest surfaces, or the presence of I compounds far less volatile than elemental I. This and the nature of the Te will be investigated further.

F. HOFFMANN

SORPTION AND DIFFUSION OF FISSION PRODUCTS IN HIGH DENSITY GRAPHITE AT HIGH TEMPERATURES

The absorption isotherms of Xe on type GS R4 high density graphite have been measured at 750° and 1000°C by using radioactive tracer Xe. A technique was developed by which graphite at high temperature is equilibrated with radioactive Xe and the sample quenched in cold Hg to seal in the absorbed gas. The measured magnitudes of the absorption and the shapes of the isotherms indicate that by far the greatest fraction of the sorbed gas is contained within the accessible pores of the graphite. It was found that the absorption can be expressed by the equation $A_g = Pv_vN/RT$ where A_g is the number of atoms absorbed per gram, v_v is the void volume per gram, N is Avogadro's number, R is the universal gas constant, T is the absolute temperature, and P is the partial pressure of the Xe. A comparison of the measured and theoretical densities, in conjunction with the measured absorptions, indicates that the Xe has completely filled the pores of the graphite. As a re-

sult of this work an explanation is offered for the high concentration of fission Xe found on graphite surfaces by other workers at BNL.

Measurements of the rate of diffusion of Xe into evacuated graphite at 750° and 1000°C were made by equilibrating for time intervals shorter than those required to achieve equilibrium. Considerable variation in rates of absorption was found for the same type of graphite fabricated as round stock and flat stock. These results indicate differences in the size and pore structure between the two batches of graphite since a considerable variation in rate of absorption was observed and the slower rate indicates that Knudsen flow can be an important flow mechanism.

The work with the Xe-graphite system has been completed and the experiments are reported fully in BNL 633.

A study of absorption and diffusion of I through high density graphite has been started. Because of the considerable difference in the physical and chemical properties of a noble gas from those of a halogen vapor, new equipment had to be built for these experiments. This equipment is shown schematically in Figure 10. The pressure of the I in the vessel will be maintained by controlling accurately the temperature of the I crystal reservoir and the rest of the equilibrium apparatus. Isotherms at 800° and 1000°C (graphite temperature) will be determined. An attempt will be made to carry out these studies with nonradioactive I because this simplifies the whole experiment very considerably. Should the absorptions prove to be so low as to make radiochemical analyses necessary, the equipment can be used for tracer experiments. In order to avoid any inaccuracies due to condensation of I vapors on the graphite surface at the end of an experiment the analyses will be performed on the graphite samples after all its external surfaces have been machined off.

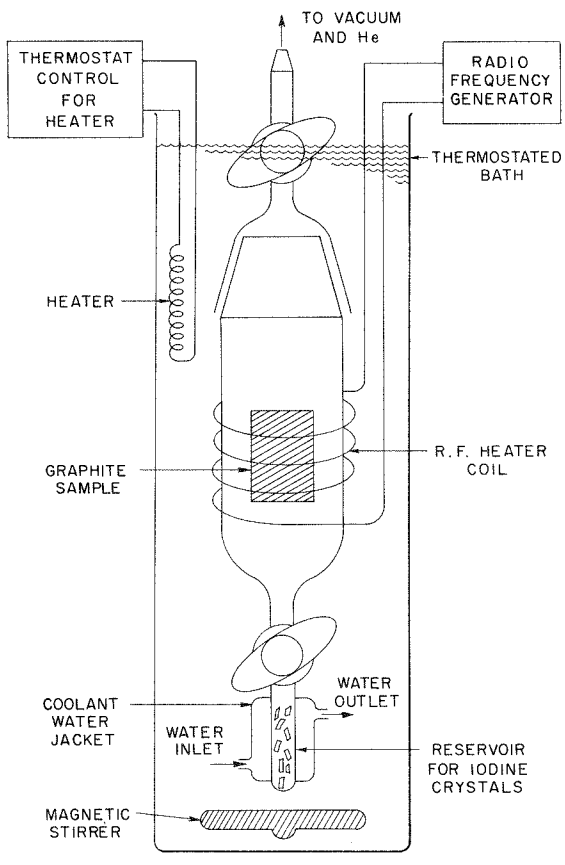

Figure 10. Iodine graphite equilibration apparatus.

During the report period eight experiments were completed with the purpose of measuring the quantities of I adsorbed in R4 type of graphite at 1000°C. The experimental conditions and results are shown in Table 3.

The experimental data are obviously inadequate as yet for arriving at any quantitative conclusions. The main concern is still to obtain greater precision and reproducibility. Both activation analyses and wet chemical analyses will be used until one method demonstrates clear advantages over the other.

One significant fact, however, is evident from the available four results and that is that I is absorbed to an extent considerably higher (10 to 50 times)

Table 3

Adsorption of Iodine by Graphite at High Temperatures

(Runs carried out at 23 mm Hg and 1000°C.)

Run	Duration, min	I_2 concentration, μg/g
A	85	[a]
B	75	11[b]
C	120	[c]
D	105	27[d]
E	105	73[d]
F	105	74[d]
G	105	[c]
H	445	[c]

[a]No iodine detected by wet chemical analysis.
[b]Activation analysis.
[c]Analysis not yet completed.
[d]Wet chemical analysis.

than what would be expected on the basis of containment of I vapor in the pores, as was the case of Xe. There is evidence, therefore, of strong adsorption on or reaction with the graphite. F. SALZANO

Liquid Metal Heat Transfer Studies

HEAT TRANSFER STUDIES WITH MERCURY

During the report period, the construction of the new Hg loop proceeded pretty much on schedule, and the present expected completion date is around October 1. The major jobs which remain are the completion of the test section and checkout of electrical systems and instrumentation. Of the 13 heating elements in the test bank, the central (or test) element will have its own power supply and instrumentation, and the other 12 will be divided in three groups of four, each group having its own power supply and instrumentation. The 20 external heaters will be divided into two groups of ten. The resistances of all these heaters have been measured and they were grouped so that the heaters in each group has, insofar as possible, the same resistances. The maximum variation in the resistances of the internal heaters was only 0.65%, and that of the external heaters 0.8%.

HEAT TRANSFER STUDIES WITH NaK

A loop will be built to determine initially heat transfer coefficients for NaK flowing in-line through unbaffled staggered rod bundles, the results of which will be applicable to the thermal design of shell-and-tube heat exchangers for handling alkali metals.

The mechanical design of the loop was slowed during August by vacation schedules. The test section presents certain design problems which arise out of the need for double containment and provision for free thermal expansion of the internal heating elements. One possible design which looks most promising is based on the principal of electrically grounding the bottom end of the test section to eliminate the problem of electrical leads at that end and to allow the heating elements to slip freely through the bottom tube sheet.

Orders have now been placed for all the major components of the loop, including the oxide-control-and-indicating system.

The present target date for completion of the loop is June 1.

Table 4

Reference	r_2/r_1	$[Nu]_2$ $\psi Pe=10^2$	$\psi Pe=10^3$	$\psi Pe=10^4$
BNL	1.948	6.13	9.84	29.85
	2.708	6.19	9.97	30.50
	3.968	6.31	10.23	31.65
	6.000	6.55	10.75	34.50
Hartnett and Irvine	1.948	6.44	11.72	45.0
	2.708	6.63	11.91	45.2
	3.968	6.91	12.19	45.5
	6.000	7.16	12.44	45.8

ANALYTICAL STUDY OF HEAT TRANSFER TO LIQUID METALS FLOWING IN CONCENTRIC ANNULI

Results have been obtained for the case of heat transfer through the outer wall only. They are based on the conditions of constant heat flux, fully-established turbulent flow, and no effect of temperature on physical properties. Table 4 summarizes the results and shows a comparison between them and those calculated from the approximate relation of Hartnett and Irvine.*

The approximate method of Harnett and Irvine gives results which are 5 to 50% above the BNL results. Moreover, their method does not give enough spread in the Nusselt number at the higher Peclet numbers as r_2/r_1 is varied. At a Peclet number of 10^4, for example, the Nusselt number remains essentially the same as the r_2/r_1 ratio is varied 3-fold. In Table 4, the following symbols apply:

$Nu]_2 = h_2 D_e/k$ = Nusselt number
h_2 = heat transfer coefficient for outer wall
D_e = 4 (cross flow area/wetted perimeter)
$\psi = \varepsilon_H/\varepsilon_M$
ε_H = eddy diffusivity for heat transfer
ε_M = eddy diffusivity for momentum transfer
$Pe = (D_e v_{av} \rho C_p)/k$ = Peclet number
v_{av} = average linear velocity
ρ = density
C_p = heat capacity
k = thermal conductivity

O. DWYER, S. KALISH,
M. MARESCA, P. TU

*J.P. Hartnett and T.F. Irvine, *AIChE Journal* 3, 313 (1957).

Fluoride Volatility Process

G. STRICKLAND

NITROFLUOR PROCESS DEVELOPMENT

The Nitrofluor process flowsheet for enriched U-Zr alloy reactor fuel consists of dissolution of an integral fuel assembly in anhydrous NO_2-HF solution, separation of the insoluble Zr salt from the soluble U salt, evaporation of the U-containing solution, fluorination of the residue with BrF_3, and purification of the UF_6 formed, by distillation. A solution containing 25 M% NO_2 is capable of dissolving a wide variety of fuel element materials, at satisfactory rates, over the temperature range 100° to 200°C. Variations in the process are necessary for low enrichment fuels. Current work is being conducted in laboratory scale equipment using up to 10 g fuel element material. Bench scale equipment capable of handling up to 100 g material has been constructed and is in the final stages of testing. Experiments pertinent to three types of fuel are described below.

Volatilization of Uranium From Bulk Zr Salt

The present flowsheet for processing enriched U-Zr fuel calls for separation of the complex Zr and U salts based on solubility. Although the salt solubilities are comparable, the high Zr:U ratio results in precipitation of nearly all of the Zr salt. Since the Zr salt settles rapidly, decantation has served as a simple means of separation, and several washes have been used to obtain high U removal. The following experiment was performed to determine the feasibility of eliminating the decantation-washing steps.

A small section of alloy fuel plate (3.3571 g containing 75.5 mg U) was dissolved in 20 ml 25 M% NO_2 – 75 M% HF solution for one hour at 100°C. The solution was evaporated to dryness over a one-hour period and the salts were further treated for three hours at 150°C, thus decomposing the complex salts to the normal fluorides. These were contacted with 10 ml BrF_3 for one hour at 121°C, after which all volatile material was evaporated and condensed. The treatment was repeated twice and the combined condensates were hydrolyzed in 1.6 N HNO_3 prior to analysis. A total of 82% U was volatilized with the BrF_3 and the remainder was found in the Zr salt. Future studies will consist of varying the treatment conditions to improve UF_6 volatilization.

Plutonium Behavior

Complex Pu salt produced by the dissolution of U-Pu alloy in NO_2-HF solution was previously shown to be soluble in that solution, even in the presence of complex Zr salt formed from Zircaloy-2 used to simulate cladding.

The conversion of complex U and Pu salts to volatile hexafluorides with fluorine was undertaken in the absence and in the presence of complex Zr salt. In each case, dissolution, evaporation, fluorination, and volatilization steps were performed starting with U-Pu alloy containing 0.056% Pu. No attempt was made to separate Pu from U.

A 0.6-g piece of the alloy was dissolved in 25 ml 25 M% NO_2 – 75 M% HF solution over a six-hour period at 103°C (100 psig). A 1¼-in.-diam Kel-F dissolution tube was used in order to minimize the interference of any corrosion product during the subsequent evaporation step. The salts were vacuum dried for five hours and then transferred manually to a Monel fluorination tube. Following evacuation, the tube was heated to 300°C for one hour to decompose the complex salts. The decomposition vapor was condensed in a liquid nitrogen cold trap. F_2 was admitted to the evacuated system to a pressure of 610 mm Hg absolute. The reaction tube was heated to 375°C for 6½ hr and the attached condenser was cooled in a bath of trichloroethylene and dry ice. A deposit of white salt collected in the bottom of the condenser tube.

The salt was dissolved in 1 N HNO_3 for analysis. The fluorination tube, which contained a slight amount of green corrosion product, was washed

Table 5

Pu-U Volatility after Alloy Dissolution and Salt Fluorination

	Plutonium, μg	Uranium, mg
Weight dissolved	332.8	594.4
Dissolution tube residue	96.3	83.5
Transferred to fluorination tube	236.5	510.9
Volatile fluoride	155.8	459.3
Fluorination tube residue	21.2	2.3
Total in fluorination apparatus	177.0	461.6
Percent volatilized	88.0	99.5
Material balance: (total found ×100/original amount)	82.2	91.7

with 1 N HNO_3 to recover the nonvolatile Pu and U. The dissolution tube was similarly flushed in order to obtain a material balance. The data are summarized in Table 5.

Of the material transferred to the fluorination tube, 88.0% of the Pu and 99.5% of the U were volatile after fluorination. The over-all material balance showed that 82.2% of the Pu and 91.7% of the U were accounted for. The lower values for Pu were probably due to the fact that it was present in microgram amounts.

A similar experiment was performed in the presence of ZrF_4, which is the decomposition product of the complex salt produced by the dissolution of Zircaloy-2. A 0.5-g piece of alloy (0.056% Pu) and a 120-mg piece of Zircaloy-2 were dissolved in 25 ml 25 M% NO_2 – 75 M% HF solution at 100°C. The solution was evaporated and the dry salts were transferred to the fluorination tube where they were decomposed *in vacuo* at 350°C for one hour. Fluorine was admitted to a pressure of 700 mm Hg abs, and the vessel was heated to 385°C for seven hours. Fluorine was added twice to maintain the original pressure. A condenser tube connected to the reaction vessel was cooled with dry ice in trichloroethylene to collect the volatile hexafluorides.

White UF_6 powder was found in the condenser tube, and a gray powder, presumably ZrF_4 containing corrosion product, was found in the reaction tube. Both samples were dissolved separately in 1 N HNO_3 and submitted for Pu and U analysis. The reaction vessel contained 73% of the Pu nominally present in the original sample; only 15% was collected as volatile Pu in the condenser tube. An additional 8% was found in the transfer line, bringing the total to 96% of that expected. A negligible amount of U was found to be nonvolatile.

It appears that most of the PuF_4 was not contacted with F_2 due to inclusion by the ZrF_4 particles formed during evaporation. This behavior will be checked at a lower Zr:Pu ratio.

Uranium Extraction From Uranium Carbide Fuel

A new fuel, uranium carbide in graphite, was tested for dissolution behavior in 25 M% NO_2 – 75 M% HF solution using a ¼-in. cube of fuel (3.5% UC). At the end of four hours contact at 190°C the cube had disintegrated to a fine powder. A second cube was disintegrated in fresh solution during a six-hour period at 260° to 270°C in order to check U removal from the graphite matrix. The decanted solution was hydrolyzed in 1.6 N HNO_3 and analyzed; it contained 83% of the U expected. The graphite residue was boiled in concentrated HNO_3 for one hour and filtered prior to analysis. It contained an additional 4% U. Of the total U found 95% was in soluble form.

A third cube was disintegrated in a 17 M% NO_2 – 83 M% HF solution over a four-hour period at 193°C. The solution, which was filtered through a 5-μ Monel filter, contained 89% of the U expected. Three subsequent two-hour contactings with fresh solution at 163°C extracted 17, 5.7, and 1.4% more U, respectively. A review of the experiment indicated that the yield of 113% was most probably due to high U content in the cube rather than analytical error or equipment contamination.

These results show that high U recovery can be achieved by repeated contacts of the residue with fresh NO_2-HF solution. Future work will consist of checking U extraction in the presence of cladding material.

Disintegration of Pyrolytic Graphite

Pyrolytic graphite shows promise of application in high temperature reactor fuel because of its exceptional anisotropic strength, thermal conductivity, and electrical conductivity. The behavior of a thin specimen prepared at BNL was determined in a 25 M% NO_2 – 75 M% HF solution. The rectangular specimen was 34.9 mil thick and weighed 35.3 mg. After it was immersed for one hour at 195°C, the specimen decreased 77% in thickness and 88% in weight. It appears that this material could be readily disintegrated in a NO_2-HF solution at a rate of approximately ½ mil/min.

Volatility Studies Laboratory

The design of a new laboratory building for engineering scale fluoride volatility studies was completed and submitted for bids. It is expected that construction will begin late this year and be complete one year later. F. Horn

MISCELLANEOUS STUDIES IN NO_2-HF SOLUTION

Effect of Gamma Radiation on Zircaloy-2 Dissolution

The dissolving power of irradiated NO_2-HF solution was checked using the 20-ml sample pre-

viously subjected to a total gamma dose of 6.8×10^8 rad over a four-month period. Although a small vapor sample from the 27 M% NO_2 – 73 M% HF solution was identified as N_2O by infrared analysis, the liquid subsequently liberated brown NO_2 fumes, and dissolved a specimen of Zircaloy-2 at an undiminished rate. Additional studies are planned when a source of greater strength is available.

Solid-Liquid Phase Diagram

Freezing point data were taken for NO_2-HF solutions in an attempt to determine the reactive species of interest in the Nitrofluor process.

The solutions were prepared by mixing measured volumes of pure NO_2 and pure HF at room temperature in a closed Monel system. The Monel cooling tube contained approximately 30 ml of solution and was provided with a needle thermocouple. The tube was mounted on a shaker and was cooled by liquid nitrogen in a Dewar flask. A Teflon sleeve was used around the tube to provide a satisfactory cooling rate. During most runs the cooling rate was 4°/min; the highest rate was 12°/min. Temperature-time plots were obtained with a recording potentiometer and changes in the cooling rate were obtained at the phase transition points. Some of the changes were barely discernible. In general, the melting points differed from the freezing points by a few degrees. A plot of the freezing points is shown in Figure 11.

A eutectic point was found at 10 M% NO_2 (−144°C); an incongruent point was evident at 20 M% NO_2 (−52°C); and compound formation was indicated by the maximum at 30 M% NO_2 (−26°C). Above 44 M% NO_2 the liquid separated into two phases at room temperature and miscibility did not occur at temperatures as high as 80°C.

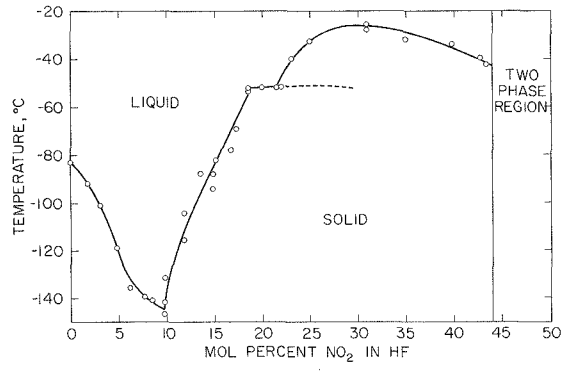

Figure 11. Freezing points of NO_2-HF mixtures.

The incongruent point could indicate another maximum, at 25 M% NO_2, hidden by the higher freezing point compound at 30 M%. It may be important to note that the incongruent composition is equal to that found by analysis for the high boiling residue previously observed during batch distillation. It was also noted that prepared solutions close to the eutectic composition exhibited a minimum vapor pressure. F. Horn

DISSOLUTION OF ThO_2-UO_2

In an attempt to find a solvent for sintered ThO_2-UO_2 fuel material, which does not react with the Nitrofluor solvent, mixtures were made up of BrF_3 with various additives: Sb_2O_3, B, CsCl, KCl, and TeO_2, each of which reacts with BrF_3 to form the corresponding fluoride. None of these mixtures reacted with ThO_2-UO_2 at a satisfactory rate. Similar negative results were obtained with SbF_5, SbF_5+HF, $NOSO_3F$, SbF_5+BrF_3, HPO_2F_2, and the last-named with additions of KF, HF, $SbCl_5$, or H_2O. R. Johnson

SPECTROSCOPY OF NO_2-HF

Work is in progress at the University of New Hampshire on the absorption spectra of NO_2-HF, under research subcontract S-522; Professor H.M. Haendler is in charge. Particular attention has been given to the infrared spectra of the vapors of NO_2, HF, and mixtures of the two. Even in the vapor state there is a definite interaction between the two compounds, or their polymers, as shown by the shifting of certain absorption bands and the appearance and disappearance of others. Observations were complicated by the fact that the spectra of mixtures change with time; whether this results from a slow gas-phase reaction or from a reaction between a gaseous species and one of the solid surfaces present (nickel, brass, or silver chloride) is not yet clear. At present a cell suitable for liquid mixtures is being developed.

Radiochemical Technology

B. Manowitz

LONG-LIVED NUCLIDE REMOVAL

Studies on the removal of Cs and Sr from synthetic radiochemical waste solutions have contin-

ued. The effect upon extraction coefficients of concentration of waste solutions and the use of complexing agents other than sodium nitrate, such as gluconic acid for aluminum, ferric, and other cations was studied.

In a sixteen-stage Mini-mixer-settler run, Cs was removed from concentrated TBP-25 type waste adjusted to a *p*H of 6.6. Sodium citrate was added as complexing agent. Mercuric ion was complexed by iodide ion. Cesium polyiodides were extracted into 0.2 *M* I_2 in nitrobenzene. Each phase had a flow rate of 1 ml/min at ~27°C. 190 ml of feed solution (6×10^{-4} *M* in $CsClO_4$ and containing 35 mC Cs^{137}) was processed in the mixer-settler until ~ 98% of the Cs^{137} activity had passed through the bank. The ratio of Cs^{137} activity in the organic phase effluent to that in the aqueous phase effluent was 1.1×10^6. Increased stage efficiency would have resulted in a much greater ratio.

L. SLATER

CHEMICAL REPROCESSING STUDIES

Laboratory and engineering scale effort continued during this period on the development of a suitable head-end dissolution step for naval reactor cores.

Studies on the Zirflex process (6 *M* NH_4F, 0.5 *M* NH_4NO_3) have shown that laboratory dissolution rates can be obtained on an engineering scale by using a boil-off type dissolution with a rate of about 6.5 lb/hr-ft² of fuel module. Hydrogen peroxide oxidation of U(IV) to U(VI) on an engineering scale was confirmed.

Studies on the modified Niflex process (HNO_3 and HF mixture) have indicated that corrosion rates during dissolution are sporadic against type 309 SCb stainless steel. Corrosion rates have averaged about 45 mil per year with rates of 250 mil per year being measured over a single cycle. Total exposure time on the test coupons was 61 hr or 6 dissolution cycles. C. PIERCE

OXIDE REDUCTION

Studies of reaction rate in the uranium oxide-calcium amalgam system have continued. No reduction of sulfated feed-material UO_3 has been observed over a 9-day run period at 300°C. This contrasts with several earlier results; however, latest experiments have utilized a more reliable sampling technique. The possibility that an induction period to reduction exists will be investigated in further work. Equilibrium studies have been set up in a salt heated rotating sampler assembly.

Galvanic cell measurements have been initiated. A suitable nonaqueous solvent for calcium amalgam activity measurements is under investigation. Apparatus for the study of reaction between calcium amalgam and various pure gases is being constructed. L. ADLER

HIGH TEMPERATURE PHYSICAL PROPERTY MEASUREMENTS

Construction of the inert argon arc has been started. Calibration of the micro-optical pyrometer and the two-color temperature meter with the use of the NBS calibrated lamp was completed. A method for measuring the true temperature using a combination of optical and two-color temperature measurements is being developed. An area is being set up to erect the x-ray diffraction equipment with a high temperature camera for making measurements up to 2000°C. M. STEINBERG

RADIATION PROCESSING PROGRAM

A series of experiments on the nitrous oxide gas dosimeter in a Co^{60} gamma field was completed. Preliminary results of irradiation of N_2-O_2 mixture at room temperature and pressures up to 12 atm in glass vials in a Co^{60} source indicated *G*-values for NO_2 formation ranging from 0.9 to 1.6. Irradiation of N_2-O_2 mixtures at pressures up to 68 atm and 538°C in stainless steel vessels indicated that part of the nitrogen was fixed on the walls of the vessel and part as NO_2 in the gas phase. Effect of some solid surfaces on the N_2-O_2 reaction was investigated. Preliminary results indicate that Al_2O_3 tends to increase the *G* (NO_2) value. BNL 612 (June 1960)on the gamma-irradiation experiments in the N_2-O_2 system was completed.

Survey gamma irradiation experiments in the NH_3-H_2O system indicated the formation of hydrazine. The yield increases with increasing ammonia concentration but then decreases beyond 65%. A maximum *G* (N_2H_4) of 0.28 has been obtained to date. This effect is being further investigated. Presence of oxygen in the system tends to markedly decrease the yield. BNL 613 (June 1960) was completed on the work performed to date in the system. M. STEINBERG, P. COLOMBO

RADIATION ENGINEERING

Research Food Irradiator

Approximately 26,000 C Co^{60} encapsulated in stainless steel tubes have been received from Oak Ridge to be used for the Research Food Irradiator. Preliminary integrity tests are being conducted on the sources as well as dose distribution tests in water. The source racks, frames, and tank are in the process of being built and assembled.

Co^{60} Low Level Studies

Additional Co was irradiated in the BNL reactor and a uniform slab of about 4×5 ft was assembled. The scintillation dosimeter required redesign and rebuilding because of inadequacy of the ¾-in. photomultiplier tubes resulting in high dark currents and low sensitivity at normal operating voltages. Anthracene crystals are being grown to replace the inefficient plastic phosphor in the original instrument.

Thermoluminescent Dosimeter

Forty-eight different calcium fluoride, manganese activated phosphors have been synthesized. An instrument is being built to read the light output of the dosimeter. O. KUHL, L. GALANTER, F. RIZZO

HIGH INTENSITY RADIATION DEVELOPMENT LABORATORY

Work with AMF on HIRDL has been completed. Final drawings were submitted by Barnes and Roe. Bids are currently being received on the construction of the facility.

Chloride-Fluoride Volatility Process Studies

L. HATCH

In the reprocessing of spent solid fuels from nuclear reactors by volatilization processes, one of the major problems is the removal of heat from the highly exothermic reactions. The problem is compounded because of the elevated temperature required, the high reaction rates, and the low heat capacities of the gaseous effluents. It has been demonstrated that it is possible to use a fluidized bed of inert granular solids, making use of the heat capacity and the heat transfer properties of fluidized beds, in order to control such exothermic reactions. Thus, the fluidized bed is used in the same sense that liquids, in the form of molten salts, interhalogens, etc., are used, without the introduction of the problems encountered in the use of such liquids.

ZIRCALOY HYDROCHLORINATION

Pilot Plant Studies

A series of three experiments was carried out to determine the effect of length (or surface area) of fuel element sections upon reaction rate and the conversion of HCl. The samples were 14 plate, Navy type, fuel element subassemblies, cut in lengths of 5, 10, and 15 in. respectively. These were box-type elements open only at the two ends. Results are presented graphically in Figures 12 and 13.

In another experiment, a 15-in. section of a 14 plate subassembly was completely reacted in about three hours. Figure 14 plots the progress of the reaction in terms of percent of unreacted sample *vs* time. J. REILLY, W. REGAN

Laboratory Studies

A number of variables were studied in the 1½-in.-diam laboratory reactor. The bed, except as noted, consisted of 60 mesh Al_2O_3 about 12 in. in depth. Samples were coupons (3¼×⅞×⅛ in.) cut from a Zircaloy-clad fuel plate.

The velocity of the fluidizing gas appears to affect the reaction rate and percent conversion to a considerable extent as shown in Figure 15. It would also appear that under the conditions specified, a superficial velocity of 0.6 to 0.7 ft/sec is optimum.

The effect of sample length was also studied with respect to reaction rate and conversion of HCl and the results are shown in Figure 16.

A series of experiments investigating the effect of bed particle size upon reaction rate and conversion of HCl was carried out. In these experiments the bed material consisted of silica sand, since a wide range of particle sizes was available. The fluidizing gas velocity was that which appeared to result in "good" bed fluidization and was, therefore, different for each particle size. Results are shown in Figure 17. J. REILLY

Uranium Fluorination

The experimental study establishing conditions for U recovery from inert beds of alumina has

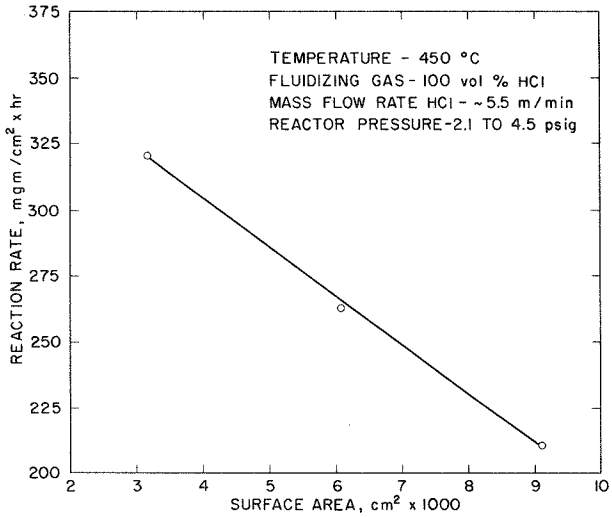

Figure 12. Surface area *vs* reaction rate, Pilot Plant.

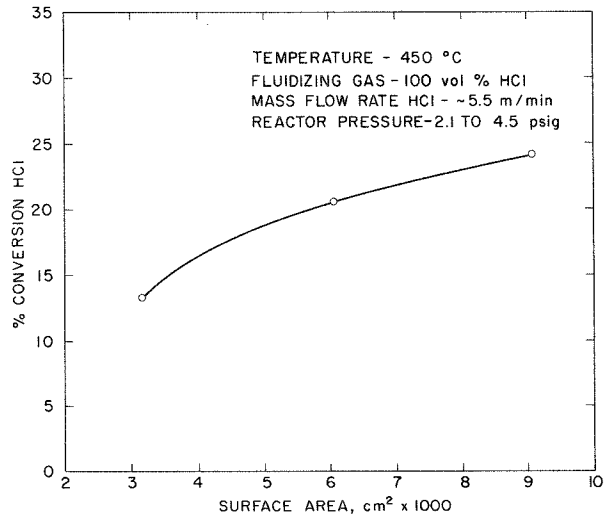

Figure 13. Surface area *vs* % conversion HCl, Pilot Plant.

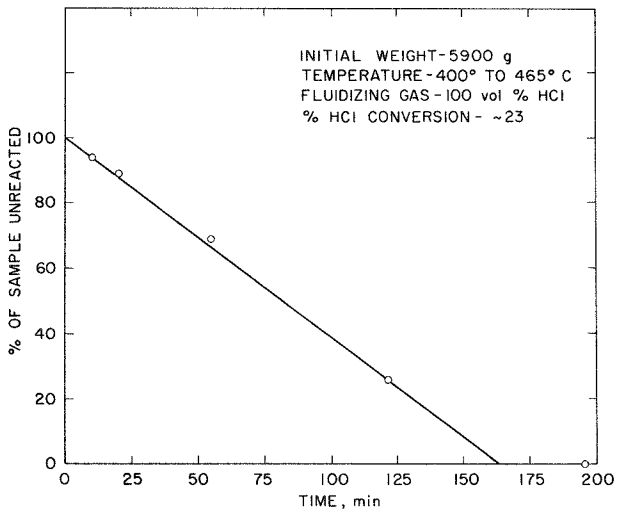

Figure 14. Hydrochlorination of 15-in. section of Zircaloy-clad, navy type element.

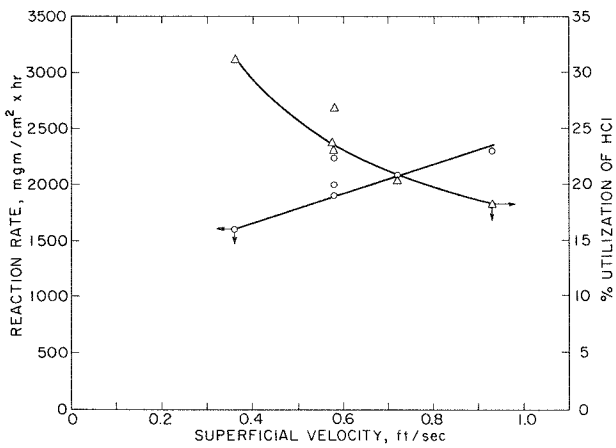

Figure 15. Superficial velocity of fluidizing gas *vs* reaction rate and % utilization of HCl.

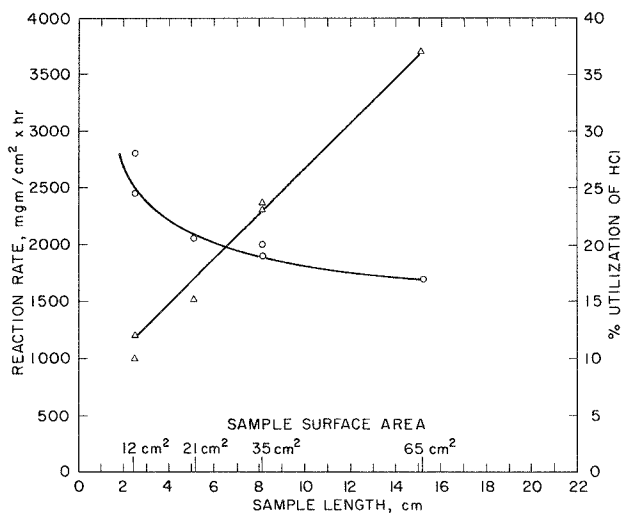

Figure 16. Sample length *vs* reaction rate and % utilization of HCl.

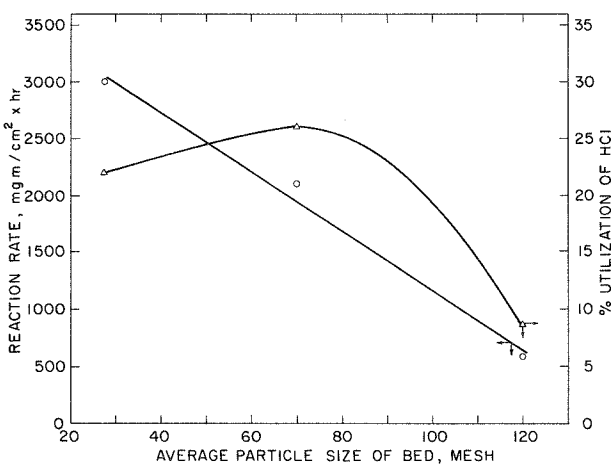

Figure 17. Particle size *vs* reaction rate and % utilization of HCl.

been continued (see BNL 595). It has been found that at temperatures of 300°C and 23% excess fluorine, U recovery from alumina beds seeded with UCl_3 (1 to 10 g) is quantitative. However, quite different results were obtained in experiments concerned with U recovery from Zircaloy fuel coupons. The procedure consisted of hydrochlorinating the Zircaloy coupon to completion and contacting the residue remaining in the inert bed with fluorine. Results of these experiments are shown in Table 6. The low U recoveries obtained indicate that the UCl_3 seeded bed experiments are not representative of the behavior of the U remaining in the bed after hydrochlorination of Zircaloy fuel and the quantitative recovery of U will have to be studied using actual fuel element coupons. E. WIRSING, J. REILLY

Chlorination of Stainless Steel

Scouting tests carried on at BNL early in this program indicated that Cl appeared promising for use as a reactant in the decladding stainless steel clad fuels. However, as shown in BNL 554, reaction temperatures of the order of 650°C are required for practical rates. This presents a serious problem with respect to corrosion of the reactor vessel. However, though a fluidized bed is a good heat conductor, the same bed in the settled state is a good heat insulator and it should be possible to establish the condition wherein the major portion of a settled bed is held at a much higher temperature than the container vessel. This temperature difference can be brought about by 1) fluidizing the bed and heating to the high temperature, 2) discontinuing fluidization, and 3) cooling the vessel to the lower temperature. Even with small (1½ in. diam) beds large temperature differentials may be produced and maintained for considerable periods of time with this technique. In the case of decladding stainless steel clad elements, wherein very high reaction temperatures may be required and only relatively small amounts of metal are involved, the central problem is no longer the control of the exothermic reaction itself but rather the maintenance of a large temperature differential between zone and the reactor vessel.

With the foregoing principles in mind, an experiment was carried out on the chlorination of a 316 SS coupon (11 g, 18 cm^2 in area) in a 1½-in.-diam Ni vessel. The temperature of the bed (silica sand) was first raised to 700°C (bed fluidized) and the vessel walls then cooled to 510°C (bed settled). At this point, 100% Cl was passed through the bed at a low rate so that the bed remained static. The run was continued for a period of 5 min at the end of which the bed temperature had dropped to 620°C and the wall (insulation removed) temperatures to 480°C. Even with the lower bed temperature, the reaction rate did not appear to fall off as noted by the deposition of $FeCl_3$ in a glass condenser. The over-all reaction rate was found to be 1240 mg/cm^2 × hr which is equivalent to a penetration rate of about 60 mil per hour. The attack was essentially uniform over the entire coupon. No attack on the reactor itself was evident upon visual inspection after the experiment. This method of high temperature decladding would seem to be applicable to spent fuel elements provided the fuel material itself is not attacked and removed in the decladding step, as a prelude to reprocessing by the inert fluidized bed method. J. REILLY, W. REGAN

Table 6

Uranium Recovery from Zircaloy Fuel Tabs
Fluorination Cycle

(60 mesh alumina bed, approx 500 g)

Experiment No.	Weight of U in bed, g	% F_2 in reactant gas	Gas flow rate, L/m	Temperature, °C	Elapsed time, min	% U recovered	Remarks
1	0.539	90	0.5	400	15	18.2	Not fluidized.
2	0.450	90	0.5	400	15	20.0	" "
2A	Remainder from experiment No. 2	100	5.0	400	10	85.1*	Fluidized.
3	0.420	100	5.0	450	3	58.5	"
4	0.494	100	5.0	450	3	48.6	"

*Total recovered in experiments 2 and 2A.

Ultimate Waste Disposal

L. HATCH

ION EXCHANGE STUDIES

As reported previously, one of the major problems in the development of the ion exchange process has been the interference due to the relatively large concentrations of nonradioactive ions in the wastes. Recently methods have been studied for suppressing such bulk ion interference in the processing of Purex type waste by absorption and fixation on mineral ion exchanger materials.

By taking advantage of proposed modification in Purex waste processing, such as the substitutions of U^{+4} and NO for $Fe(NH_2SO_3)_2$ and $NaNO_3$, formaldehyde destruction of HNO_3 and the use of titanium evaporators to reduce corrosion, bulk ions may be very considerably reduced. However, even with these reduced amounts of the bulk ions, low decontamination factors for the fission products would result when the solutions were passed through columns of mineral exchanger such as clinoptilolite or montmorillonite. One of the major difficulties arises when the *p*H of the solution increases as it flows through the column thereby causing precipitation of the corrosion products. Radioactive ions may adsorb on the $Fe(OH)_3$ colloids and pass through the column without being exchanged while large accumulated masses of the precipitate eventually cause plugging of the column.

Studies of methods of suppressing bulk ion interference have involved chelation and pretreatment of the ion exchanger to prevent the rise of *p*H as the solution moves through the column. Corrosion products form citric acid chelates of very high stability whereas Cs and Sr have little or no tendency to form such groups. Thus by the use of chelating agents, essentially all the corrosion products may be sequestered without the interference with Cs and Sr as independent cations. It is therefore possible to remove Cs and Sr by ion exchange from solutions containing bulk ions which remain in solution. The chelation step is beneficial in two ways in that it prevents precipitation and renders the bulk ion nonexchangeable.

In an attempt to determine the effect of temperature on the kinetics of Sr adsorption on clinoptilolite, four runs were made at 65°C using citric acid as a chelating agent in three runs, and the hydrogen form of clinoptilolite in the fourth run. With 1-ft columns of the exchanger the decontamination factors were 10^5 for the chelated system and 10^6 for the hydrogen clinoptilolite; the throughput was 57 column volumes in each case. Since the amout of Sr present in the effluents was thus reduced by large factors, the matter of iso-

Influent Solution	Citrate Conc.	Influent Activity d/m/ml Sr^{90}	Temp.	Column Length	Volume Passes	Composite Effluent Activity d/m/ml	Composite D.F.	Total D.F.
#1 Purex Type	.0065 m	$1x10^7$	65°	1 ft.	3.8 L	18.8	$5.5x10^5$	
#1 Effluent to $2.3x10^{-4}$m Sr with inactive Sr	"	$6.8x10^4$ d/m/ml Sr^{90} added	65°	1 ft.	3.8 L	10.4	$6.5x10^3$	$3.25x10^9$
#2 Purex Type	.007 m	$9.73x10^6$	65°	1 ft.	3.8 L	13.8	$7.0x10^5$	
#2 Effluent to $2.3x10^{-4}$m Sr with inactive Sr	"	$5.35x10^4$ d/m/ml Sr^{90} added	65°	1 ft.	3. L	7.7	$7.0x10^3$	$5.0x10^9$
#3 Purex Type	.00825 m	$8.7x10^6$	65°	1 ft.	4.1 L	67.5	$1.3x10^5$	
#3 Effluent to $2.3x10^{-4}$m Sr with inactive Sr	"	$5.48x10^4$ d/m/ml Sr^{90} added	65°	1 ft.	4.1 L	4.4	$1.25x10^4$	$1.6x10^9$

Figure 18. Citric acid treated waste solutions.

topic dilution as a means of obtaining further decontamination by ion exchange was investigated. As indicated in Figure 18, the composite from the citric acid experiments were respiked and inactive Sr was added to give the original Sr concentration of 10^{-4} molar. These solutions, after standing one week, were then passed through a second 1-ft column of clinoptilolite (65°C) and the decontamination factors were about 10^3. There is obviously a question involved here as to whether complete equilibrium was attained between the chelated Sr which had passed through the first column and the inactive Sr which was added. However, the results indicate that considerable advantage may be realized through the use of the isotopic dilution technique as a final step in the ion exchange process.

Returning to the hydrogen clinoptilolite, Figure 19 shows that with a single 1-ft column (65°C) the decontamination factor for Sr was of the order of 10^6 with a throughput of 57 column volumes. Again the composite effluent was respiked (no inactive Sr was added) and passed through a second 1-ft column. It should be noted that the amount of Sr^{90} added to the respike was only about one-tenth that of the total Sr present so that there was no appreciable buildup in the Sr concentration. Combining the decontamination factor from the first column, 2.0×10^6, with that of the second column, 3.2×10^3, gives an over-all value of 6.4×10^9 for the two 1-ft columns. Although Cs and Sr are exchanged to a very high degree in these systems, Y and the rare earths, as represented by Ce, remains in solution under the low *p*H conditions. Further experiments are indicated in which sufficiently high activities are used in the original feed solution so that the respike is not necessary. Only in this way could one determine whether the high decontamination factors shown are realistic.

E. TUTHILL, G. WETH

GLASS PREPARATION

The process steps required in forming glasses and other ceramic bodies containing the fission products with the raw liquid waste, although simple enough in principle, present a somewhat complex problem in the design of process equipment. For example, the blending of fission products with the glass forming additives, either before or after the removal of water, the decomposition of nitrates and other salts, and the transfer of heat to the system, all become matters of concern in the design, operation, and maintenance of plant equipment. However, if the glass forming material were introduced as a liquid which remained stable at suitable temperatures so that rapid volatilization of the water and consequent concentration of the waste products occurred without the usual accumulation of solids residue, the first phase of the glass making process would be considerably simplified. In other words, bumping during evaporation due to excessive temperature gradients and poor blending of the solid components would not be a problem with an all-liquid system. Phosphoric acid seems to be suitable for this purpose in that the raw liquid waste can be added directly to the boiling acid and the entire concentration and denitration step carried out in the liquid medium. Phosphoric acid dissolves or otherwise reacts, possibly by complex formation, with the waste components so that no solid formation or stratification of ingredients occurs when evaporation and denitration proceeds at temperatures ranging from about 120° to 300°C. At the end of the denitration step, the product, now in a thickening state, becomes a homogeneous green glass upon heating to a temperature of 1100°C. The glass is free of bubbles and has a density of approximately 2.9. Sulphates are apparently decomposed during the final heating stage.

Influent Solution	Citrate Conc.	Influent Activity d/m/ml Sr^{90}	Temp.	Column Length	Volume Passes	Composite Effluent Activity d/m/ml	Composite D.F.	Total D.F.
Purex Type	0	8.8×10^6 d/m/ml Sr^{90}	65°	1 ft.	3.8 L	4.4	2.0×10^6	
						↓		6.4×10^9
Effluent	"	1.14×10^4 d/m/ml Sr^{90} added	65°	1 ft.	3.8 L	3.5	3.2×10^3	

Figure 19. Hydrogen form clinoptilolite.

Sample	Volume Reduction	H_3Po_4 Grams	Oxides from Waste Grams	Leach Solution	% Leached 5 days	11 days	21 days	30 days	44 days
Unground (surface area ~20 cm^2)									
A	~500	72	10	H_2O	7.0×10^{-2}		0.82	1.4	2.4
B	~500	72	10	HNO_3*	4.8×10^{-2}		0.54	0.84	1.4
C	~800	72	20	H_2O		5.5×10^{-2}	0.29		
D	~800	72	20	HNO_3*		0.13	0.43		1.0
E	~1000	72	30	H_2O	ND**		4.2×10^{-3}	3.9×10^{-3}	7.94×10^{-3}
F	~1000	72	30	HNO_3*	ND		2.1×10^{-3}	8.5×10^{-3}	9.7×10^{-3}
G	~1100	72	40	H_2O		ND	ND		ND
H	~1100	72	40	HNO_3*		ND	ND		ND
Ground (through 35 on 45 mesh)									
E′	~1000	72	30	H_2O		7.8×10^{-2}	6.9×10^{-2}		5.65×10^{-2}
				HNO_3*		7.3×10^{-2}	0.10		8.4×10^{-2}
G′	~1100	72	40	H_2O			2.1×10^{-2}		
				HNO_3*			2.1×10^{-2}		

*pH 4.0
**ND - none detectable

Figure 20. Phosphate glasses made with simulated future Purex waste containing Sr^{90} tracer.

Sample	Volume Reduction	H_3Po_4 Grams	Oxides from Waste Grams	Leach Solution	% Leached 11 days	20 days	30 days	44 days
Unground (surface area ~20 cm^2)								
A	~ 800	72	20	H_2O	0.36	1.1		1.4
B	~ 800	72	20	HNO_3*	0.32	1.23		1.9
C	~ 1000	72	30	H_2O	ND**	ND	ND	ND
D	~ 1000	72	30	HNO_3*	ND	ND	ND	ND
E	~ 1200	72	50	H_2O	ND	ND	ND	ND
F	~ 1200	72	50	HNO_3*	ND	ND	ND	ND
Ground (through 35 on 45 mesh)								
C′	~ 1000	72	30	H_2O	ND	ND		6.4×10^{-2}

*pH 4.0
**ND - none detectable

Figure 21. Phosphate glasses made with simulated Purex wastes containing Ce^{144} tracer.

Sample	Volume Reduction	H_3Po_4 Grams	Oxides from Waste Grams	Leach Solution	% Leached 5 days	11 days	21 days	30 days	44 days
Unground (surface area ~20 cm^2)									
A	~160	72	29	H_2O	ND**	ND	ND	ND	ND
B	~160	72	29	HNO_3*	ND	ND	ND	ND	ND
Ground (through 35 on 45 mesh)									
A′	~160	72	29	H_2O	ND	ND	ND	ND	ND

*pH 4.0
**ND - none detectable

Figure 22. Phosphate glasses made with simulated present day Purex wastes containing Ce^{144} tracer.

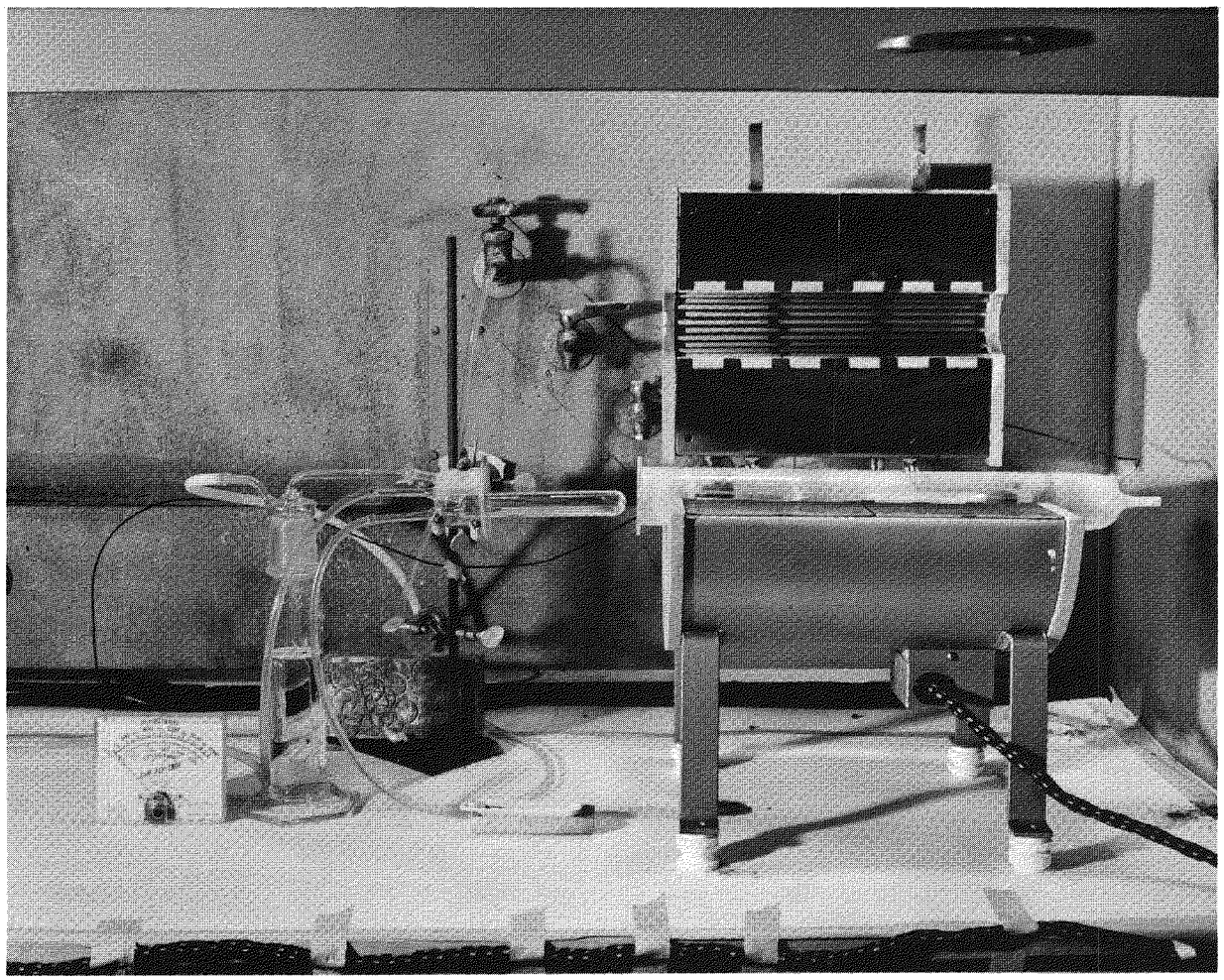

Figure 23. Apparatus for studying Cs volatility.

In recent months, a number of phosphate glasses have been made with various concentrations of representative waste products and a program of leaching is now under way. Up to this point, studies on the phosphate glasses have emphasized the elements of simplicity in carrying out the process steps for the entire glass forming operation rather than the quality of high stability in the final product. Stability of product, however, must be considered a matter of first importance if the principle of ultimate disposal by fixation in solids is maintained. A few results of preliminary leaching tests have been obtained for periods of up to 90 days duration (Figures 20, 21, and 22). Since Ce is not readily leached from glasses, its removal by the liquid may be taken as an indication of the solubility of the glass itself.

Since the problem of volatilization of Cs and Ru is encountered in all high temperature waste processing, a preliminary study in this regard has been made in connection with the formation of phosphate glasses. Figure 23 shows the equipment in which Cs volatilization experiments were conducted. These experiments involved glass samples of the order of 5 g and showed that some 0.4% Cs was volatilized after 4 hr at 1100°C.

It has been estimated that volume reductions from the raw waste to the glass product by factors greater than 160 would pose serious decay heat removal problems. Assuming a core temperature of 400° and outside wall temperatures of 100°C, glass cylinders 6 in. in diam and 5 ft long are indicated.

E. Tuthill, G. Weth, W. Regan

Hot Laboratory Division

L.G. STANG JR.

Radioisotopes Development

W.D. TUCKER

YTTRIUM-90

Dowex-50, the resin used in the Brookhaven Y^{90} generator, is no longer commercially available, and has been replaced with Dowex-50-W by the manufacturer. To test the milking system under conditions which simulate actual usage, a column of the new resin loaded with 100 mC Sr^{90} will be milked once or twice a week. Thus far, assays of early milkings have shown considerably less Sr^{90} contamination than corresponding ones obtained in the past with the older-type resin, which indicate that the new resin, thus far, is performing even better than the old. Y^{90} elution curves are similar for both resins. R. DOERING

CALCIUM-47

$Ca^{46}(n,\gamma)Ca^{47}$ Szilard-Chalmers Reaction

Calcium Phthalocyanine. The proposed use of calcium phthalocyanine (Ca-Pc) as a possible target for the Szilard-Chalmers production of Ca^{47} involves irradiating the Ca-Pc, dissolving it in 30% oleum, reprecipitating the Ca-Pc with ethyl acetate, and extracting the recoiled ionic Ca^{47} from the aqueous layer by carrying it on $Fe(OH)_3$. Contrary to earlier results, this sytem apparently produces some chemical decomposition of the Ca-Pc although no correlation could be found between decomposition and either the strength of the acid or the length of contact time with the acid.

Subsequently, the infrared absorption spectra were examined for Ca-Pc, free phthalocyanine (H_2-Pc), and Li_2-Pc, as well as for thenoyltrifluoroacetone (TTA) and the calcium complex of TTA. Distinguishing peaks were found for each compound, and from this study it is concluded that the Ca-Pc which has been used has had little, if any, free H_2-Pc in it.

Tracer techniques will be used to study the chemical reaction between Ca-Pc and other reagents by repeating the work with Ca-Pc labeled with Ca^{47}. To this end, some Ca^{47} tracer was made by irradiating purified CaO. An examination of the gamma spectrum of the material produced revealed no Na^{24} contamination which indicated that the CaO is suffiiently pure for these purposes.

The preparation of Ca-Pc by mixing a solution of Ca-TTA in alcohol with an alcoholic solution of Li_2-Pc was found to be much easier than previous methods of preparation, which involved anhydrous $CaCl_2$ as a starting material. A. WEISS, M. HILLMAN, E. YELLIN, J. DAANE

Calcium-TTA. The thenoyltrifluoroacetone complex of calcium (Ca-TTA) is also being studied as a possible target for the Szilard-Chalmers production of Ca^{47} using two different approaches. In the first approach solid Ca-TTA is irradiated, then dissolved in cyclohexanone from which solution ionic Ca^{47} is then extracted with water. Inasmuch as early experiments gave inconsistent results, an extensive experiment was performed to test the reproducibility of the extraction method and also of the method of analysis. The experiment, which involved determining the amount of Ca extracted by distilled water and by 2 N HCl, indicated that a single extraction of cyclohexanone containing Ca-TTA by an equal volume of reagent removes 1) 99% of the extractable Ca when 2 N HCl is the reagent, 2) 5.3% of the Ca when H_2O is the reagent, and 3) the combined reproducibility of the method of analysis together with the extraction procedure was good. Subsequent use of this procedure gave an average enrichment factor of 1.40 ± 0.24. This is too small a value to be of practical importance, and, although the data are the most precise obtained thus far, the enrichment factor is too close to unity to be trusted. The reaction will, therefore, be repeated on a scale 10-fold larger in order to get better counting statistics. M. HILLMAN, J. DAANE

The second approach using Ca-TTA involved the irradiation of paper impregnated with Ca-TTA, eluting the unreacted Ca-TTA, leaving the recoiled Ca^{47} behind (as reported in BNL 595).

Two irradiations were made this period to test out the method. The first, performed at 200°C, decomposed the paper itself and possibly the material impregnated in it; furthermore, the paper was eluted with a mixture of benzene and ethyl alcohol and it was subsequently discovered that the alcohol might have dissolved some of the recoiled ionic calcium. Hence, it is not surprising that no Szilard-Chalmers reaction was observed. The second irradiation, performed at 50°C, apparently did not decompose the material. Analysis is in progress. R. DOERING

$Ti^{50}(n,\alpha)Ca^{47}$

Cross Section. The computed excitation function for this reaction, reported in BNL 595, indicated a maximum cross section of 4 to 8 mb at a neutron energy of 17.5 ± 2.0 Mev, and a cross section of 0.3 to 5.75 mb for 14-Mev neutrons. The cross section for this reaction at 14 Mev is being determined experimentally by irradiating in the nuclear reactor appropriate foils around which are pressed Li^6D. The use of Li^6D to produce 14-Mev neutrons has been discussed in previous progress reports and is further discussed in a separate subsection below. Pellets irradiated thus far have included foils of Ti and V. The known 30 mb cross section for the $V^{51}(n,\alpha)Sc^{48}$ reaction permits the V to serve as a monitor for the 14-Mev neutron flux produced by the Li^6D. Although this work has been hampered somewhat by disintegration of the foils and the presence of many gamma-emitting impurities, a very rough value of $10 \pm$ mb has been obtained. A more precise value will be determined. M. HILLMAN, E. YELLIN, J. DAANE

COPPER-67

Using enriched Ni^{64} and the $Ni^{64}(\alpha,p)Cu^{67}$ reaction, 2.7 mC Cu^{67} to be used in the study of Wilson's disease have been supplied. The material contained only about 7% Cu^{64} and negligible amounts of other radioimpurities. The 61-hr half-life of Cu^{67} was confirmed. The target was such as to intercept the entire 40-Mev alpha beam. "Thick target" yields of approximately 2 μC/μah were obtained. M. GREENE

IODINE-124

About a quarter of a millicurie of I^{124} was produced by the irradiation with 40-Mev alphas of a sample of antimony metal powder pressed into a 10-mil thick disc. The "thick target" yield was about 100 mC/mah. The I^{124}, separated chemically by previously published methods, contained no antimony impurity and only a small amount of $I^{123,125,126}$. Fabrication of an antimony target large enough to produce 10 mC I^{124} is under way. The I^{124} is to be used in iodinating blood proteins.

M. GREENE

SCANDIUM-47

Reagent-grade CaO has been shown to be suitable for use as a target material for production of millicurie quantities of Sc^{47} free of gamma-emitting impurities. R. DOERING, J. DAANE

ARGON-38

The method of production of high-purity, stable Ar^{38}, used as a standard for calibrating spectrographs which are used in geological dating, was outlined in BNL 595. A proposed method of assaying and determining the isotopic composition of the product Ar^{38} involved sealing an aliquot of the gas into a short length of glass capillary tubing which would then be melted within the mass spectrograph; the purpose of this technique was to introduce the argon sample into the instrument without loss and without contamination by atmospheric air. However, it was found that the glass itself from which the capillary was made contained normal atmospheric Ar occluded inside of it. When the glass was melted this Ar contaminant was introduced into the mass spectrograph and vitiated the results. Attempts to seal the Ar^{38} aliquot into a short length of Cu tubing, the ends of which were crimped shut, was unsuccessful because none of the crimps produced effective vacuum seals.

Hexachlorobenzene, a possibly better target than KCl for the production of Ar^{38}, crystallizes in fine needles. An attempt to grow larger crystals in order to minimize the loss of Ar^{38} by diffusion to the surface, resulted only in longer needles of about the same diameter. Meanwhile 98 g KCl were placed in the reactor for a 3-month irradiation at maximum flux. Eleven different institutions in six countries have expressed an interest in obtaining Ar^{38}. During this period shipments have been made to Germany, Canada, Australia, and New York. A. WEISS

POLONIUM-210 ALPHA NEEDLE

Preparation of a 5-mil diam W wire having a flat, square end on which is plated 0.005 μC Po^{210} was continued. To anchor the Po in place it must be covered by a metal plate which is thin enough (less than 10 μ) to permit the alphas to pass through it. The original work of Munro, who recommended covering the Po with a layer of Cr-Fe followed by a layer of pure Cr, could not be duplicated, but it was found that the needle could be covered by a plate of Cu followed by one of pure Cr.

The electron microscope was used successfully to measure the diameters of W wires which had been electroplated with Cu in one series and Cr in another series under conditions where only the length of plating time was varied. By subtracting the diameter of the bare wire from the plated wire, the thicknesses of the various plates were measured and from these data straight-line graphs were plotted correlating the plate thickness with the electroplating time. Thus, it is now possible both to control and to measure the thickness of these plates to within a few tenths of a micron for thicknesses of about 2 μ or more. R. DOERING

KRYPTON-83m

A method recently proposed for determining if a Stellarator is capable of containing a plasma involves using a radioactive gas to produce ions isotropically, eliminating current effects as a possible source of instability. To satisfy the requirements the radionuclide must be short-lived, emit only low-energy electrons, be available in relatively large amounts, and must be exceedingly pure. Kr^{83m} apparently is the only nuclide which can fulfill all of these requirements, according to the Project Matterhorn people who have proposed the idea. To be useful 3 to 4 C Kr^{83m} would have to be produced, the maximum time between reactor discharge and use at Princeton would have to be less than 4 hr, the Kr^{83m}/Kr^{83} ratio would have to be at least 0.1 at the time of use, and all other atoms other than those of Kr would have to be excluded. It is calculated that as much as 1 kg Se may have to be irradiated for at least 4 hr in the BNL reactor in order to produce the required amount of Kr.

Preliminary experiments were performed in which Se was irradiated in the reactor accompanied by a flux monitor, then melted in the presence of Kr carrier, the radiokrypton then being pumped off, suitably purified and collected on charcoal, and counted. From these experiments it was concluded that the literature value for the neutron capture cross section for Se^{82} is approximately correct and that 50% of the radiokrypton emanated from the quiescent pool of Se. Although future experiments using either gas-sweeping or eddy-current techniques should be able to increase the yield, the present figure is both encouraging and useful. M. HILLMAN

GALLIUM-68

Ga^{68} is of interest in the study of brain tumor localization because it is a positron emitter, has a short half-life (68 min), and is potentially readily available inasmuch as it is formed from decay of a relatively long-lived parent Ge^{68} (275-day half-life). Therefore, a simple milking system for separating Ga^{68} from Ge^{68} is being sought. A system which shows promise involves adsorbing Ge^{68} on Dowex-1 anion exchange resin in the basic form and eluting the glycerol or glucose complexes of Ga^{68}. M. GREENE

MAGNESIUM-28

The present Mg^{28} production process was modified to improve the purity of the product and to reduce the processing time required. This was accomplished by adding an ion exchange step to remove F^{18} and by removing H^3 in the final step where the volume to be taken to near dryness is less than the volume at previous steps.

A subsequent proposal (see below under Radioisotope Production) for producing Mg^{28} involves the use of enriched Mg^{26}. The new procedure will involve handling only very small amounts of Mg at any one time. Tests have shown that suitably small amounts of Mg could be handled and that when it is alloyed with Li^6 the resulting foils are homogeneous. Irradiation of Li^6-Mg^{26} confirmed the fact that the new proposal was feasible.

Anticipating the possibility that Mg^{26} may have to be purchased as the oxide, consideration was given to the possibility of reducing the oxide with Li^6 and simultaneously forming the desired Li^6-Mg^{26} alloy. Thermodynamic calculations of the equilibrium constant for the Li reduction indicated that if 30 mg Mg^{26} as the oxide is mixed

with 70 mg Li^6 at 700°C, at equilibrium 74% of the Mg will be reduced to metal.

A. Weiss, J. Baranosky, J. Daane

LITHIUM-6 DEUTERIDE

Previous progress reports have described the use of Li^6 deuteride as a source of 14-Mev neutrons when irradiated with thermal neutrons. A comparison is being made between this method and other methods of obtaining fast neutrons such as the use of an accelerator or the irradiation of enriched U^{235} in a nuclear reactor. The $Vi^{51}(n,\alpha)Sc^{48}$ reaction, which requires 13-Mev neutrons, is being used as a monitor. A. Weiss

SHORT-LIVED ISOTOPES FOR TUMOR TREATMENT

Equipment is being assembled for testing a previously proposed method for continuously measuring, recording, and controlling the B concentration in the blood of a patient undergoing neutron capture therapy for brain tumors. Consideration is also being given to adapting the equipment and the method in order to produce beta emitters of very short half-lives and to introduce these into a patient in such a way that the emitted radiation can be used in appropriate localized areas in the patient without danger of contamination from the radioisotopes themselves. E. Yellin

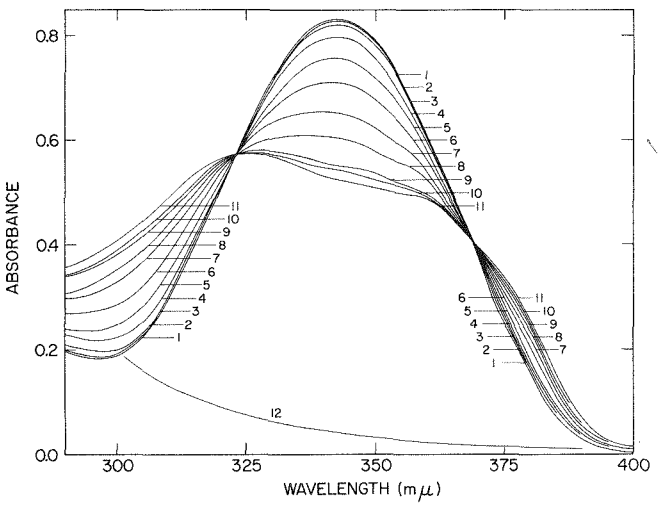

Figure 24. Absorbance of benzene solutions containing thenoyl-trifluoroacetone (HT) and varying amounts of tri-n-octylamine (R_3N). Curve 12 shows the absorbance due to the highest amine concentration used. Curve 11 is the absorbance due to 5×10^{-5} *M* HT in the absence of any amine. Curve 1 is the absorbance corresponding to the complete conversion of HT to its association product with the amine. All intermediate curves show the absorbance corresponding to a mixture of HT and its association product.

Radiochemical Analysis

H.L. Finston

EXTRACTING CHARACTERISTICS OF LIQUID ION-EXCHANGER AND CHELATING AGENT

The investigation of the reaction of tri-n-octylamine (R_3N) with HCl reported in the last progress report has been extended. The equilibrium constant and the mechanism of the reaction between R_3N and 2-thenoyl-trifluoroacetone (HT) has been determined. The assumption that the reaction product would demonstrate an absorption spectrum was verified, making possible the application of a spectrophotometric method.

Eleven benzene solutions were prepared each containing HT (5×10^{-5} *M*) and R_3N (varying from 0 to 50×10^{-3} *M*). Each solution was pretreated with dilute HCl to equilibrate the HT with its monohydrate – the prevailing situation when HT is used as an extractant for metals from an aqueous solution; the concentration of HCl was not high enough to convert a significant amount of the amine to the hydrochloride form.

The absorbences of the solutions were measured against blanks prepared in the same manner and containing the corresponding concentration of R_3N but no HT. The compilation of the spectra is shown in Figure 24. Curve No. 12 demonstrates that there is a negligible contribution to the total absorbence for those concentrations of amine for which appreciable amounts are used up by reaction with the HT. Therefore, the absorbences due to the free amine are accurately subtracted out by the blanks. The fact that the two isosbestic* points shown in Figure 24 remain fixed over a 5000-fold change in amine concentration indicates that there is only one product from the interaction of R_3N with HT.

It is assumed that in benzene a reaction of the following type occurs:

$$q[R_3N]+[HT]=[(R_3N)_qHT] .$$

*An isosbestic point is a wavelength at which the absorbence indices are the same for two species in equilibrium.

The following equation is derived by means of a procedure of Newman and Hume:*

$$\log \frac{[(R_3N)_qHT]}{[HT]} = q \log [R_3N] + \log k_q ,$$

where $k_q = [(R_3N)_2HT]/[R_3N]\,q[HT]$. Figure 25 shows a plot of log $[(R_3N)_qHT]/[HT]$ *vs* log $[R_3N]$. It is seen that the relationship is a straight line and that its slope, which is equal to the association ratio, q, is equal to unity. Therefore, the reaction between tri-*n*-octylamine and 2-thenoylfluoroacetone in benzene is shown to be

$$R_3N + HT = R_3N \cdot HT .$$

The intercept gives the formation constant, $k_q = (1.43 \pm 0.10) \times 10^3$.

The extent of hydration of the HT has been reported as 10% when a benzene solution of HT is contacted with an aqueous phase.** However, since the addition of more amine decreases the concentration of free HT, the concentration of a hydrate should also be decreased. This would appear to present an anomaly inasmuch as the HT is involved in two equilibria, and the well-defined isosbestic point should not have been present. However, it was shown that the rate of attainment of equilibrium between the nonhydrated form and the hydrate in benzene is reached very slowly and that consequently the 10% of the HT initially present as the hydrate remains unchanged during the experiment. L. NEWMAN, P. KLOTZ

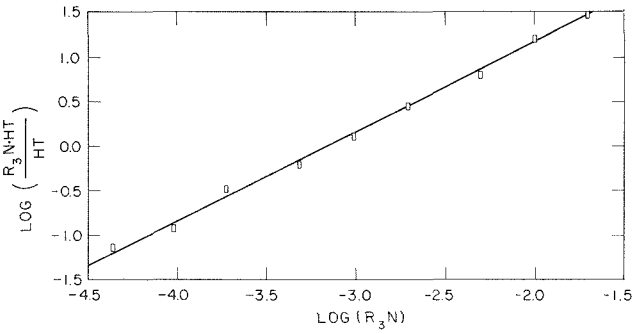

Figure 25. Plot of log ($R_3N \cdot HT/HT$) *vs* log (R_3N).

EMISSION SPECTROSCOPY

Manganese Analyses in Blood

Tracer techniques in which Mn^{54} and Co^{60} were equilibrated with blood were used to study the erratic Mn assays obtained at first and to develop a satisfactory ashing technique.

Co is not suitable for use as an internal standard because over a period of time the rate of volatilization of Co relative to that of Mn changes. However, Cu was found to volatilize at the same rate as Mn, and a spectral line of Cu was found which permitted the use of a Cu concentration high enough so that variations in Cu normally present in blood would have no effect on the Cu intensity. Therefore, Cu is shown to be suitable for use as an internal standard, and with its aid a sample of dog plasma was analyzed and found to have a concentration of 0.0033 μg Mn/ml with a precision of about ±10%. J. FORREST

Fluoride Analyses in Zircaloy

The investigation of the flame photometric procedure for the determination of fluoride in Zircaloy solutions was continued with the study of the flame emission of the Ca-F band at 529 mμ. This emission band was measured for solutions containing $CaCl_2$ and various mixtures of fluoride and Zr. No limiting Zr concentration was observed beyond which further suppression of Ca-F emission did not occur. Furthermore, the shallow slopes of the curves showing emission *vs* fluoride concentration limit the precision to approximately 12 to 15% at fluoride concentrations of 0.1 *M*. Consequently, prior adjustment of sample solutions to constant Zr concentration levels would not improve precision. It has been concluded that the poor emission of Ca-F in the presence of Zr precludes further investigation of the flame photometric technique. J. FORREST, R. WILSON, C. BACHSMITH

ELECTROCHEMISTRY OF FUSED SALTS

Sulphate Medium

The feasibility of molten sulphate as a medium for electrochemical studies is being investigated. The solvent system being studied is the Li_2SO_4-K_2SO_4 eutectic at 625°C (80 *M*% Li_2SO_4; mp, 535°C).

Suitable equipment has been constructed of quartz and Vycor, and a Ag^+-Ag electrode was made. A current-voltage curve of Ag_2SO_4 solution was determined against a 25 mm^2 Pt foil electrode. Silver ion behaved as a depolarizer at the expected potential. No limiting current was observed be-

*L. Newman and D.N. Hume, *J. Am. Chem. Soc.* **79**, 4571 (1957).

E.L. King and W.H. Reas, *J. Am. Chem. Soc.* **73, 1806 (1951).

cause of the large electrode area and the relatively high concentration of Ag^+.

The density of the molten Li_2SO_4-K_2SO_4 eutectic at 625°C was determined pycnometrically to be 2.12+0.01 g/ml. Quantitative measurements require knowing how much salt is present in each compartment of the electrolysis apparatus. Conventional analytical methods for sulphate determination are not feasible for the present study and were avoided by passing the sulphate through a Dowex-1 anion exchange column in the chloride form and titrating the chloride released.

The limiting electrode reactions in the sulphate melt at a Pt electrode have been examined. At the anode, the electrode reaction appears to be

$$SO_4^{=} \rightarrow \tfrac{1}{2}O_2 + SO_3 + 2e^- .$$

In the cathode compartment considerable amounts of both sulphite and sulphide have been found. Three possible reactions are postulated, and the content of the cathode compartment is being analyzed to determine the correct mechanism.

The Ag^+-Ag electrode in the melt at various Ag^+ concentrations was examined in detail. It was found that this electrode obeyed the Nernst equation closely when the $[Ag^+] > 5\times10^{-3}$ molal. At lower concentrations positive deviations were observed, the cause for which is still under investigation. Particular efforts were made to determine the utility of this electrode as a reference electrode, and it was found to be satisfactory when $[Ag^+] > 1\times10^{-2}$ molal.

Coulometric studies of the *n* values and potentiometric measurements showed that the Pd^{+2}-Pd and Cu^+-Cu electrodes gave reversible potentials in accordance with the Nernst equation. Potentials were found to be +0.541 and −0.206, respectively, relative to the Ag^+-Ag reference electrode.

Examination of the effect of Cl^- on the potential of the Ag^+-Ag electrode indicated that when $[Cl^-] < 0.2$ molal and $[Ag^+] < 0.02$ molal, the following equilibrium occurs:

$$AgCl \rightleftharpoons Ag^+ + Cl^- , \quad K = 2\times10^{-1} .$$

Irregularities which were observed at higher chloride concentrations warrant further investigation.

C. Liu

Nitrate Medium

A fused $LiNO_3$-KNO_3 eutectic is being studied polarographically and coulometrically. This system is sufficiently low melting (mp, 132°C) to permit the use of Hg as an electrode.

Appropriate equipment has been constructed. A Ag-AgCl electrode and a Ag-$AgNO_3$ electrode have been used and polarograms have been obtained. In some cases cathodic currents of 0.5 to 1 mμa were obtained with some indication of a composite cathodic-anodic wave, especially upon prolonged contact between salt and Hg. This will be investigated further.

Polarograms were taken for two particular cases: 1) 1.3×10^{-3} *M* $Cd(NO_3)_2$, and 2) the same to which had been added enough KCl-$Pb(NO_3)_2$ to obtain approximately 0.6×10^{-3} *M* $Pb(NO_3)_2$. The two polarograms coincided and indicated near reversible two-electron reductions of identical half-wave potential. The same result was observed when the order of addition was reversed. This is very remarkable because 1) in most ordinarily used aqueous media the half-wave potential of Cd is approximately 0.2 v more negative than that of Pb, and 2) others, using approximately 0.05 molal KCl in a nitrate melt, have obtained a separation of nearly 0.1 v with the Cd more negative. The stability constants of the chloro-complexes of Pb and Cd are not sufficiently different to account for such a large discrepancy. This will be studied further.

C. Auerbach, G. Kissel

Chloride Medium

Further investigation of the behavior of Bi^{+3}/Bi system in the chloride eutectic indicates that both the chloride eutectic and the Bi can be purified and that oxide contamination can be minimized. Consequently this study has been extended to include investigation of the chronopotentiometric stripping of metals from a Bi pool.

A Cd-Bi alloy of nominal concentration 2×10^{-5} *M* Cd/cc Bi was made. The potential of this alloy when used as a molten electrode in the chloride eutectic at 450°C was found to be −1.01 v *vs* a 0.05 *M* Pt^{+2}/Pt reference electrode. Very little Cd^{+2} was found initially in the chloride melt, as evidenced by the cathodic chronopotentiometric behavior of the pool in contact with the chloride eutectic. However, no well-defined anodic chronopotentiogram of Cd in the Bi could be noted even at currents as high as 20 ma.

Anodization of the pool at a controlled potential of −0.9 v gave an initial electrolysis current of approximately 3 ma. This potential is too negative to oxidize Bi, and the current must be attributed to the oxidation of Cd to Cd^{+2} in the chloride melt. After 5 min anodization at −0.9 v the cathodic

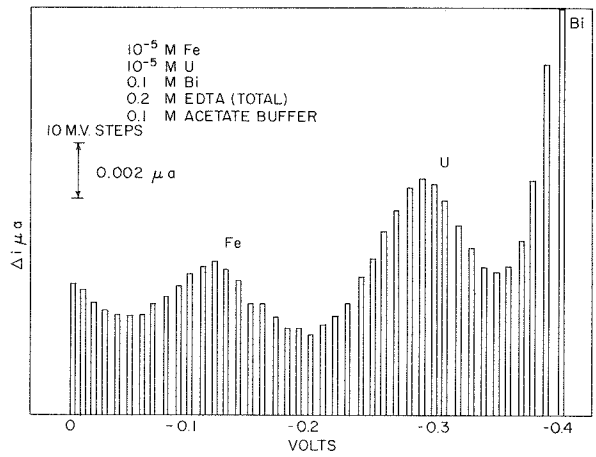

Figure 26. Incremental polarogram of Fe and U in Bi and EDTA.

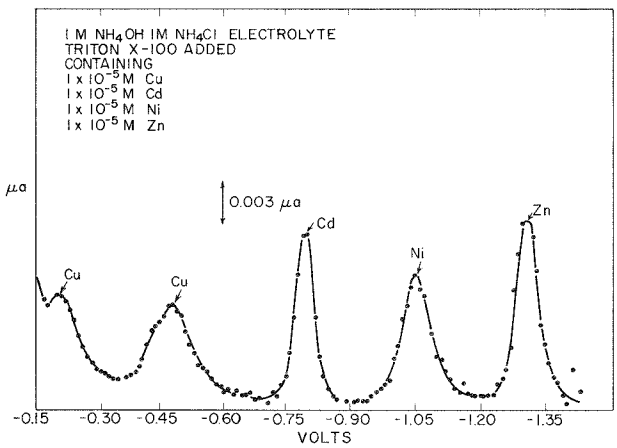

Figure 27. Polarogram of Cu^{+2}, Cd^{+2}, Ni^{+2}, and Zn^{+2} (each 10^{-5} M).

chronopotentiometric behavior of the electrode was studied and a definite holdup of potential attributable to the reduction of Cd^{+2} was demonstrated. The quarter-wave potential was measured at -1.33 v and agreed well with the E^0 of -1.316 v for the Cd^{+2}/Cd couple found by Laitinen and Liu.

The Zn-Bi system was studied, and the diffusion coefficient of Zn in Bi was calculated to be $(5.2\pm 20\%)\times 10^{-5}$ cm^2 sec^{-1} at 450°C. Although this diffusion coefficient is somewhat higher than those of ions in fused salts, it is about the same as that found by King for Sn in Bi at 420°C.

The anodic stripping of Li from Bi into a LiCl-KCl eutectic melt at 450°C was also studied using a Bi pool electrode, and a value of 2.1×10^{-5} cm^2 sec^{-1} was obtained for the diffusion coefficient. This value is much smaller than that of Zn in Bi, although from the sizes of the atoms one would expect approximately equal diffusion coefficients. However, Li forms an intermetallic compound of Bi, the effect of which would be to lower the diffusion coefficient of Li in Bi. Further evidence of this intermetallic compound formation is the low activity coefficient of Li in Bi. Using the measured potentials of the Li-Bi pools, their concentrations, and the E^0 potential of the Li^+-Li couple as measured by Laitinen and Liu, an activity coefficient of 4×10^{-7} was calculated. (Note that Egan and Wiswall obtained the value of 1×10^{-5} for this activity coefficient.) J. Van Norman

INCREMENTAL POLAROGRAPHY

The problem of determining U and Fe simultaneously in U-Bi fuel was mentioned in the last progress report; it has been shown that small amounts of Fe can be determined in the presence of U using an EDTA-acetate-buffer supporting electrolyte. However, this is of little practical value in the present case of interest where Bi, U, and Fe are present in the approximate ratio 10^5:10^2:1. Further experiments have been performed and Figure 26 shows an incremental polarogram of Fe and U, each 10^{-5} M, in the presence of 10^{-2} M Bi and 10^{-2} M excess EDTA. Lesser amounts of EDTA gave less satisfactory resolutions.

Studies have shown that when DCTA is substituted for EDTA highly distorted current-time curves with resulting irregularities in the incremental response are obtained. Apparently, DCTA has pronounced surface active properties.

Figure 27, a polarogram of a mixture of Cu^{+2}, Cd^{+2}, Ni^{+2}, and Zn^{+2}, each 1×10^{-5} M, further illustrates the resolution afforded by the present instrument. C. Auerbach, G. Kissel

MECHANISM OF ELECTRODE REACTIONS

All quantitative applications of dc voltammetry are crucially dependent upon equations which involve many parameters including an area term. In an intensive research effort begun at the Pennsylvania State University in 1955 the significance of all the relevant parameters has been elucidated with the exception of the area term. For Hg and liquid amalgam electrodes the area is known to be equal to the corresponding geometric area of

the electrode, but for solid electrodes the geometric area has been found to differ appreciably from the value of the area parameter in the analytical equation. The obvious implication is that on solid electrodes only certain specific sites are active as heterogeneous catalysts in reversible oxidation-reduction electron transfer processes. Identification of these "active sites" is of fundamental interest in connection with the detailed mechanism of electrode reaction.

Work has begun using radioactive tracers to locate such active electron transfer sites unambiguously. It is hoped this will lead to quantitative measurements of the kinetics and mechanisms of electrode reactions and a general refinement of solid electrode voltammetry into a reliable quantitative analytical tool.

Evaporation of solutions of Tl^{204} onto stainless steel surfaces followed by contact autoradiography showed the feasibility of localizing and identifying discrete spots of deposited material.

In order to determine whether electrodeposition occurs selectively on preferred electrode sites, the reduction of Tl^+ to Tl at a bright Pt electrode in 0.1 *M* NaOH(aq) was studied. The electrolyte contained 7.2 mC Tl^{204} and 1.7×10^{-4} *M* Tl^+. Contact autoradiographs were made of the thallium electrodeposits. Similarly, contact autoradiographs were made of thallous adsorbates obtained on electrodes immersed in the electrolyte in an open circuit for time periods equal to the duration of the foregoing electrolysis experiments. The autoradiographs together with a photograph of the pristine electrode before treatment are shown in Figures 28a, b, and c.

On visual examination in direct light, the adsorbate obtained in the absence of electrolysis exhibited a pink reflectance, reminiscent of the color of thallous hydroxide, and the even density autoradiograph (Figure 28c) shows the presence of a virtually uniform deposit. In contrast to this, the autoradiograph of electroplated thallium (Figure 28b) indicates several circular dark spots corresponding to relatively thick thallium deposits.

Considering the fact that 10^{16} to 10^{17} atoms of Tl including 10^5 to 10^6 atoms of Tl^{204} tracer were present in each deposit, the non-uniformity of the

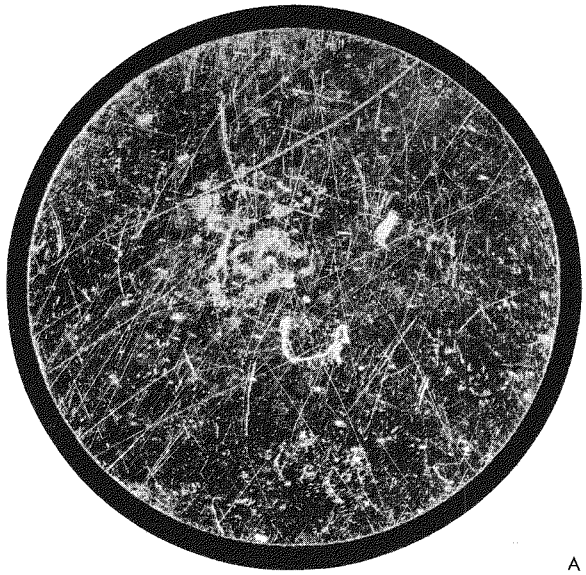

A

B

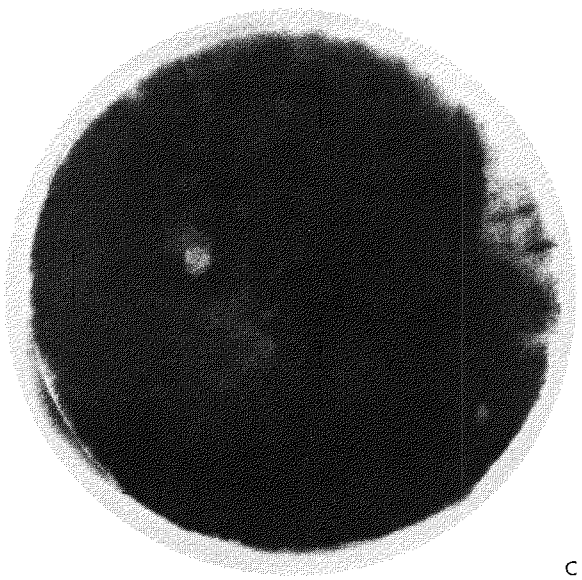

C

Figure 28. Demonstration of occurrence of electroreduction on preferred electrode sites. Figures are enlarged. A is a photograph of pristine electrode surface prior to treatment; light lines represent scratches or depressions in an otherwise plain surface. B is an autoradiograph of a platinum cathode following electroreduction of Tl^{204}. C is an autoradiograph of a platinum "electrode" following immersion without electrolysis in solution of Tl^{204}.

autoradiograph of the electrodeposited thallium cannot be accounted for by random statistical fluctuations, but instead reflects differences in the relative rates at which Tl was electroreduced at various electrode sites. J. JORDAN

ACTIVATION ANALYSIS OF BIOLOGICAL TISSUE FOR GOLD

Activation analysis is being used to determine trace amounts of Au in sections of mouse brain tissue in cooperation with a study by the BNL Medical Department. A 3-hr irradiation in the reactor at a flux of 5×10^{13} n/cm^2-sec has been determined to be optimum for this analysis. The Au concentration is determined by comparison of the 0.411 Mev gamma of Au^{198} with that of a pure Au standard. S. TASSINARI, H. FINSTON

CONTROLLED POTENTIAL COULOMETRY OF ORGANIC DISULFIDE GROUPS

The feasibility of selective reduction of some of the disulfide groups in the insulin molecule is a matter of current interest in the BNL Medical Department. Controlled potential electrolysis, which would not introduce extraneous chemicals into this highly sensitive system, is being tried on two relatively simple disulfides: the amino acid cystine (RSSR) and the disulfide form (GSSG) of the tripeptide glutathione (GSH). From experiments performed it is concluded that the disulfide-sulfhydryl reduction in compounds of this type can be carried out coulometrically with 100% current efficiency. C. AUERBACH

Hot Laboratory Operations

P. RICHARDS

RADIOISOTOPE PRODUCTION

J. BARANOSKY

All routine production of processed isotopes is being put on a self-supporting basis, and to that end production costs of all isotopes have been reviewed and, where necessary, selling prices revised.

Iodine-132

Nine I^{132} production runs were made during this period with only minor difficulties. A total of 35 shipments including another one to Melbourne, Australia were made as follows:

CUSTOMER	NO. OF SHIPMENTS	TOTAL NOMINAL ACTIVITY (mC)
Mayo Clinic, Rochester, Minn.	9	90
UCLA Medical Center, Los Angeles, Calif.	7	70
Oak Ridge Institute of Nuclear Studies, Oak Ridge, Tenn.	4	40
Commonwealth X-Ray and Radium Laboratory, Melbourne, Australia	1	10
St. Joseph's Hospital, Houston, Tex.	4	40
BNL Medical Dept.	2	20
VA Hospital, Birmingham, Ala.	3	30
University of Texas, Galveston, Tex.	1	10
National Naval Medical Center, Bethesda, Md.	2	20
Lawrence Radiation Laboratory, Berkeley, Calif.	1	100
Johns Hopkins Hospital, Baltimore, Md.	1	10
TOTAL	35	440

Magnesium-28

In reviewing production costs it was discovered that the use of fully enriched Mg^{26} rather than natural Mg for the production of Mg^{28} would not only increase the specific activity by a factor of about 20, but would also be surprisingly economical in spite of the high price of Mg^{26} ($3,000/g). An irradiation of Mg^{26}-Li^6 foil confirmed the expected increase in specific activity and showed the new process to be feasible. Meanwhile, pending receipt of more Mg^{26} from Oak Ridge, 22 production runs were made with the old process from which 53 shipments totaling 12,500 μC were made. Two of these shipments were to the French Atomic Energy Commission at Saclay, the most distant point to which this isotope has been shipped.

CUSTOMER	NO. OF SHIPMENTS	TOTAL NOMINAL ACTIVITY (μC)
University of Colorado Medical Center, Denver, Colo.	12	2400
Los Angeles County Hospital, Los Angeles, Calif.	7	3500
University of Tennessee, AEC Agricultural Laboratory, Oak Ridge, Tenn.	2	900
State University of New York, Brooklyn, N.Y.	5	800
Harvard School of Public Health, Boston, Mass.	1	500

Atomic Energy Commission, Saclay, France	2	100
VA Hospital, Minneapolis, Minn.	7	700
Montreal General Hospital, Montreal, Canada	4	200
State University of Iowa, Iowa City, Iowa	1	100
Massachusetts General Hospital, Boston, Mass.	7	1700
University of California, Davis, Calif.	1	1000
Stanford University, Palo Alto, Calif.	1	50
National Institute of Health, Bethesda, Md.	1	50
Tulane University, New Orleans, La.	1	500
General Atomic, San Diego, Calif.	1	50
TOTAL	53	12,550

Iodine-133

Only eight I^{133} production runs were made this period from which 11 shipments totaling 200 mC were made. During this lull the hood and processing equipment were rebuilt to include more shielding and a new method of opening, transporting, and inserting the uranium oxide into the dissolver vessel.

CUSTOMER	NO. OF SHIPMENTS	TOTAL NOMINAL ACTIVITY (mC)
Roswell Park Memorial Institute, Buffalo, N.Y.	3	60
BNL Medical Dept.	2	20
Medical College of South Carolina, Charleston, S.C.	6	120
TOTAL	11	200

Fused Beads

Six shipments totaling 180 fused Y^{90} clay beads were made to the UCLA Medical Center at Los Angeles. Each bead averaged approximately 1.3 mm diam and 1.5 mC.

SPECIAL PROJECTS

Radiography

A total of 289 service radiographs and autoradiographs were made of which 39 were for groups outside of the Nuclear Engineering Department. Several radiographs were produced using a 1 mm diam Lu^{177} bead as a source; such a source has proven to be useful in cases requiring a point source having gamma-ray energies falling between those of Tm^{170} and Ir^{192}. Of the autoradiographs, 14 were of mice brain and liver tissues (for the BNL Medical Dept.) and 43 were of Tl^{204} deposits on Pt electrodes (Radiochemical Analysis Group). J. AUSTIN, H. RUGE, E. KRIEDEMAKER, T. ROBINSON, JR.

Iodine-132 Standard

Repeated counting experiments indicate that Cs^{134} and I^{132} have the same counting efficiency and that Cs^{134} makes a satisfactory long-lived counting standard for calibrating equipment for counting I^{132}. Lucite standards incorporating Cs^{134} have been made up for distribution to I^{132} customers. J. BARANOSKY, H. FINSTON, P. RICHARDS

Processed Isotopes Catalog

Brookhaven has just published its first catalog describing all of the isotopes which are supplied routinely by the Hot Laboratory Division. Distribution of the 2500 copies printed has begun.

L. STANG, P. RICHARDS, W. TUCKER

REMOTE CONTROL DEVELOPMENT AND STAFF SHOP OPERATIONS

Work was continued this period on the development of glove boxes and related equipment for use in the handling of alpha-emitting material. A commercially supplied polyester Fiberglas vat is being modified and tested as a possible glove box.

A special shielding door for the introduction port to the first section of the Metallurgy Hot Cell was designed in order to provide a better means of introducing items into the cell using the General Mills Model 100 manipulator. A test of the boot changing operation from the cold side of this cell was performed satisfactorily.

Other items fabricated included four Al source holders each holding 16 Co^{60} sources, 6 Y^{90} generators, a glove box for storing heavy-water standards, a dry box for use in alloying Li^6 with Mg^{26}, a dust-free box for handling materials to be analyzed on the emission spectrograph, and a special rolling pig and storage cave. A. BANSLABEN, C. KIESLING

LIQUID WASTE OPERATIONS

A total of 3100 gallons of "A" waste has been disposed of this period by pumping approximately 150 gal from the underground "A" storage tanks

into each "blowdown" from the Waste Concentration Plant.

A number of leaks were discovered in the auxiliary steam coil in the Waste Concentration Plant. The coil was removed with appropriate decontamination. When the tubes were cut off and remounted into a new tube sheet by rolling and welding, the leaks persisted, and examination showed that the stainless steel had crystallized and was cracking during the rolling operation. An entire new steam coil was fabricated, and two-shift operation of the Waste Concentration Plant was resumed. The net change in the "D" waste inventory was a decrease of 16,140 gal during this period.

The vacuum receiver tank for the house vacuum system in the Hot Laboratory (Building 801) became contaminated and had to be removed for decontamination. After re-installation of the tank the entire vacuum system was flushed out.

Table 7 summarizes the liquid waste operation during this period. J. BARANOSKY

Table 7

"F" Waste Processing

Comparative figures on waste released to the sewer for the period

	Gal	Average activity level, C/ml	Total activity, mC
May – Aug.	1,371,320	2.47×10^{-11}	210.4
Jan. – Apr.	1,338,995	9.3×10^{-12}	51.4

Waste Concentrator Operations

	Waste to evaporator	Concentrate to drums	Volume reduction	Activity in mC: Feed	Activity in mC: Distillate
May – Aug.*	218,480	1,867	117:1	213,915	5.04
Jan. – Apr.*	257,620	1,948	132:1	239,160	7.49

Waste Sample Analysis

	"F" waste	Pile canal	Concentration	Misc.	Total
May – Aug.	204	50	238	19	511
Jan. – Apr.	198	20	231	10	459

Waste Containers

	"D" waste	"A" waste	Total
May – Aug.	98	0	98
Jan. – Apr.	93	0	93

Waste Inventory

	Gal start	Gal received	Gal to evaporator	Gal end
"D" Waste				
May – Aug.	167,835	206,580	222,720	151,695
Jan. – Apr.	203,825	221,730	257,720	167,835
"A" Waste				
May – Aug.	4,136	19	3,100	1,055
Jan. – Apr.	4,415	21	300	4,136

*Nominal months (all other months are calendar months).

Metallurgy Division

D.H. GURINSKY

Corrosion Studies and Engineering Tests

THERMAL CONVECTION LOOPS

As of August 31, 1960, there are 6 thermal convection loops in operation. One loop contains U-Bi plus Zr and Mg, while the remaining 5 loops contain Pb-Bi eutectic (55.5% Bi – 44.5% Pb) plus inhibitors and additives. During this report period, an additional 10 loops were shut down. These consisted of 7 U-Bi or Bi loops and 3 Pb-Bi eutectic loops. The operating conditions of the entire 16 loops are summarized in Table 8.

Loops 83, 87, 91, 94, 95, 96, and 107 (all U-Bi or Bi loops) and loops 118, 120, and 121 (all Pb-Bi eutectic loops) were shut down in order to place greater emphasis on the boiling Hg and Na programs. Radiographs of loop 91 showed the presence of a slight deposit in the cold leg but no corrosion was detectable. There was no corrosion or deposition detectable on radiographing the other 9 loops.

The Pb-Bi eutectic loops presently in operation have no indication of deposition or corrosion. The addition of Ti or Zr to Pb-Bi eutectic decreases the corrosion rate of carbon steel and 1¼ Cr – ½ Mo steel.

Two new loops containing Hg (loops 124 and 125) have been started up during this report period. The loops are pressurized, so that the Hg will not boil and are operating at a temperature differential of 1000° – 600°F (538° – 315°C). Loop 125 is uninhibited but contains 25 ppm Mg to act as a getter while loop 124 contains a Ti insert in the cold leg as well as 50 ppm Mg. The operating conditions are summarized in Table 8. There is no corrosion or deposition detectable on radiographs taken of the Hg loops.

PUMPED LOOPS

HVL 1 – Run 7

The purpose of this run is to study the effects of flow velocity of liquid, inhibited Pb-Bi eutectic on

Table 8

Status of Metallurgical Thermal Convection Loops as of August 1960

Loop	Material of construction	Contents of additives in solution, ppm			Temperature, °C		Date started	Hr of operation	Radiographic inspection	
		Mg	Zr	U	Hot leg	Cold leg			Hot leg	Cold leg
83[a]	carbon steel (stress relieved)	260	1000	930	550	550	11/18/58	1,891	No corrosion	No ppt.
					550	510	2/5/59	506	"	"
					550	425	2/26/59	8,142	"	"
					550	550	2/4/60	647	"	"
					650	500	3/2/60	3,495	"	"
87[a,b]	carbon steel (stress relieved)	280	350	940	550	550	1/22/59	737	No corrosion	No ppt.
					550	510	2/26/59	507	"	"
					550	400	3/19/59	11,686	"	"
88[b]	carbon steel (stress relieved)	250	280	940	550	550	1/29/59	666	No corrosion	No ppt.
					550	510	2/26/59	507	"	"
					550	405	3/19/59	12,400	"	"
91[a]	1¼ Cr (stress relieved)	300	250		550	550	3/13/59	1,412	No corrosion	No ppt.
					550	510	5/14/59	5,490	"	"
					650	500	12/31/59	5,045	"	Slight ppt.

Table 8

Status of Metallurgical Thermal Convection Loops as of August 1960

Loop	Material of construction	Contents of additives in solution, ppm			Temperature, °C		Date started	Hr of operation	Radiographic inspection	
		Mg	Zr	U	Hot leg	Cold leg			Hot leg	Cold leg
94[a]	AISI 4130 steel (stress relieved)	225	250	850	550	550	3/6/59	740	No corrosion	No ppt.
					550	510	4/6/59	1,130	"	"
					550	405	5/23/59	9,833	"	"
95[a]	carbon steel inside 1¼ Cr (stress relieved)	275	1000	965	550	550	4/10/59	815	No corrosion	No ppt.
					550	510	5/14/59	509	"	"
					550	405	6/4/59	7,069	"	"
					575	575	3/28/60	690	"	"
					650	500	4/26/60	2,095	"	"
96[a]	carbon steel inside 1¼ Cr (stress relieved)	260	1000	940	550	550	4/11/59	935	No corrosion	No ppt.
					550	510	5/20/59	1,283	"	"
					550	400	7/14/59	6,147	"	"
					575	575	3/28/60	690	"	"
					650	500	4/26/60	3,360	"	"
107[a]	1¼ Cr (stress relieved)		300		550	550	8/25/59	622	No corrosion	No ppt.
					550	510	9/21/59	2,558	"	"
					550	400	1/11/60	4,686	"	"
113[c]	1¼ Cr (stress relieved)	350	45		550	550	1/14/60	390	No corrosion	No ppt.
		(Bal., Pb-Bi eutectic)			650	500	2/8/60	4,850	"	"
117	1¼ Cr (stress relieved)	Pb-Bi eutectic (No inhibitors)			400	320	1/8/60	1,119	No corrosion	No ppt.
					400	200	2/24/60	4,200	"	"
118[a]	carbon steel inside, with 1¼ Cr outside (stress relieved)	350	45		550	550	2/23/60	335	No corrosion	No ppt.
		(Bal., Pb-Bi eutectic)			600	450	3/8/60	3,425	"	"
119	carbon steel inside, with 1¼ Cr outside (stress relieved)	350	70		550	550	2/2/60	689	No corrosion	No ppt.
		(Bal., Pb-Bi eutectic)			625	625	3/2/60	173	"	"
					650	500	3/9/60	4,080	"	"
120[a]	1¼ Cr (stress relieved)	Mg 350 - Ti 80 (Bal., Pb-Bi eutectic)			575	575	3/1/60	975	No corrosion	No ppt.
					650	500	4/11/60	2,616	"	"
121[a]	carbon steel (Si-killed; stress relieved)	Ti chip in cold leg Mg 350 - Ti 20 (Bal., Pb-Bi eutectic)			400	400	3/11/60	407	No corrosion	No ppt.
					500	300	4/21/60	2,020	"	"
122	carbon steel inside, 1¼ Cr outside (stress relieved)	Mg 350 - Ti 95 (Bal., Pb-Bi eutectic)			575	575	4/1/60	760	No corrosion	No ppt.
					650	500	5/4/60	2,820	"	"
123[d]	carbon steel inside, 1¼ Cr outside (stress relieved)	Zr chip in cold leg Mg 350 - Zr 85 (Bal., Pb-Bi eutectic)			650	450	4/12/60	3,310	No corrosion	No ppt.
124[d]	carbon steel inside, 1¼ Cr outside (stress relieved)	Ti chip in cold leg Mg 50 (Bal., Hg)			583	315	8/9/60	528	No corrosion	No ppt.
125	carbon steel inside, 1¼ Cr outside (stress relieved)	Mg 25 (Bal., Hg)			538	315	6/17/60	1,525	No corrosion	No ppt.

[a]Loop shut down to make room for experiments under the new program and subsequent examination.
[b]½ hot leg Al-killed + ½ hot leg Si-killed.
[c]Henceforth the Pb-Bi eutectic is taken to mean 55.5% Bi and 44.5% Pb.
[d]Loops 121, 123, and 124 contain a chip of inhibitor suspended on a flexible rod and located at the coldest point in the loop.

corrosion and mass transfer of several steels and weld metals. Flow was 1.6 ft/sec and the ΔT was 600° – 450°C. The eutectic contains 70 ppm Zr and 350 ppm Mg. The test section consists of 2¼ Cr – 1 Mo steel, 1¼ Cr – ½ Mo steel, ½ Cr – ½ Mo steel, RH 1081 steel (carbon steel with low Mn, high Ti), carbon steels (Si-killed) and weld metals of similar compositions. The loop has been operating at the design conditions for 1355 hr, and radiographs taken of the test section and cooler have shown no detectable corrosion or deposition. A failure in one of the heater circuits has caused a temporary shutdown.

BOILING MERCURY LOOPS

The purpose of these tests will be to develop corrosion information on container materials for a Hg cycle turbine. Test parameters are: boiling at 1000°-1100°F; superheating the vapor to 1150°-1250°F; condensing at 1000°-1100°F; and cooling the condensate to approximately 600°F. The materials to be tested in this program will include carbon steels, 1¼ Croloy, 2¼ Croloy, Cb, and Cb – 1% Zr.

The first boiling loop, of carbon steel co-extruded with 1¼ Cr – ½ Mo steel, has been completed and is ready for startup. The loop will operate at the design conditions mentioned above and will contain a Ti insert in the cold leg as well as 50 ppm Mg.

SODIUM PURIFICATION

A purification apparatus with a two pound capacity has been designed for producing high purity Na containing less than one ppm oxygen. A cold trap will reduce Na_2O to 30 ppm and a hot trap utilizing Zr sheet as a getter is expected to reduce Na_2O to less than 1 ppm.

Assembly of the components for the apparatus is in progress and will be completed next month. Analytical problems in determining the oxygen concentration in Na at this level are being investigated. A. ROMANO, A. FLEITMAN, C. KLAMUT

LOOP EXAMINATION

HVL 4 – Run 1

The purpose of this experiment was to study the effects of liquid metal velocity on corrosion and mass transfer of several low alloy steels and weld metals. The liquid metal used in this test consisted of 350 ppm Zr and 350 ppm Mg in Bi circulating through a steel loop at 9 to 10 ft/sec. The materials tested in the furnace section were 2¼ Cr – 1 Mo and 1¼ Cr – ½ Mo steels with various heat treatments and 2¼ Cr – 1 Mo, 1¼ Cr – ½ Mo, and 32 CMS (low carbon steel) weld metals deposited by the inert arc process.

The piping was completely sectioned. Visual examination revealed that the 2¼ Cr – 1 Mo portion of the piping was very severely attacked by a dissolving type of transgranular corrosion. Cavitation-like attack was also evident on the 2¼ Cr – 1 Mo pipe wall. The 1¼ Cr – ½ Mo steel showed little or no attack.

Although both the sandblasted and polished areas of each 2¼ Cr – 1 Mo specimen were severely attacked, the corrosion of the sandblasted portions was more general.

Portions of both the 2¼ Cr – 1 Mo and 1¼ Cr – ½ Mo longitudinal welds were attacked severely in the sandblasted sections of the piping. The 1¼ Cr – ½ Mo welds seemed to resist attack in the polished regions, while the 2¼ Cr – 1 Mo welds showed areas of severe attack in the polished portions of the piping. All the transverse welds (32 CMS low carbon steel) appeared to be unaffected.

Microexamination of the 1¼ Cr – ½ Mo piping showed some slight corrosion.

J. SADOFSKY, A. CENDROWSKI

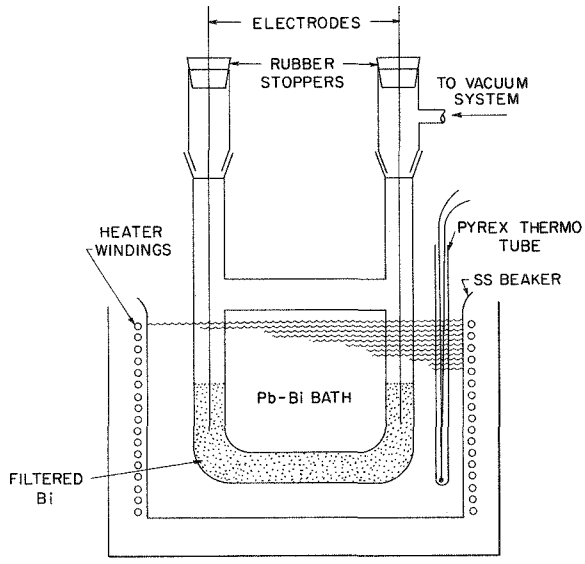

Figure 29. Apparatus for measuring emf between metals immersed in liquid Bi.

Corrosion Fundamentals

ELECTROCHEMICAL EFFECTS IN CORROSION OF IRON AND STEELS BY LIQUID BISMUTH

It was reported previously that electrolysis of Fe-Bi and Cr-Bi melts produced migrations of Fe to the anode and Cr to the cathode. It remained to be seen whether these are in phase with or opposite to the current flow due to the steel-Bi thermocouples, or whether or not these currents are responsible for the selective attack seen on certain materials.

The emf's between specimens of a number of steels immersed in liquid Bi were measured. The apparatus used is shown in Figure 29. A Pyrex U-tube containing 40 g filtered Bi was heated by immersion into a molten bath of Pb-Bi eutectic. Electrodes, consisting of approximately ⅛- to 1/16-in. rods of the steels studied, passed into the U-tube through rubber stoppers, permitting them to be lowered into the Bi after it melted. At all times during an experiment, the U-tube was under rough vacuum ($\sim 10^{-3}$ mm Hg). The temperature of the Pb-Bi bath was controlled by a variac in series with the heater windings. The Pb-Bi bath temperature was measured by immersing a glass-tubing-shielded chromel-alumel thermocouple into it. Since the Bi level in the U-tube was approximately 1 in. lower than the level of the Pb-Bi eutectic, it was assumed the temperatures of the two liquid metals were essentially the same, provided the temperature of the Pb-Bi bath remained constant, ±1°C, for 10 min prior to reading the potential between the electrodes. Increasing the temperature equilibration time to 30 min did not produce measurable changes in the emf. The upper ends of the 12-in. electrodes were connected to a type K L&N potentiometer. Care was taken that this connection was sufficiently remote from the Pb-Bi bath to insure it was at room temperature. Room temperature remained at 24° ±2°C during these experiments.

In this manner the electromotive force generated between pure Fe, pure Cr,* and a number of steels immersed in Bi** was measured as a function of temperature over the range 300°-525°C. The compositions of the electrodes are listed in Table 9. The emf's measured are listed in Table 10 and are plotted as a function of the measured temperature of the Pb-Bi bath in Figure 30. It can be seen that a straight-line, or nearly straight-line, dependence was obtained in all the systems measured. Also, the "additive" rule applies, i.e.,

$$E_{AB}=E_{AC}+E_{CB}\,.$$

Thus at 450°C, $E_{9Cr^+,\ 32\ CMS^-}=4.27$ mv, which is the sum of $(E_{9Cr^+,\ 2\ 1/4^-})+(E_{2\ 1/4^+,\ 32\ CMS^-})=(1.20)+(3.03)=4.23$ mv, within reasonable experimental error. Thus sufficient data were obtained to permit the estimation of the potential between any possible combination of the materials listed in Table 9 within ±0.2 mv.

In some cases, as in run 40, the electrodes were left immersed in the Bi overnight; the potentials measured the second day differ slightly from those measured the first day, probably resulting from mass transfer between the electrodes. The data are plotted as the potential against carbon steel as a function of the Cr content in Figure 31, and as the potential against 2¼ Cr – 1 Mo steel as a function of Cr content in Figure 32. (These are the two base materials with which most Bi corrosion experience has been obtained.) In both cases, a sharp maximum in potential in the vicinity of 5% Cr is observed; this correlates well with the selective attack so often found on this material. Further experiments, it is hoped, will determine if this emf maximum is indeed related to the observed corrosion.

Two additional points are of interest. The potential of pure Fe is essentially the same as that of 32 CMS at 450°C, but slightly more negative at lower temperatures. The potential of pure Cr is only slightly more positive than that of 5 Cr steel. It would be of interest to obtain data in the range of Cr concentrations 15 to 95% Cr.

It is difficult to compare the values for the Fe-Cr thermocouple with those in the published literature. However, a graph in the Metals Handbook (p. 32) suggests Fe has approximately 14 μv/°C against Pt at 450°C. A curve published by Udy* gives a number of 31.5 μv/°C for Cr against Pt at 450°C. One might guess from these data that the temperature dependence of the potential of Cr against Fe would be of the order of 18 μv/°C, which is slightly less than the 21 μv/°C measured in the

*The pure Cr wire was obtained through the courtesy of Mr. H. Kato, U.S. Bureau of Mines, Albany, Oregon.

**The liquid Bi served merely to flux the hot junction.

*M. J. Udy, *Chromium* (Reinhold, New York, 1956), Vol. 2, p. 106.

Table 9

Analyses of Electrodes Used in Thermocouple Measurements

Sample	Cr	Mo	Mn	Si	Fe	Other	Source
Pure Fe	N.D.	Tr	Tr	Tr	Major	0.003 %C	"Ferrovac E"
						0.1 %O	Bare weld rod
32 CMS	0.32	0.07	1.08	0.25	Bal.	0.15 %B	Bare weld rod
1¼ Cr – ½ Mo	1.33	0.49	0.57	0.33	Bal.		Bare weld rod
2¼ Cr – 1 Mo	2.62	1.02	0.66	0.34	Bal.		Bare weld rod
5 Cr – ½ Mo	5.4	0.30	0.5	0.1	Bal.		Swaged from pipe stock
9 Cr	7.9	0.2	0.5	0.5	Bal.		Bare weld rod
410 SS	13.33	0.15	0.5	0.5	Bal.	0.11 %C	U.S. Bureau of Mines, Albany, Oregon
Pure Cr	Major	—	—	—	—	—	

Table 10

Thermocouple Potentials Measured in Liquid Bi

Run	Electrodes +	Electrodes −	Temperature range, °C	E_{meas} at 450°C, mv*	$\Delta E/\Delta T$ at 450°C, μv/°C
27	410 SS	2¼ Cr	302 to 523	−0.02	2**
28	2¼ Cr	32 CMS	298 to 498	+3.03	8.5
29	5 Cr	2¼ Cr	302 to 537	+2.58	5.5
31	5 Cr	410 SS	299 to 502	+2.57	3.5
32	5 Cr	32 CMS	300 to 503	+5.47	14.0
33	410 SS	1¼ Cr	308 to 540	+2.01	8.0
34	1¼ Cr	32 CMS	327 to 525	+0.95	3.0
35	Cr	Fe	312 to 532	+5.36	21.0
36	410 SS	32 CMS	295 to 518	+3.01	10.5
37	9 Cr	32 CMS	291 to 546	+4.27	13.0
38	9 Cr	2¼ Cr	275 to 533	+1.20	4.0
39	2¼ Cr	Fe	295 to 546	+2.94	11.5
40	Cr	32 CMS	277 to 533	+5.48	20.0
26	2¼ Cr	1¼ Cr	302 to 500	+2.14	5.0

*Room temperature (cold junction) was 24° ±2°C; this corresponds to zero potential.
**The potential of 410 SS to 2¼ Cr was zero at 452°C; above 452°C, 410 SS was positive; below 452°C, 2¼ Cr was positive.

present work. Udy indicated that the data he used scatter, so the discrepancy is not too serious.

Initial attempts were made to measure the emf generated by an Fe-liquid Bi thermocouple. Large thermal gradients in the Bi made temperature measurements difficult, and the data scatter badly. The emf measured is generally much lower, by a factor of at least 10, than the Fe-solid Bi emf reported in the handbooks. It is also highly sensitive to the concentration of Fe in the Bi, changing sign during the course of an experiment as the Fe from the electrodes dissolves. As an example, for 450° – 400°C we measure +0.08 mv (hot leg+) early in the experiment, and −0.55 later in the same experiments. Experimental techniques are being revised to reduce thermal gradients in the vicinity of the electrodes and permit evaluation of the effect of Fe concentration. J. Weeks, A. Minardi

LIQUIDUS CURVES OF Mg-Bi AND Sm-Bi SYSTEMS

An attempt was made to examine all binary liquidus curves obtained at BNL to see if the curves of Strauss, et al.,* could be verified. These authors calculated the heat of solution of a num-

*S.W. Strauss, J.L. White, and B.F. Brown, *Acta Met.* 6, 604 (1958).

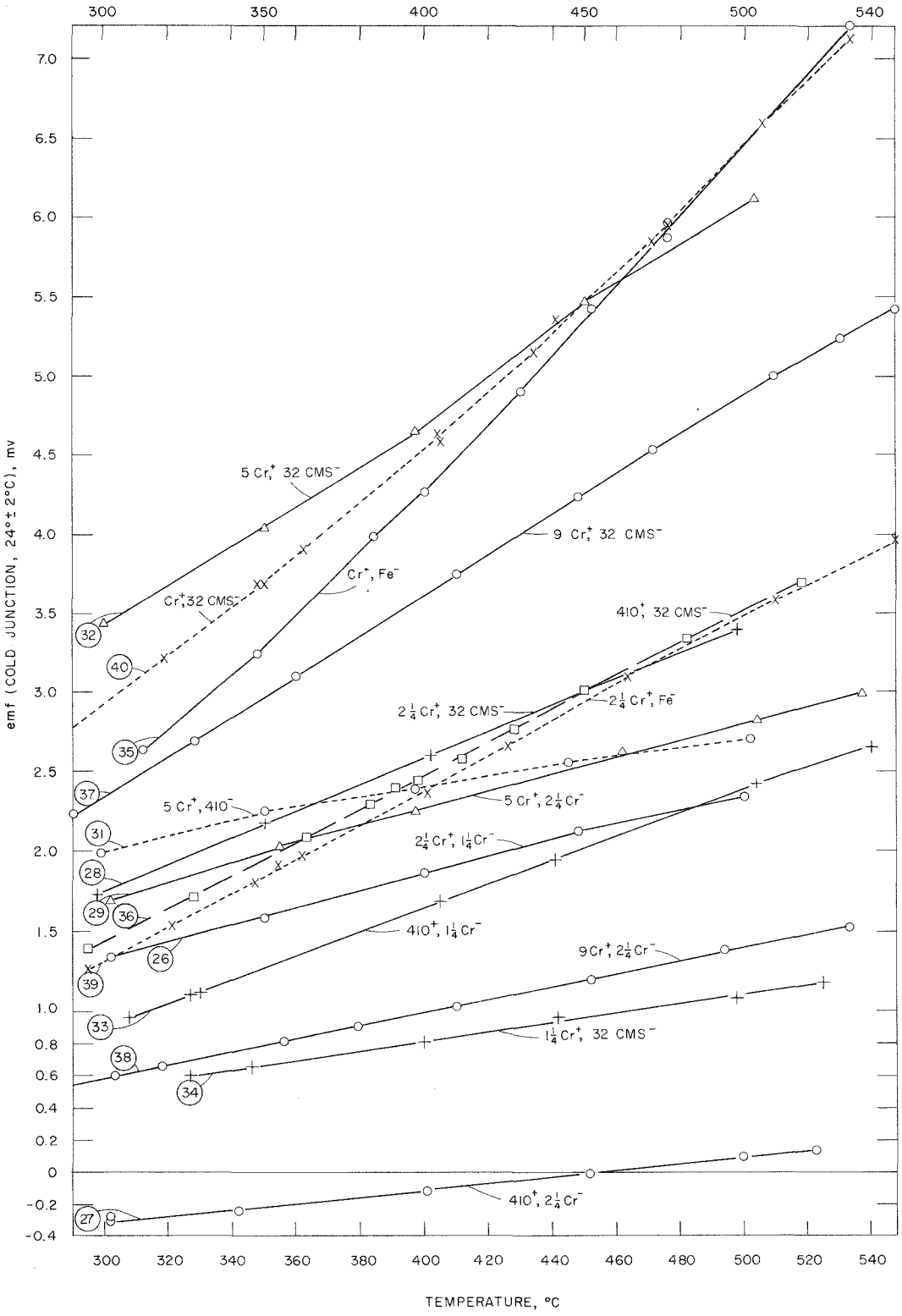

Figure 30. Thermocouple potentials between Fe, Cr, and several steels immersed in liquid Bi. Cold junction: 24° ±2°C.

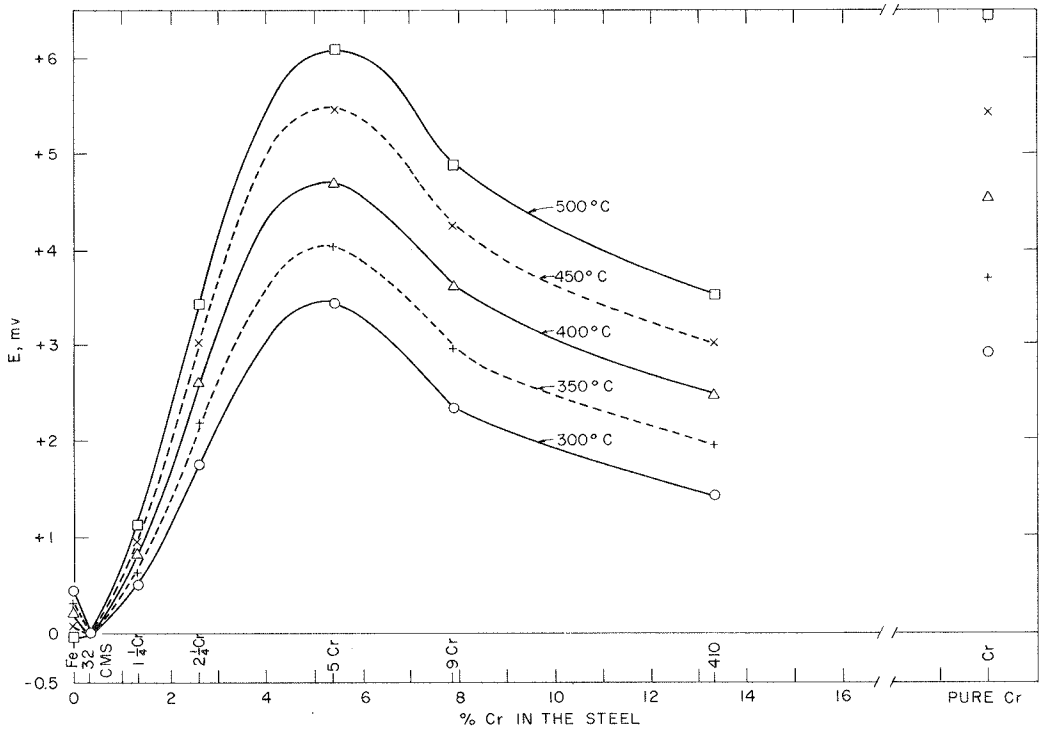

Figure 31. Effect of Cr concentration on the potential against 32 CMS. Reference junction: 24° ±2°C.

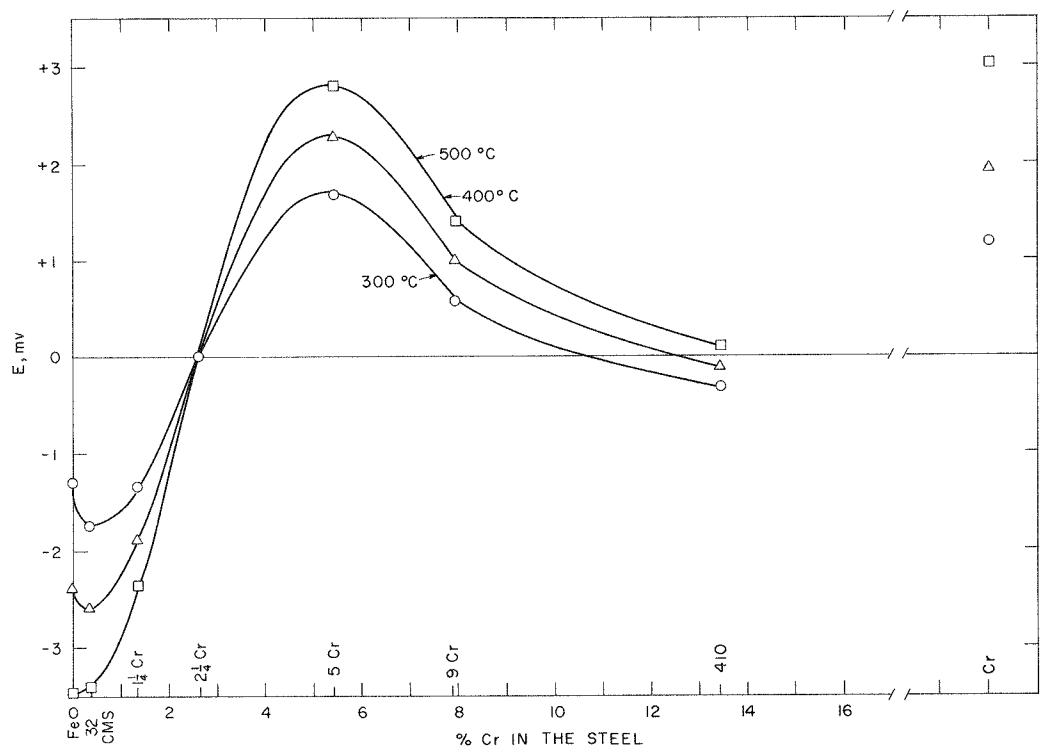

Figure 32. Effect of Cr concentration on the potential against 2¼ Cr–1 Mo steel. Reference junction: 24° ±2°C.

ber of solute elements in several solvent liquid metals, and reported a relationship between the heat of solution and the ratio of solvent/solute atomic radii. The data obtained here are more self-consistent than those Strauss used and should therefore provide a test for his theory. They do not, as seen in Figure 33, where they are plotted and compared with Strauss' curve. However, a series of lines of nearly constant slope can be drawn through several families of elements, i.e., Ba and Sr, the rare earths and Th, Fe and Ru, etc., as shown in Figure 33. The possible significance of this is not clear, but it was felt desirable to obtain additional solubility curves to fill out some of these groups of solutes and determine how inclusive this trend might be. The first ones, measured this period, were Mg and Sm. The data are shown in Figures 34 and 35, and the heats of solution from these are included in Figure 33. The data used in plotting Figure 33 are listed in Table 11.

The Mg-Bi eutectic temperature was measured by solidifying the melt with the shielded thermocouple immersed, and was found to be 261°C. The solubility curve extrapolates (from 300°C) to a eutectic composition at this temperature of 0.21 wt % Mg. This compares with 0.5 wt % reported in Hansen.* At temperatures 300°-500°C, the data are in general agreement with those in Hansen.

The large amount of Mg_3Bi_2 that precipitated from the original (5 wt %) melt on cooling and floated on its surface made it impossible to obtain samples over more than a 100°C range with any one melt. Consequently, three original melts were used in this determination, containing approximately 5, 3, and 1.5 wt % Mg. Data from all three alloys are in agreement and shown in Figure 34.

The Sm-Bi data are in good agreemnt with the 3 points reported earlier by Schweitzer and serve to substantiate his measurements. Schweitzer's data were also used in plotting Figure 35.

J. Weeks, A. Minardi

*M. Hansen and K. Anderko, *Constitution of Binary Alloys* (McGraw-Hill, New York, 1958), p. 317.

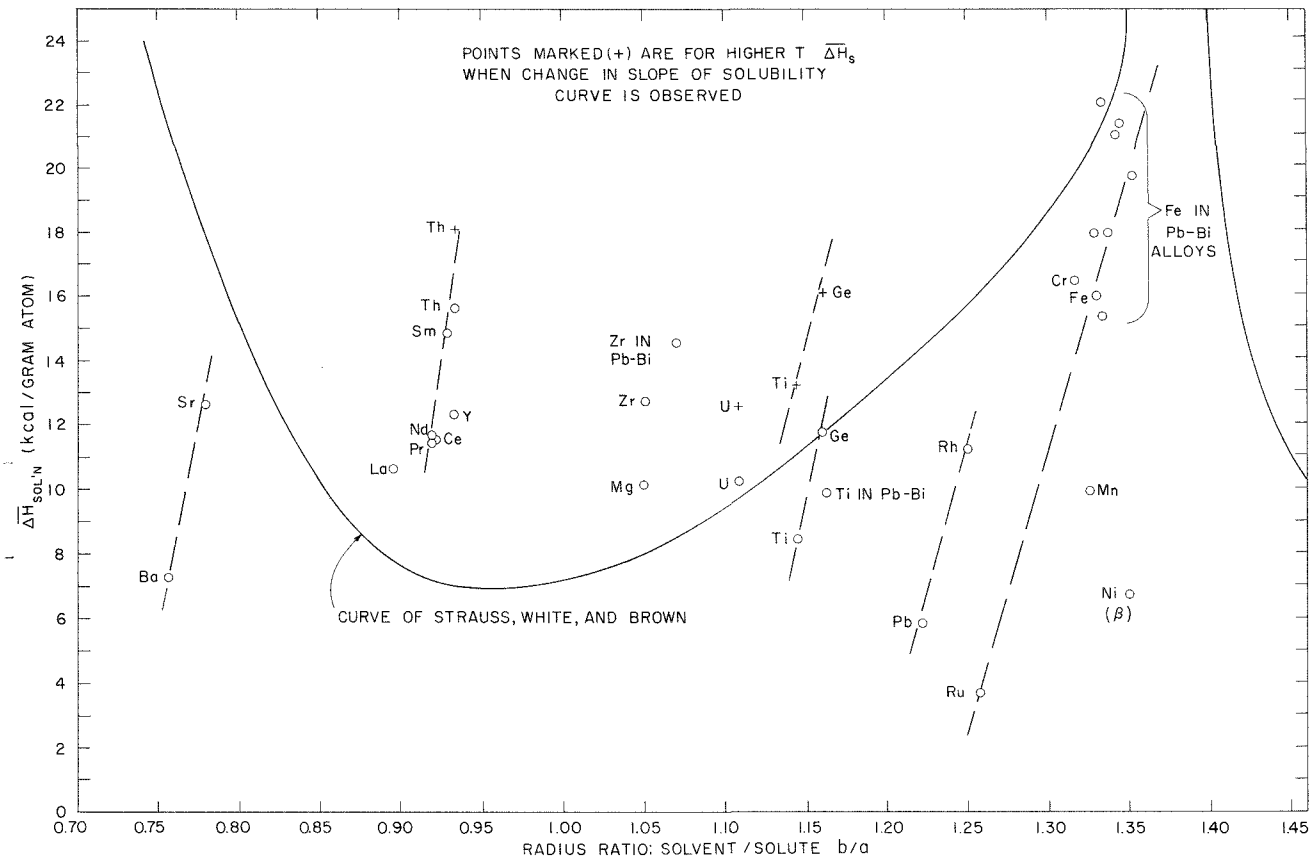

Figure 33. Effect of (radius of solvent/radius of solute) on heat of solution of metals into Bi or Pb-Bi.

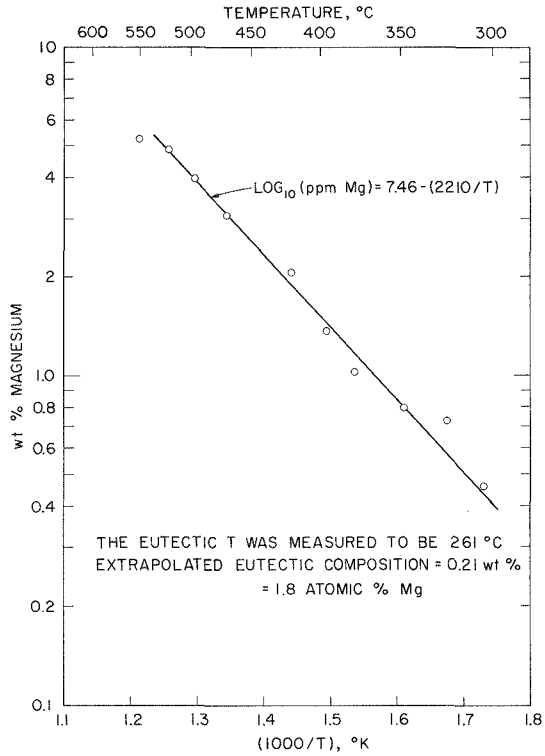

Figure 34. Solubility of Mg in Bi.

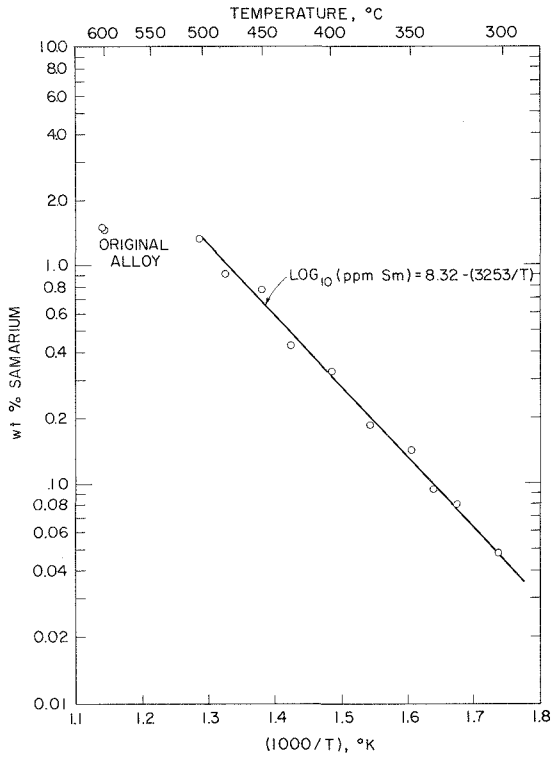

Figure 35. Solubility of Sm in Bi.

Table 11

Heats of Solution of Solute Atoms in Liquid Bismuth

System	ΔH, kcal/g-atom*	Solute radius** (a)	Solvent radius*** (b)	(b)/(a)
Mg-Bi	10.17	1.598	1.678	1.050
Sr-Bi	12.62	2.148	1.678	0.780
Ba-Bi	7.27	2.215	"	0.757
Y-Bi	12.30	1.797	"	0.933
La-Bi	10.65	1.871	"	0.896
Ce-Bi	11.52	1.818	"	0.922
Pr-Bi	11.45	1.824	"	0.919
Nd-Bi	11.68	1.824	"	0.919
Sm-Bi	14.88	1.804	"	0.929
Ti-Bi	8.45 (275° to 475°C)	1.467	"	1.145
Ti-Bi	13.2 (475° to 700°C)	"	"	"
Ti-$^{46.5\ Pb}_{53.5\ Bi}$	9.87 (300° to 700°C)	"	1.705	1.163
Zr-Bi	12.72	1.597	1.678	1.051
Zr-$^{51.4\ Pb}_{48.6\ Bi}$	14.50	"	1.705	1.070
Cr-Bi	16.40	1.276	1.678	1.316
Mo-Bi	Insoluble	1.386	"	1.212
Mn-Bi	9.92	1.286	"	1.325
Fe-Bi	15.98	1.26	"	1.33

Table 11

Heats of Solution of Solute Atoms in Liquid Bismuth

System	ΔH, kcal/g-atom*	Solute radius** (a)	Solvent radius*** (b)	(b)/(a)
Fe-$^{6.6\ Pb}_{93.4\ Bi}$	17.90	"	1.685	1.337
Fe-$^{16.2\ Pb}_{83.8\ Bi}$	"	"	1.675	1.328
Fe-$^{26.4\ Pb}_{73.6\ Bi}$	15.30	"	1.68	1.333
Fe-$^{36.5\ Pb}_{63.5\ Bi}$	21.35	"	1.695	1.345
Fe-$^{48.4\ Pb}_{52.6\ Bi}$	19.7	"	1.705	1.352
Fe-$^{42.2\ Pb}_{57.8\ Bi}$	21.0	"	1.69	1.342
Fe-$^{39.3\ Pb}_{60.7\ Bi}$	22.0	"	1.68	1.333
Ru-Bi	3.70	1.336	1.678	1.258
Rh-Bi	11.25	1.342	"	1.250
Pd-Bi	5.85	1.373	"	1.220
Ni-Bi	6.70	1.244	"	1.35
Ge-Bi	11.75 (270° to 485°C)	1.444	"	1.161
Ge-Bi	16.05 (485° to 670°C)	"	"	1.161
U-Bi	10.25 (300° to 480°C)	1.516	"	1.109
U-Bi	12.55 (480° to 725°C)	1.516	"	"
Th-Bi	15.6 (300° to 550°C)	1.795	"	0.934
Th-Bi	18.08 (475° to 900°C)	"	"	0.934

*Calculated from slope of solubility curve.

**From L. PAULING (for co-ordination number 12), *Nature of Chemical Bond*, 3rd ed., 1960, p. 402.

***From P.C. SHARRAH, J.I. PETZ, and R.F. KRUH, *J. Chem. Phys.* **32**, 291-246 (1960). Obtained by x-ray and neutron diffraction of liquid Bi, Pb, and Pb-Bi alloys.

SURFACE REACTION STUDIES

On the Composition of Zr-Bearing Films Formed on Steel by Reaction with Liquid Bi-Zr Alloy

An attempt was made to obtain more information on the composition of a film deposited on a 2¼ Cr – 1 Mo steel (U.S.S. "G") dipstick after reaction with Bi, containing 238 ppm Zr, at 752°C for 168 hr (Run 2-D-8).

The adherence of the deposit was weakened by immersing the dipstick in a methanol solution of bromine (10% Br_2 by volume) for about 5 min at room temperature. After rinsing the dipstick 2 times in methanol, Scotch tape was pressed onto the film-bearing surface and then peeled off. The Scotch tape, to which the film adhered, was then pressed onto a glass miscroscope slide.

Results of an x-ray diffraction analysis of this film are given in Table 12, in which *d* values and relative intensities are compared with those of ZrN given in the ASTM Index.

It is apparent that ZrN is present, along with some other compounds. Compounds which may possibly correspond with these *d* values are Cr_3C_2, αSiC (type V), Cr_2N, and Fe_3N. These results suggest that either the film is a mixture of ZrN with these compounds, that the ZrN is bonded to the steel through these compounds, or that the film is a Zr compound, not yet catalogued in the ASTM Index. It is planned to try to obtain a powder pattern. J. WAGNER, J. SADOFSKY

Uniformity of Zr-Bearing Films Deposited on Steel From Liquid Bi-Zr Alloy

Effect of prereaction ion bombardment of steel surfaces was studied. Rectangular shaped specimens of 2¼ Cr – 1 Mo steel (U.S. Steel Co. special steel "G"), 13×45 mm, were given a series of pol-

Table 12

Comparison of X-Ray Diffraction Analysis of Stripped Film with That of ZrN

Stripped film		ZrN (ASTM)		
d	Relative intensity	*d*	Relative intensity	hkl
2.64	100	2.64	100	111
2.53	16			
2.35	16			
2.29	92	2.29	100	200
2.23	28			
2.08	16			
2.07	16			
1.76	16			
1.62	36	1.62	80	220
1.59	20			
*		1.38**	70	311

*The machine was not run at an angle higher than $2\theta = 65.5°$. This would correspond to a *d* value of 1.43 as the cut-off point.

**All other *d* values are less than 1.38.

ishing cuts on standard metallographic papers, 240 through microcut, rinsed with reagent grade benzene, and then anhydrous methanol at room temperature (Run 1-115).

Specimen No. 1 was mounted on the cathode in a standard cathodic etching attachment for a Kinney model SC-3-Ct vacuum evaporator unit. The unit was evacuated to a pressure of about 0.04 μ. Argon, previously passed over Mg chips at 450°C was admitted. The sample was then bombarded with argon ions for 30 min at 3.5 to 4 kv, 50 ma. Ion bombardment was stopped by evacuating to *ca* 0.03 μ. Bi was then vapor deposited onto the ion-cleaned surface from two filaments in the same equipment in sequence. The specimen was then stored under the vacuum of a roughing pump.

Specimen No. 2 was given the same surface preparation and ion bombardment except that the anode was cooled with dry ice in 75 vol % methanol/25 vol % H_2O mixture; reaction time was 1 hr at 3 kv and 30 ma; and Bi was vapor deposited in one heavy coat (*ca* 1 g Bi evaporated from a Ta strip heater) in about 20 min.

Figure 36 shows contact prints from autoradiographs of the specimens after reaction with Bi-Zr alloy, containing Zr^{95}, for 168 hr at 698°C. Control specimens contacted with the same melts, but not bombarded, are shown for comparison. There does not appear to be any improvement in uniformity by ion bombardment.

X-ray surface reflection diffraction patterns taken near the ZrN (111) peak indicate that ion bombardment does not make any significant difference in the structure of these deposits.

It was noticed that the vapor-deposited Bi films on both specimens appeared to be very thin as judged by reflection of visible light. The next step might be to devise a technique for increasing the thickness of the Bi coating. J. WAGNER, J. KELSCH

Kinetics of Formation of Zr-Bearing Films on 1¼ and 2¼ Cr Steel

The procedure for determining the rate of film growth, described in a previous report (BNL 618), was repeated using the same steels at temperatures of 650° and 697°C (Runs 1-113 and 1-112 respectively).

In Figure 37, the data obtained in all three runs from the nitride-film-forming 2¼ Cr – 1 Mo steel are plotted on cartesian coordinates. Figure 38 is a log-log plot of the same data. It appears that during the first 2 hr the film grows rapidly then decreases, possibly due to spalling. From 2 to 8 hr the film again grows. The dotted lines in Figure 38 are fitted with a slope of ½. This slope suggests that the films grow by the rate process $d\Upsilon/dt = k\Upsilon^{-1}$ (Υ = film thickness, t = time, and k = rate constant), which integrates to $\Upsilon^2 = 2kt$. The rate process for a diffusion controlled reaction is described by a similar equation and suggests that diffusion is rate controlling.

In Figure 39, the data obtained in all three runs from the carbide-film-forming 1¼ Cr – ½ Mo steel are plotted on cartesian coordinates. Figure 40 is a log-log plot of the same data. The dotted lines in Figure 40 have been fitted with a slope of 2 to regions of film growth, although the scatter in the data make any such coordination questionable. This slope would correspond to a growth rate process of the type $d\Upsilon/dt = k\Upsilon^{1/2}$, which integrates to $\Upsilon^{1/2} = \frac{1}{2}kt$. These data also suggest that a growth-spall cycle occurs during the first 4 hr.

Activation energies cannot be estimated in either case from the present data until an estimate of the activity of Zr^{95} in the melt is obtained.

J. WAGNER, A. MINARDI, S. FINK, J. WEEKS

Radiation Effects

RADIATION LOOP

The Radiation Loop is being operated in the Brookhaven reactor to determine the effect of in-

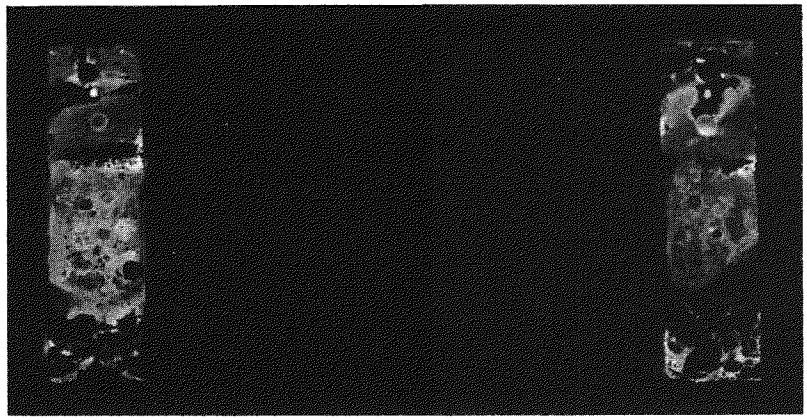

1 2

ION BOMBARDED, Bi VAPOR DEPOSITED BEFORE REACTION

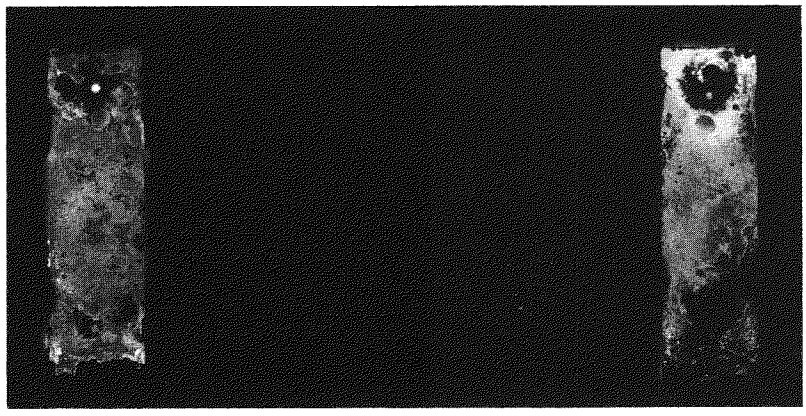

1 CONTROL 2

Figure 36. Autoradiographs of bombarded specimens.

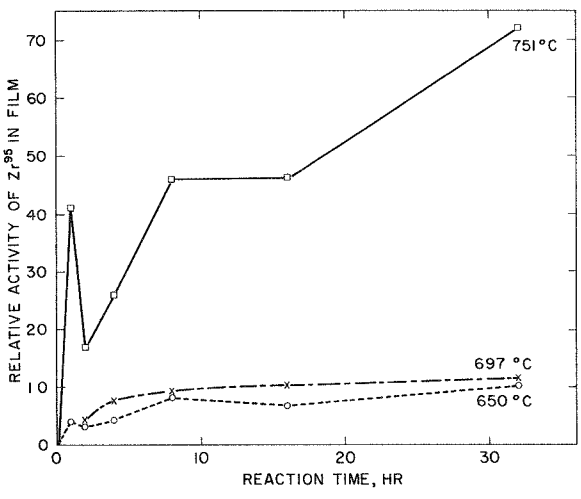

Figure 37. Growth rate of Zr bearing films on 2¼ Croloy steel reacting with liquid Bi-Zr alloy.

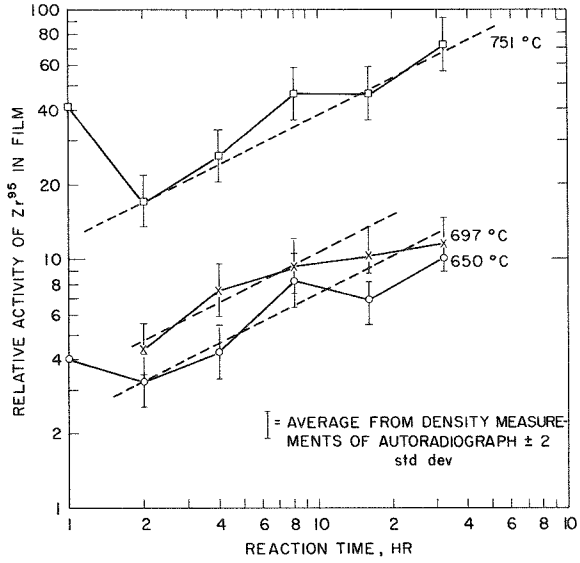

Figure 38. Growth rate of Zr bearing films on 2¼ Croloy steel reacting with liquid Bi-Zr alloy.

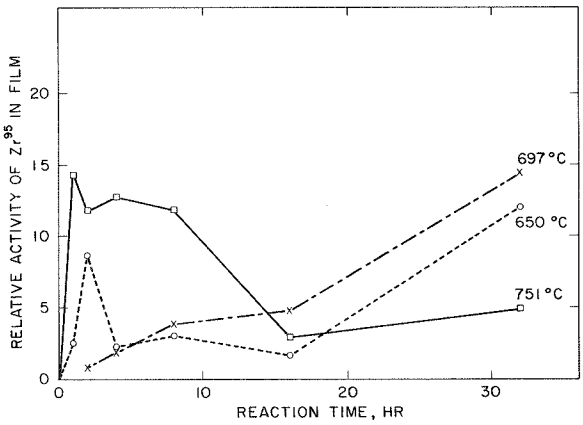

Figure 39. Growth rate of Zr bearing films on 1¼ Croloy steel reacting with liquid Bi-Zr alloy.

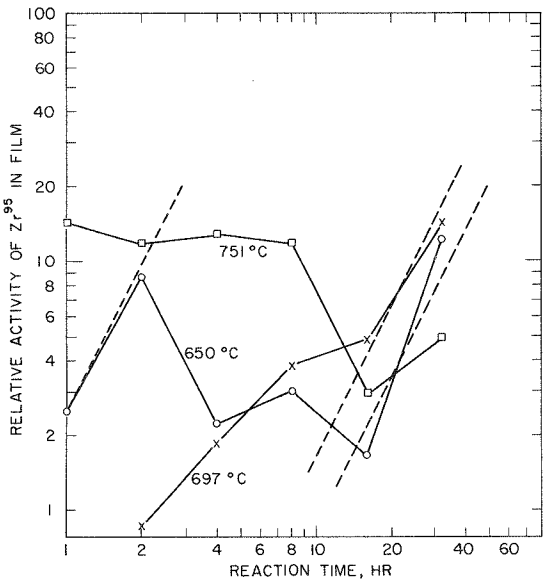

Figure 40. Growth rate of Zr bearing films on 1¼ Croloy steel reacting with liquid Bi-Zr alloy.

pile radiation on the corrosion of materials subjected to fissioning U-Bi solution circulating through a loop upon which a temperature difference is imposed. The materials being studied are carbon steel, low-chrome steels, Be, Mo, Ta, and graphite.

The addition of enriched U to the Bi charge, which was first circulated in the reactor in April, was started in May 1960. The U was added stepwise in units of approximately 1, 10, 45, and 100% of the final U inventory. Following each addition, the loop was operated long enough to obtain samples and verify that the shielding was adequate for operation at the next U level. A considerable amount of shielding was added in some areas and special shielding arrangements had to be worked out where adjacent experiments required low neutron and gamma background. A number of surveys were made by the Health Physics Division during this part of the operation.

The design temperature difference (500° to 425°C) was applied to the loop on June 9, 1960, and has been maintained since that time, except for pile shutdowns and one sampling requirement. As of August 31, 1960, the loop has operated in-pile for a total of 1817 hr of which 1552 hr have been at ΔT conditions.

Two failures of the in-line sampler occurred during the report period. The first, caused by wear of a positioning unit in the sampler cup transfer mechanism, was successfully repaired during a pile and loop shutdown without hazard to the personnel involved. The second failure was caused by Bi clogging the sampler mechanism during the sampling procedure. It is considered probable that this was the result of mal-operation rather than a defect in the sampler itself. The sampler is not readily repairable and rather than delay loop operation to replace the unit the loop is now sampled by dumping the charge to the melt-dump tank at the time of pile shutdowns and sampling manually using the thief-probe method.

Additive concentrations during the run have been constant at the following values: 967 ppm U^{235}, 353 ppm Mg, and 240 ppm Zr. Corrosion product analyses indicate Fe concentrations of less than 10 ppm. Cr, Mn, Mo, and Ni are not detectable. C. WAIDE, L. KUKACKA

FUNDAMENTAL STUDY OF NEUTRON IRRADIATION ON THE PROPERTIES OF IRON AND OTHER BCC METALS

The objectives of this program are to study how material and irradiation variables effect the changes in properties of body-centered cubic metals and from this information to evolve an explanation on the mechanism of these changes. Because of their importance in reactor technology, the initial work will be on high purity Fe and synthesized "steels" made by alloying high purity Fe with the various elements generally found in steels.

A vacuum still is being set up by the Materials Development Section for remelting the pure Fe to

lower its oxygen content. A series of melts will be made to study the effect of varying time, temperature, and the type of crucible used on the oxygen content.

Modification of the Instron tester for remote testing at temperatures down to the boiling point of liquid He has been completed. Tests at room temperature down to 50°K have been made on the "as received" ferrovac "E" pure Fe (not remelted) which had been cold swaged to 0.279 in. diam from the hot rolled 1 in. diam bar and annealed at 600°C for 6 hr. Data of these tests are being analyzed to determine the various parameters.

Remote metallographic techniques on pure Fe are being developed. A specimen that was broken at 50°K was sectioned longitudinally and mechanical twins were observed in the plastically deformed material.

A capsule containing 14 tensile specimens and 2 electrical resistivity specimens of the "as received" Fe was inserted in the pile on August 12. This capsule will be irradiated for 2 cycles. The specimens are being irradiated in air and are kept at about 50°C by cooling with compressed air.

Construction of an in-pile furnace for exposing specimens up to 500°C has been completed and the furnace is being tested out-of-pile. J. CHOW, S. MCRICKARD

Graphite Studies

MONITORING AND RADIATION DAMAGE PROGRAM

It is desired to determine and improve some of the experimental techniques and parameters affecting the dimensional and energy changes in the graphite used in the BNL reactor. A program has been prepared to clarify 1) the magnitude and temperature range of the stored energy associated with growth and recovery changes, 2) the effects of annealing frequency, soak time, annealing temperature, and temperature cycling on the physical, thermal, and electronic properties of the graphite.

D. SCHWEITZER

POROSIMETRY

Pore volumes and distributions between 125 and 200,000 Å for natural graphite powder (received from the Southwestern Graphite Co.) have been measured.

The data in Table 13 reveal similar distributions and total pore volume penetrable by Hg for various aliquots. Generally 75% of the available volume in the observed range of pore diameters exists in pores of 4000 Å diam and larger, 10% in the 125 to 300 Å range, 10% in the 600 to 4000 Å range, and 5% from 300 to 600 Å. Total pore volumes for the natural graphite powders examined vary from 2 to 2.3 ml/g sample. These volumes and distributions will be compared to other natural and artificial graphites.

It must be noted that the volumes referred to are the accessible volumes measured within the operating limits of the Hg Porosimeter. Methods to measure indirectly and to calculate pore volumes contributed by pores below ~120 Å in diam and those above 500,000 Å are under investigation.

Compacts of these natural graphites have been prepared by pressing at 15,000 psi at room temperature. These compacts exhibit very high densities but little mechanical strength. Total pore

Table 13

Pore Volumes and Distributions for a Natural Graphite Powder

	Sample 1		Sample 2	
Pore diameter, Å	Pore volume, ml	% of total	Pore volume, ml	% of total
124 to 194	0.138	5.9	0.157	7.9
194 to 318	0.108	4.6	0.072	3.6
318 to 436	0.046	2.0	0.043	2.2
436 to 581	0.026	1.1	0.014	0.7
581 to 4,260	0.220	9.5	0.229	11.5
4,260 to 8,320	0.575	24.8	0.60	30.0
8,320 to 200,000	1.210	52.1	0.89	44.3
Total	2.323	100.0	2.00	100.2

Table 14

Pore Volumes and Distributions for a Natural Graphite Compact Formed at 15,000 psi, Before and After Removal of Mercury Under Vacuum at 250°C

	First impregnation		Reimpregnated after Hg removal	
Pore diameter, Å	Pore volume, ml	% of total	Pore volume, ml	% of total
124 to 194	0.012	8.6	0.010	6.8
194 to 318	0.013	9.3	0.012	8.2
318 to 436	0.013	9.3	0.010	6.8
436 to 581	0.021	15.0	0.014	9.6
581 to 4,260	0.077	55.0	0.095	65.1
4,260 to 8,320	0.003	2.1	0.002	1.4
8,320 to 200,000	0.001	0.7	0.003	2.1
Total	0.140	100.0	0.146	100.0

Table 15

Pore Volumes and Distributions for Natural Graphite Compacts Formed at Various Pressures

	5,000 psi		10,000 psi		15,000 psi	
Pore diameter, Å	Pore volume, ml	% of total	Pore volume, ml	% of total	Pore volume, ml	% of total
124 to 194	0.039	9.3	0.014	6.9	0.012	8.6
194 to 318	0.027	6.5	0.012	5.9	0.013	9.3
318 to 436	0.013	3.1	0.010	5.0	0.013	9.3
436 to 581	0.010	2.4	0.014	6.9	0.021	15.0
581 to 4,260	0.279	66.7	0.139	68.8	0.077	55.0
4,260 to 8,320	0.020	4.8	0.005	2.5	0.003	2.1
8,320 to 200,000	0.030	7.2	0.008	4.0	0.001	0.7
Total	0.418	100.0	0.202	100.0	0.140	100.0

Table 16

Pore Volumes and Distributions of Virgin AGOT Graphite

(¼ in. diam × ½ in. long)

	Sample 1		Sample 2	
Pore diameter, Å	Pore volume, ml	% of total	Pore volume, ml	% of total
125 to 194	0.021	11.1	0.020	10.5
194 to 318	0.020	10.6	0.020	10.5
318 to 436	0.011	5.8	0.011	5.8
436 to 581	0.009	4.8	0.009	4.7
581 to 4,260	0.021	11.1	0.021	11.0
4,260 to 8,320	0.006	3.2	0.005	2.6
8,320 to 27,000	0.021	11.1	0.020	10.5
27,000 to 57,000	0.015	7.9	0.015	7.9
57,000 to 180,000	0.055	29.1	0.060	31.4
180,000 to 500,000	0.010	5.3	0.010	5.2
Total	0.189	100.0	0.191	100.1

volumes for the compacts for the same operating limits as the powders are 0.14 to 0.16 ml/g sample. This is about a 15-fold decrease in available pore volume upon forming a compact at 15,000 psi. Distribution of the volumes is also altered considerably on pressing. Whereas, in the powders, the principal fraction of the available volume is in pores greater than 4000 Å, the major share (97% at 15,000 psi) of the volume of the compacts is in pores below 4000 Å in diam (Table 14). This decrease in volume and disappearance of the larger pores may be the result of creating closed (unavailable) pores or of completely filling some of the pores upon forming a compact. Determination of the He displacement volumes for the samples should clarify the picture. Table 14 also lists the volume and volume distribution for the compact after complete removal (by weight) of the Hg by heating at 250°C under vacuum for 24 hr. The total available pore volume does not appear to vary. Further work will be attempted to determine whether or not the structure is altered during Hg impregnation and release.

Table 15 relates the total pore volume and volume distribution to the compact formation pressures. It was found that the total pore volumes and percentages of total volume existing in pores larger than 4000 Å appear inversely proportional to the formation pressure. This may be a real effect of a "skin" effect; that is, upon pressurizing, the larger pores become blocked at the surface and become inaccessible or filled, thus preventing penetration into the interior of the sample.

In conjunction with the expanded reactor monitoring program, representative virgin AGOT specimens have been examined (Table 16). Pore volume and distribution studies will be completed at regular time intervals over the next several years on similar in-pile samples. Effects of annealing frequency, length of "soak" time, annealing temperature and flux on the volume and distribution of the pores in graphite will be investigated.

An effort is under way to accrue experimental information regarding the shapes of the pores existing in graphite via Hg desorption (release) techniques employing the Porosimeter.

V-shaped pores or those of uniform diameter should, upon lowering of the hydraulic pressure in the Porosimeter, release all of the Hg that had penetrated. "Ink-bottle" type pore shapes, those with narrow necks and wider bodies, would upon lowering of the pressure in the system to some specific value, release Hg trapped in the neck while retaining that in the bulb of the pore.

Table 17 reveals preliminary results to date. After maximum instrument pressure is achieved (15,000 psi), the pressure is lowered in increments and pore volumes recorded. It is found that all of the Hg introduced originally into the graphite is not released. For natural graphite powders ~80% Hg remains, for compacts prepared from the powder ~50% remains, and for AGOT cylinders ~70% remains in the pores. R. SINGER, D. SCHWEITZER

DENSITY DISTRIBUTION

The system for measurement of the degree of inhomogeneity of graphite powders is ready for operation. A schematic is presented in Figure 41. By dilution of a light liquid (benzene), with a heavier one (bromoform), samples of graphite powder can be separated into density fractions. The density of the liquid mix is measured with a Westphal balance. The density distributions of the samples are determined from the weights of the fractions collected in a fritted Pyrex funnel and the densities at which they floated. R. SINGER, D. SCHWEITZER

Table 17

Mercury Pickup and Release (ml/g) for Natural and Artificial Graphites

Material	Hg pickup	Hg remaining	Hg released	% Hg remaining
Powder #1	3.0	2.4	0.6	80
Powder #2	2.0	1.7	0.3	85
Compact #1 (15,000 psi)	0.17	0.08	0.09	47
Compact #2 (15,000 psi)	0.19	0.10	0.09	53
Compact #3 (10,000 psi)	0.20	0.09	0.11	45
AGOT #1, ¼ in. diam, ½ in. long	0.17	0.115	0.055	68
AGOT #2, ¼ in. diam, ½ in. long	0.17	0.114	0.056	67

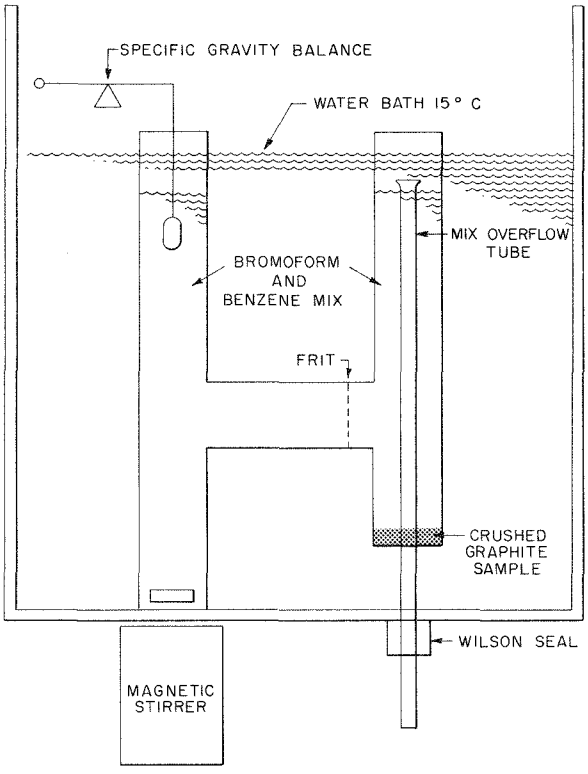

Figure 41. Density determination by sink-float method.

HELIUM DENSITY MEASUREMENTS OF GRAPHITE

A schematic of the He density apparatus is presented in Figure 42. The method of measurement essentially involves expansion of a definite quantity of He into a sample tube of known volume containing a sample of known weight. The He will fill the space between the sample particles and all accessible pores within the particles. A known volume of Hg is then introduced from a reservoir in order to return the system to its original volume which is so indicated by a manometric reading utilizing fixed Pt contacts sealed into the apparatus at appropriate locations. The unit sits in a constant temperature bath. The apparent density of the graphite to the gaseous He is found by dividing the specimen weight by the volume difference of the sample tube with and without a specimen.

A second similar glass system has been constructed and will be employed principally for measurements of any drift in the He density values as a function of time.

Table 18

Volume of the He Density System Without a Sample

Run		Volume, ml
1		34.22
2		34.21
3		34.14
4		34.17
5		34.21
6		34.21
	Av	34.19
	Av deviation	±0.027

Repeated determinations of the volume of the system without a sample check to 0.1% (Table 18). He density values for AGOT graphite cylinders outgassed at 500°C for 1 hr are presented in Table 19.

The accessible and inaccessible volumes are listed in Table 20. R. SINGER, D. SCHWEITZER

SURFACE AREA MEASUREMENTS

The Perkin-Elmer-Shell Sorptometer as received has been significantly modified to produce more dependable surface area results. This effort to adapt the instrument was undertaken because of the narrow limits of operation.

The modified external system permits a much wider range of investigation, as to sample size, sample surface area, sample pretreatment (outgassing, etc.), compensation for pressure changes upon desorption of large amounts of nitrogen and permits a measurement of the true internal system pressure. D. SCHWEITZER, R. SINGER

URANIUM CARBIDE STUDIES

Work has begun on a program to measure the rate of release of gaseous fission products from slightly irradiated uranium carbide powders.

The initial part of the program is concerned with the preparation of high purity uranium carbide by the reaction between uranium metal and methane. To this end, a vacuum system has been constructed which will permit the reaction to take place under closely controlled conditions.

In the second part of the program, a series of postirradiation anneals will be made on the powders and the evolved fission gases collected. The

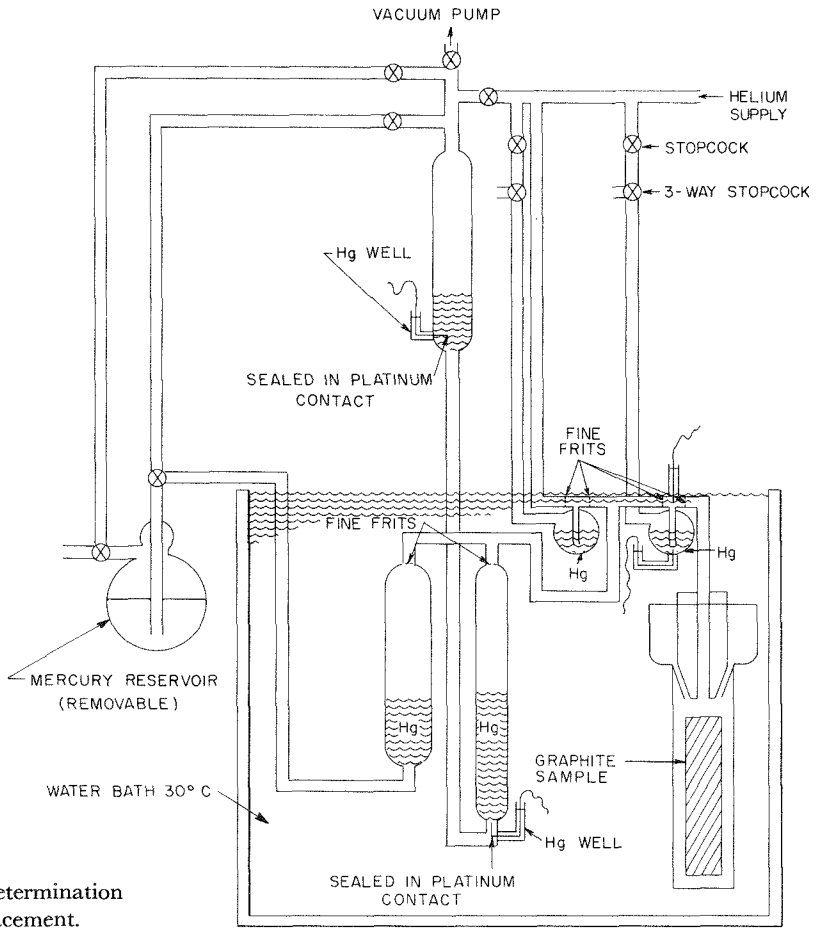

Figure 42. Density determination by helium displacement.

Table 19

Helium Density Values for AGOT Graphite

(¾ in. diam × 2 in. long)

Sample	System volume without sample, ml	System volume with sample, ml	Sample volume, ml	Sample weight, g	Density, g/ml
1	34.19	22.19	12.00	24.318	2.027
2	34.19	22.17	12.02	24.180	2.012

Table 20

Accessible and Inaccessible Pore Volumes for AGOT Graphite

Sample weight, g	Bulk volume, ml	Volume displaced by sample in He, ml	Theoretical volume, ml	Accessible pore volume, ml	Inaccessible pore volume, ml	Total pore volume, ml	% total pore volume	% of total pore volume inaccessible
24.318	14.51	12.00	10.76	2.51	1.24	3.75	25.8	33.1
24.180	14.50	12.02	10.70	2.48	1.32	3.80	26.2	34.7

Xe^{133} activity of the collected gases will be measured. Analysis of the time-rate of Xe^{133} evolution can give the diffusion coefficient for Xe in UC.

A. AUSKERN, D. SCHWEITZER

Metallography

EXAMINATION OF IMPERFECTIONS IN U^{235} FUEL ELEMENTS

A visual examination of a U^{235} fuel element for the BGRR revealed an irregularity in the surface of one of the plates that had developed during storage in the vaults. A section containing a pimple was submitted for examination. Radiographic inspection showed three spots in the plate, one of which was in the region of the original pimple.

The plate was sectioned transversely adjacent to each irregularity, mounted, and ground down to the points of imperfection.

A large globular mass of grey material was removed from the pimpled area and the powder submitted for x-ray diffraction. Analysis of the resulting film showed only the pattern for UAl_4. However, chemical analysis of the grey powder showed it contained 0.14% C and approximately 1% U.

The spots in the areas that were not pimpled showed a similar grey deposit protruding into but not through the cladding. Plate radiographs suggest these occur in stringers. It is postulated that they are a carbide of U which, when large enough, penetrates the cladding and reacts with moisture in the air causing the observed swelling. Apparently, the x-ray pattern from this hydrolyzed oxide was diffuse and masked by the corrosion-resistant UAl_4.

J. SADOFSKY, J. WEEKS

EFFECTS OF HEAT TREATMENT ON PLATES OF GREENBANK OBSERVATORY TELESCOPE

Metallographic examination of the telescope plates indicated that both steels were fairly clean and of good quality. Further microscopic examination revealed that heat treatment refines the grain size appreciably in the 4-in. plate but alters the grain size only slightly in the 2-in. plate. Much of the improvement in properties after heat treatment was believed due to the refinement in grain size.

J. SADOFSKY, O. KAMMERER

HIGH LEVEL HOT CELL

Research with the high-level hot cell has been restricted during this period. It is set up and ready to handle the Radiation Loop #1 on 48-hr notice. Since this would not be enough time to dismantle equipment in a contaminated cell and set up again for the loop, the *status quo* arrangement has been maintained. Nonradioactive testing and equipment setup for the pure Fe irradiation program were carried on in the third compartment of the cell.

In preparation for the loop, a lifting winch was installed on the General Mills manipulator crane to facilitate opening of the coffin door. The auxiliary shielding block outside the isolation room was covered with polyethylene to reduce exterior contamination. An additional roller assembly was built to support the empty coffin during its removal into a waste disposal trailer.

The setup for the remote low temperature tensile testing in the pure Fe irradiation program has been completed and tested at various temperatures. A report has been written about the facility (BNL 4952) and is tentatively scheduled to be given at the winter A.N.S. meeting. An optical comparator was received and set up in the north isolation room. This piece of equipment is used to measure the profile of the tensile specimen before and after testing. A small lead pig has been designed and constructed for the purpose of passing the fractured halves of the hot tensile specimen out of the cell and positioning on the comparator for measurement. Eventually, it is planned to completely remotize the comparator for operation in the cell.

The new impact tester was fitted with remote temperature conditioning equipment and was subsequently used to study the impact transition temperature of "as received" and annealed samples of the steel being used in the new A.U.I. Greenbank Radiotelescope Observatory.

S. MCRICKARD, J. CHOW

FISSION FRAGMENT DAMAGE TO THIN FILMS

In the first month of this period, work was continued in the electron microscopic investigation of fission fragment damage in metal foils thinned by electropolishing. It was found that there is an increase in dislocations and in vacancy loops correlating with increasing exposure to thermal neu-

trons. The mechanism of production of such damage remained elusive. Beginning in June, a new approach was made consisting of causing fissioning of U^{235} within evaporated films of Al, Ca, Ag, Pt, and Ge. Fission fragments produce tracks in such films when the films are $\geqq 100$ Å in thickness. The tracks are light in a dark matrix indicating loss of material, thereby increasing electron "transparency." In thicker films, the tracks are characterized by being dark in a lighter matrix and by containing larger crystallites.

On the basis of a theoretical consideration of the transfer of energy from fragment to matrix, it was concluded, after direct measurements showed close agreement with theory, that in thin films the matrix is vaporized; in thicker films, it is melted and recrystallized; and in still thicker films, exceeding 250 Å, no visible effect is produced. However, since the evaporated films are polycrystalline, small effects such as lattice dislocations and vacancy clusters would not be visible. Accordingly, toward the end of this period work was begun to produce thin, evaporated, single-crystal films by epitaxy. The effects of the dissipation of fission energies on the crystal lattice should be readily visible in the electron microscope under these conditions in the thickness range from 50 to 1000 Å. This should enhance understanding of such radiation damage in bulk material.

This work will continue and in addition, a thorough study of film thickness determination will be carried out.

During this period, a letter to the editor was submitted to the *Brit. J. Appl. Phys.* and accepted for publication; its title is "A New Technique for the Direct Investigation of Fission Events," by J. J.

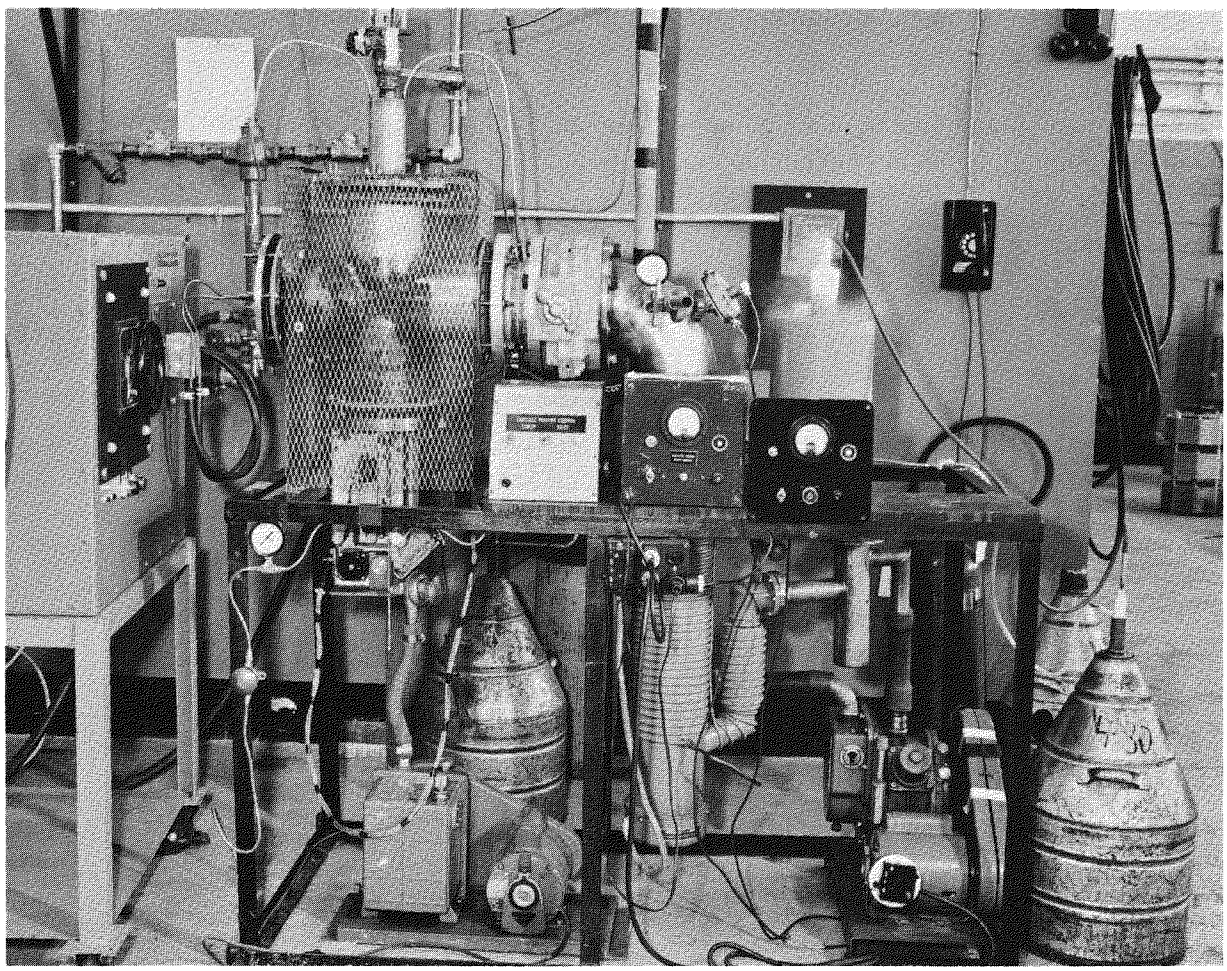

Figure 43. High vacuum furnace for melting pure Fe.

Kelsch, O.F. Kammerer, and P. Buhl. A paper entitled "Experimental Observation of Fission Fragment Damage in Thin Films of Metals," by J. J. Kelsch, O.F. Kammerer, and P. Buhl, was submitted to *J. Appl. Phys.*

J. KELSCH, O. KAMMERER, P. BUHL

General Metallurgical Studies

PREPARATION OF HIGH PURITY IRON

A high temperature, high vacuum furnace has been built to purify Fe required by the Radiation Effects Group. This furnace is similar to the one used by Prof. M. Gensamer at Columbia University. Purification of the Fe is accomplished by melting in a vacuum good enough to decompose iron oxide. A liquid nitrogen freeze-out located just above the crucible (less than the mean free path of the gas) makes the system operate essentially as a molecular still.

The completely assembled apparatus is shown in the photograph in Figure 43. The furnace chamber is made from a standard 6-in. Pyrex pipe and cross-attached to one horizontal leg is a 6-in. Hg diffusion pump, while the power leads from a 50-kw, 10,000-cycle inductive heater are put through the other horizontal leg. A 6-in. vacuum valve separates the vacuum chamber from the diffusion pump. A liquid nitrogen freeze-out coil is put through the top opening and located about 1 in. above the crucible. An elevator mechanism, located at the bottom of the vacuum chamber, is used to lower the crucible after melting in order to effect a "hot top," thus reducing the size of the pipe in the solidified ingot.

Efforts to date have been in assembling the furnace and going through test runs.

C. KLAMUT, F. ISELI, M. SCHUSTER

BRAZED GRAPHITE JOINTS

A requirement for the spatially fixed, nonrigid fuel element proposed at BNL is to make a leak-tight graphite-to-graphite seal, which would be compatible with most heavy liquid metal coolants at high temperatures.

Mo was chosen as the first braze material to try, since it has known good corrosion resistance to heavy liquid metals and has a lower melting point than either W or Ta, which also have good corrosion resistance.

To make these tests, the high temperature, high vacuum furnace, shown schematically in Figure 44 and in the photograph in Figure 45, was built. A water-cooled jacket (from an old single-crystal furnace) was modified to house a graphite resistor which served as the heater element. Graphite reflectors and graphite powder provide insulation. Power is supplied by a 60-kw, 18-v secondary Sorgel transformer. The vacuum system consists of a 4-in. oil diffusion pump backed by a mechanical fore pump.

Test runs are made with the sample cups shown in Figure 46. All sample cups are outgassed prior to making a brazing run. After outgassing, a Mo ring made from 0.035- or 0.065-in. wire is inserted.

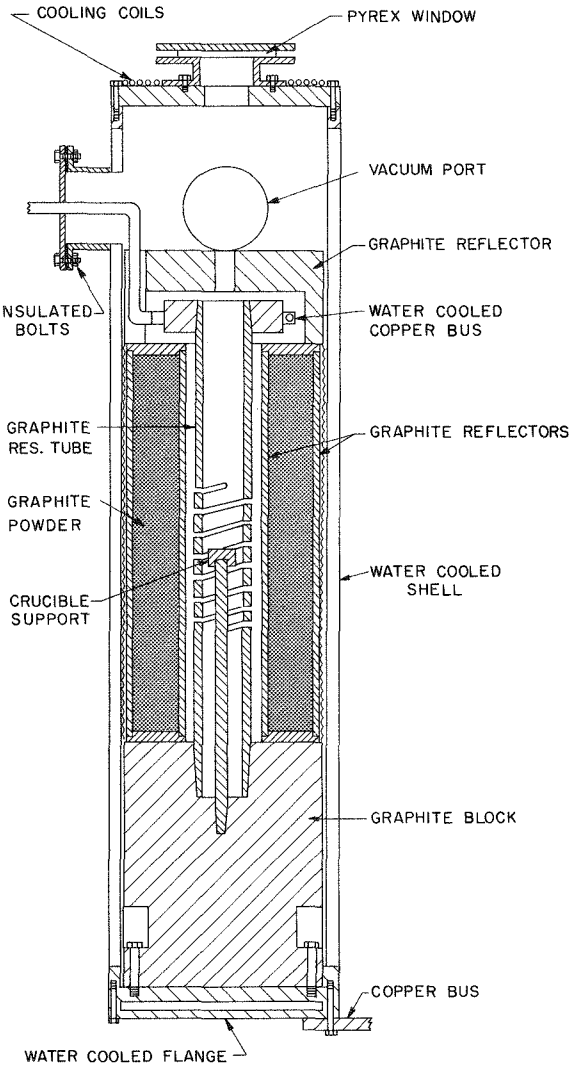

Figure 44. High temperature vacuum furnace.

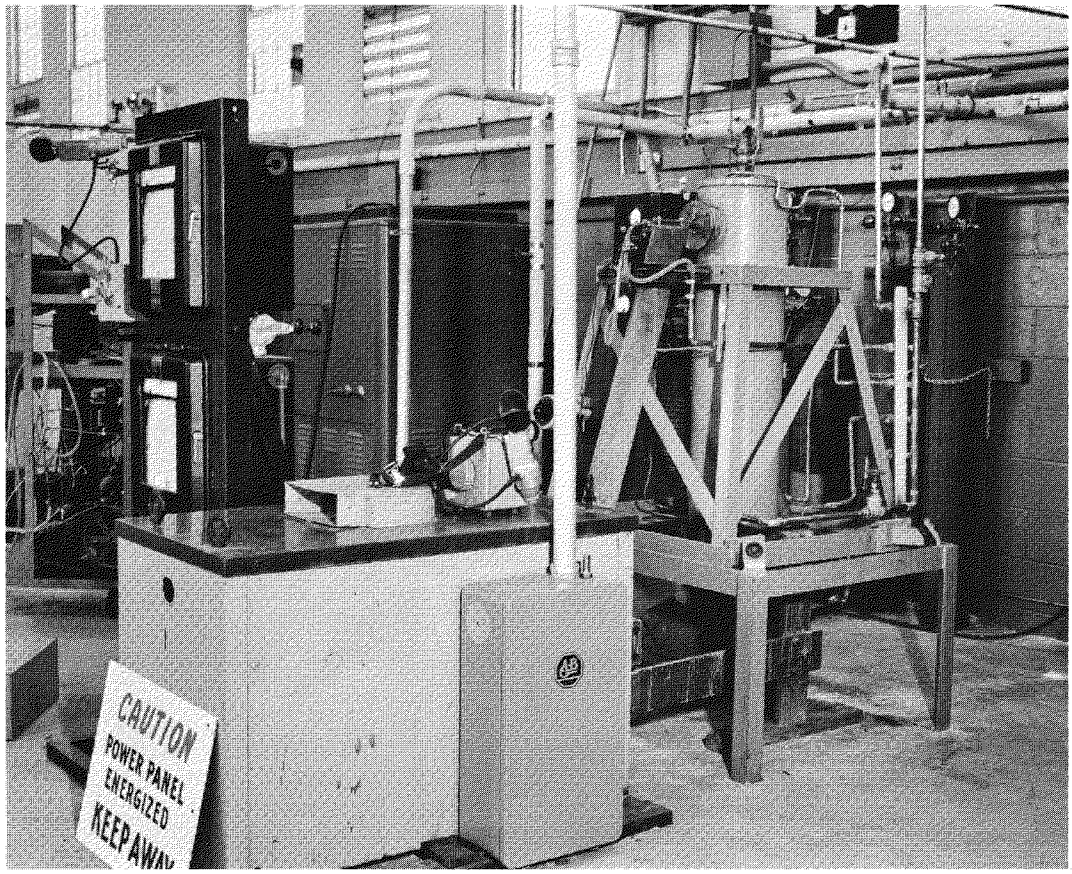

Figure 45. High temperature vacuum furnace.

Runs are made at temperatures up to 2500°C at a vacuum of 10^{-3} mm Hg.

In runs made thus far, indications are 1) the material which flows into the joint is a Mo-C alloy rather than pure Mo (Figure 47), 2) with the particular joint design used, the filler will not flow through clearances of 0.002, 0.004, or 0.008 in., but will readily flow through 0.016-in. clearances, and 3) metallographic examination of the graphite-metal interface reveals a reaction layer (Figure 48), indicating the possibility of attaining a good tight joint. C. KLAMUT, F. ISELI, M. SCHUSTER

BBRR FUEL ELEMENT TEST

The type D-5 fuel elements proposed for the BBRR are similar to the MTR and ETR elements with the exception of having thicker end plates. Calculations have indicated that at reactor operating conditions, there is a great enough temperature difference between the inner and outer plates to cause bowing of the inner plates if the element remained completely rigid.

An apparatus was built to impose a temperature differential on a section of an element (Figure 49) and observe any dimensional changes which might take place. The apparatus is shown schematically in Figure 50 and in the photograph in Figure 51. The apparatus consists of a pump and associated piping which circulates hot water through the element. The outer plates are sealed from the inner plates with "O" rings in order not to impose any external stress on the element. The side plates are cooled with tap water.

Deflections of the plates are determined by sighting through a plate glass window and taking photographs at the various temperature conditions. The deflection is also measured by inserting between the plates a liquid filled neoprene tube which is connected to a long capillary tube. Any changes in the spacing between the plates will increase or decrease the "squeeze" in the neoprene

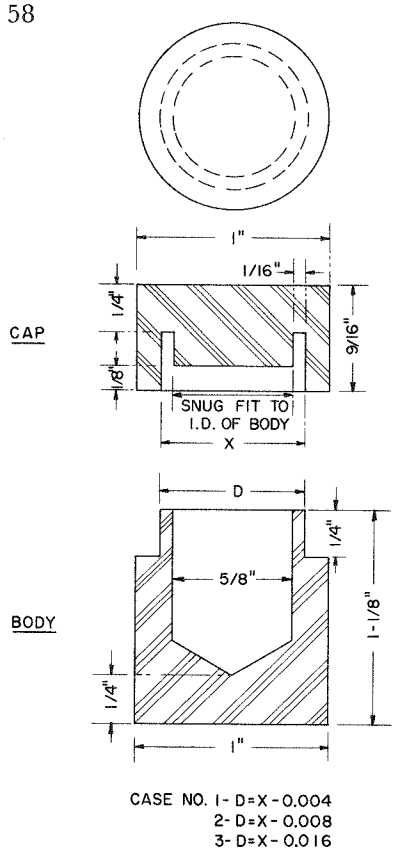

Figure 46. Graphite sample cups for high temperature brazing.

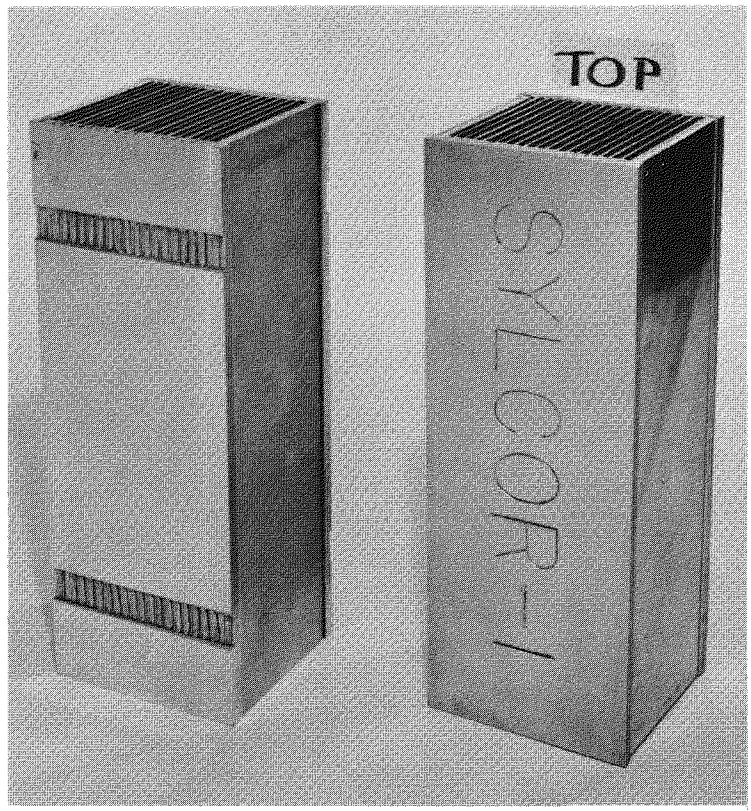

Figure 49. BBRR type D-5 fuel element mockup.

Figure 47. Mo-C alloy formed at Mo-brazed graphite joint. Estimated C, 7 to 10%. 250×, unetched.

Figure 48. Graphite-Mo interface showing possible reaction layer. 400×, unetched.

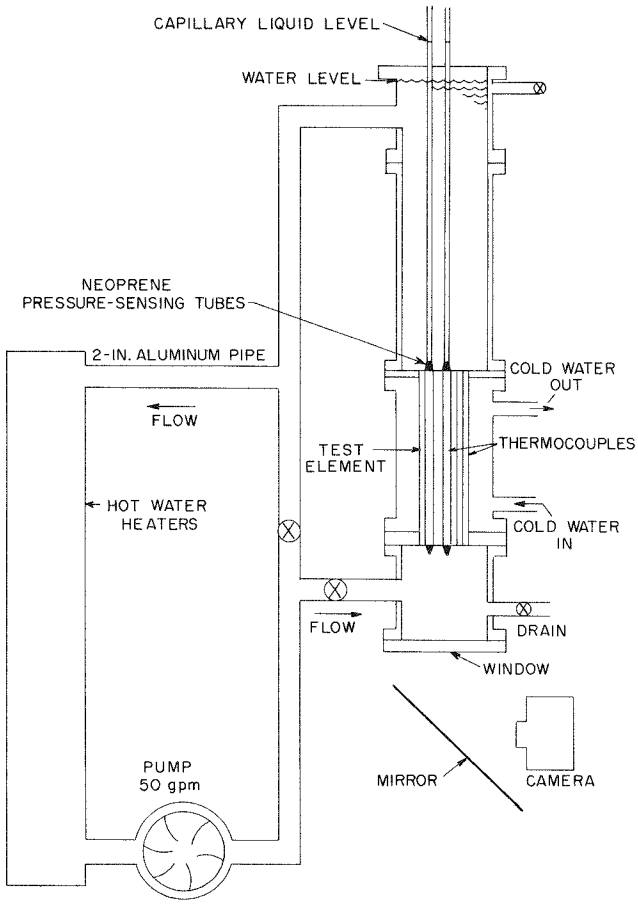

Figure 50. BBRR fuel element thermal testing unit.

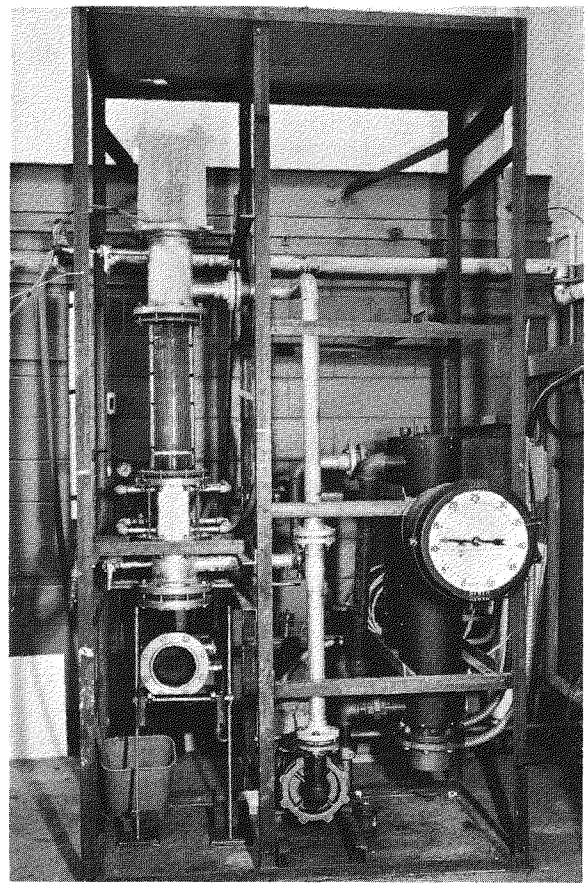

Figure 51. BBRR fuel element thermal testing unit.

tube, thus changing the height of the column in the capillary. The tube and capillary are calibrated, thus allowing quantitative measurements of plate deflections during testing.

The equipment is now undergoing shakedown runs. It was necessary to replace the silicone oil with ethylene glycol as the measuring fluid when it was found the silicone oil reacted with the neoprene, causing it to swell. C. KLAMUT, A. HOLTZ

Fuel and Blanket Development

SPATIALLY-FIXED, NONRIGID FUEL ELEMENT

Migration of Soluble Constituents Under a Temperature Differential

Additional experiments were carried out to study the migration of U and Th in Bi alloys held stagnant under a temperature differential. Alloys of 5% Th and 10% U in Bi were prepared in graphite containers 9 in. long by ⅜ in. i.d. and subjected to a temperature differential of 800° – 271°C in the manner described in the previous progress reports, except that the container for the U-Bi alloy was divided into two equal compartments by a porous graphite disk. When no further change in the moments of the specimens could be detected, the specimens were cooled and examined.

In the Th-Bi alloy it was observed that nearly all of the Th initially present in the hotter four inches of the specimen (corresponding to the temperature range of 800° – 590°C) had migrated into the cooler five inches within 72 hr. Over 80 percent of the total change in moment occurred within the first 7 hr after the temperature differential was applied, and very little further change was noted after 48 hr.

In the U-Bi alloy, it was found that the porous graphite disk (at a position corresponding to 580°C) had acted as a barrier to the migration of U. Within 87 hr, U had migrated out of the hottest 3½ in. and deposited in a region from the disk to a position corresponding to 675°C. On the cooler side of the disk, U had migrated out of the next 2 in. and deposited in the region below 375°C.

In these experiments as in previous experiments, the deposited material was concentrated most heavily in the region immediately on the cooler side of the final hottest liquid-solid interface. The deposits were invariably found in the upper part of the cooler end of the specimen, while the bottom part was virtually depleted of U or Th. Chemical analyses of samples taken from the hot ends of these and previous specimens revealed U and Th concentrations which were lower than the respective solubilities in Bi at the temperatures of the final liquid-solid interfaces.

From the data obtained in these experiments, it is possible to calculate an apparent diffusion coefficient for U or Th in liquid Bi at the temperature of the final hottest liquid-solid interface. The calculation is based on the assumptions that the alloy is stagnant and that the total migration of U or Th past the position of the final hottest interface is caused by diffusion down the concentration gradient in the liquid resulting from the change in the solubility of U or Th in Bi with temperature. Results of these calculations are shown in Table 21.

These calculated diffusion coefficients are at least 10 to 100 times higher than diffusion coefficients reported in the literature for other metals dissolved in liquid Bi and in other liquid metals. It is evident, therefore, that diffusion played a minor part, if any, in the observed migration. These results, combined with the other reported observations, indicated strongly that most of the observed migration must have been caused by mass transfer of the soluble U or Th by means of thermal convection currents in the molten alloys. The results suggested that migration under a temperature differential might be minimized or prevented by using more concentrated alloys in which thermal convection currents would be prevented by high viscosity due to a high volume concentration of solids.

Attempts were made to test this possibility using an alloy of 15% Th in Bi. This composition corresponds to that of the highly viscous settled layer in a stagnant $ThBi_2$-Bi slurry. Several efforts to prepare this alloy in the 9 in. long by ⅜ in i.d. graphite containers by allowing the solids from larger, more dilute alloys to settle into the container through a graphite funnel were unsuccessful, because the solids became concentrated in the funnel. One such effort yielded an alloy having the desired concentration in approximately 3 in. of one end of the container and approximately 2.5 percent Th in the other 6 in. This specimen was tested under the 800° −271°C temperature differential for 67 hr with the concentrated end at 800°C. After testing, it appeared that very little Th, if any, had migrated out of the hottest inch (ΔT=800° −773°C), but that nearly all of the Th in the next 4 in. (773° −545°C) had migrated toward the cooler end. This result appeared to indicate that increasing the volume concentration of

Table 21

Apparent Diffusion Coefficients of U and Th in Liquid Bismuth

Test number	Alloy composition	Time, hr	Temperature, °C	Diffusion coefficient, (cm^2/sec) $\times 10^5$
1352-20[a]	5% U-Bi	86	380	627
1352-21[b]	5% U-Bi	48	515	88
1352-23[b]	10% U-Bi	185	543	48
1387-35[b]	5% Th-Bi	72	590	150
1387-36[c]	10% U-Bi	87	675	50
1387-36[d]	10% U-Bi	87	375	656

[a]Specimen 6 in. long. ΔT=700° −271°C.
[b]Specimen 9 in. long. ΔT=800° −271°C.
[c]Hot half of specimen 9 in. long with porous graphite disk at center. ΔT=800° −580°C.
[d]Cool half of specimen 9 in. long with porous graphite disk at center. ΔT=580° −271°C.

solids in the hot end had prevented rapid migration of Th toward the cold end. Microscopic examination of the hot end of the specimen revealed the presence of a relatively high concentration of nonmetallic inclusions (possibly ThO_2) in addition to the $ThBi_2$ particles. Since this material may have acted as a barrier to migration, the results of the experiment are inconclusive. The specimen preparation equipment was modified to overcome previous difficulties. Before the test could be repeated, it was necessary to discontinue these experiments because of lack of manpower.

Behavior of Inert Fission Product Gases

Experiments were carried out to determine whether the escape of inert fission product gases from irradiated U-Bi alloys during subsequent heat treatment could be detected by scanning an evacuated void space above the alloy using a single-channel pulse height analyzer to measure the amount of the 0.081-Mev gamma radiation from the decay of Xe^{133}. Alloys of 5 to 6% natural U in Bi were prepared in graphite crucibles and sealed under vacuum in tight-fitting steel capsules, so that the alloy occupied approximately the bottom half of the capsule leaving a void space above it. One capsule containing a 50-g, 5% U-Bi alloy was irradiated for 2 hr in a flux of 10^{13} neutrons/cm^2/sec. After 100 hr, the capsule was scanned in the counting apparatus to measure gamma activity at the Xe^{133} energy level. In the portion of the capsule containing the alloy, the gamma activity was approximately twice the average activity in the void space above the alloy. The capsule was heated at 800°C for 2½ hr to dissolve the solids in the alloy and release any trapped fission product gases, and then water quenched. Scanning revealed that the activity in the void space had increased by about 3%, while the activity in the alloy had decreased by about 10%, thus possibly indicating the escape of some Xe^{133} from the alloy into the void space.

A second similar capsule containing an identical alloy irradiated for 2 hr at the same neutron flux level was scanned after 168 hr and then scanned again after an 18-hr treatment at 800°C. Although the activity had decreased in both the alloy and the void space, the ratio of void space activity to alloy activity had increased by approximately 19 percent. Scanning after a second heat treatment at 800°C for 69 hr showed that the activity in both the alloy and the void space had decreased, but that the ratio of void space activity to alloy activity had increased by approximately 10 percent. The decrease in alloy activity after each heat treatment was appreciably less than the decrease expected from decay of Xe^{133}. Based upon a comparison with the counting rate observed when scanning a glass capsule of similar size containing a roughly known concentration of Xe^{133}, the total relative increase in void space activity during the two heat treatments corresponded to that which could be expected if 60 to 100 percent of the Xe^{133} present had escaped from the alloy into the void space.

A third similar capsule containing a 70-g alloy of 5.7 percent natural U in Bi was irradiated for 7 hr in a neutron flux of 0.784×10^{13} neutrons/cm^2/sec. The irradiated capsule was scanned after periods of 23, 46, and 112.5 hr. Initially, the activity in the void space was 82 percent of that in the alloy. The activity in both the alloy and the void space decreased with time over the entire period, whereas the amount of Xe^{133} present should rise to a maximum and then decrease during this period. The decay rate of the void space was appreciably faster than that of the alloy. These results indicated that a major fraction of the observed activity came from radioactive species with half-lives shorter than that of Xe^{133}, and that the source of the activity of the void space was at least partly different from that of the alloy. The capsule was heat treated at 800°C for 4 hr, and then scanned again. The activities in both the alloy and the void space had decreased. However, the activity of the void space was approximately 6 percent higher than the amount indicated by the void space decay curve, again indicating the possible escape of radioactive species from the alloy into the void space during the heat treatment. This relative increase in void space activity corresponded to that expected if 6 to 10 percent of the Xe^{133} atoms present had escaped from the alloy into the void space.

The data from these experiments are consistent with an indication of escape of Xe^{133} atoms into the void space. It is questionable, however, whether Xe^{133} escape caused the observed results. It is certain that most of the void-space counts before and after heat treatment did not come from Xe^{133}, but were caused rather by scatter of radiation from the alloy. The energy-range window of the counter (approximately 0.06 to 0.10 Mev) could have detected direct or coherently scattered radia-

tion from at least ten other fission products plus the fluorescent K-radiation from Bi and the Pb shielding. Unfortunately, none of the heat-treated capsules were scanned after further decay, so that the decay rate of the excess activity in the void space could be determined and compared with the decay rate of Xe^{133}. If the observed results were indeed caused by Xe escape, the data indicate that the rate of escape from the stagnant molten alloy is quite slow at 800°C. Thus, the escape of Xe from fine solid particles in a two-phase alloy might be masked by the slow rate of escape from the more massive liquid. It must be concluded that this capsule technique will not be adequate for the experiments planned.

A new experimental technique has been devised in which escape of fission product Xe from the liquid phase after heat treatment will be facilitated by agitation under an atmosphere of nonradioactive natural Xe. The entire Xe atmosphere containing an evolved Xe^{133} will then be withdrawn and transferred to an ionization counting tube, so that the Xe^{133} content can be measured by beta decay. Work is in progress to assemble the necessary equipment. J. BRYNER, A. FLEITMAN

Mechanical Engineering Division

T.V. SHEEHAN

Brookhaven Beam Research Reactor

In June the Lummus Co. changed its nuclear adjunct from Curtiss-Wright Co. to Combustion Engineering. However, in spite of this change in the companies involved the key people remained unchanged.

The preparation of the preliminary design report was completed at the end of August. In the course of developing material for this report a considerable quantity of detailed design work was completed on the vessel, shields, core, building, and site work. In mid-August a site report was submitted to the AEC. R. BALDWIN

CRITICAL EXPERIMENTS

The new 7-ft spherical containment vessel for the Critical Experiments has been designed and bids for fabrication were solicited. A vendor was selected and a contract was awarded. The tank will be delivered during the month of November 1960. This spherical containment vessel will approximate as closely as possible the Brookhaven Beam Research Reactor concept. It will be complete with Tangent beam tubes, one radial tube, and a cold neutron facility. The supporting structure and service platform will be supplied by the vendor with the vessel. It is intended to use the existing pump, piping, etc., and couple directly to the spherical tank by means of flanged joints. The design for the control rod plate locations and accessory equipment is now in progress. F. PALLAS

FUEL HANDLING MOCKUP

Modifications were made to the tank for the Fuel Handling Mockup consisting of a 48-in. cylindrical section. Shutters and the indexing carriage and the respective supporting structures were designed, fabricated, and installed, and testing is now in progress. A new handling tool and cooling bonnet are now in the design stages. Six dummy fuel elements were modified to conform with the present BBRR fuel element concept.

F. PALLAS

FUEL ELEMENT TEST LOOP

All of the equipment for the BBRR, Fuel Element Test Loop, has been delivered. The framework has been completed and fabrication of piping spool pieces is proceeding. K. HOFFMAN

Mercury Test Loop – Mark IV

Erection of the Mercury Test Loop framework and piping has been completed and all components have been installed. Final testing of the system in now in progress. K. HOFFMAN

NaK Heat Transfer Loop

The pipe and fittings for the NaK Loop have been received. All other equipment is on order with the exception of the oxide control system. Bids have been received for the oxide control system and negotiations are proceeding. A reference design for the test section has been completed.

K. HOFFMAN

Laminar Fluidized Bed Reactor

A conceptual design has been accomplished for a Laminar Fluidized Bed Reactor utilizing small fluidized UO_2 particles as the fuel. An evaluation of the economics of this system was made.

K. HOFFMAN

High Temperature Critical Facility

A preliminary flow sheet and cost estimate has been made for a high temperature water critical facility to operate at 600°F and 2000 psi.

K. HOFFMAN

New Fans for Brookhaven No. 1 Research Reactor

All three fans have now been on the line for about two months and are performing according to the specifications. There are still a few minor items to be completed such as final balancing of the fans and finer damper control. Early indications show that the power savings will amount to about $10,000/month. G. NUGENT

High Level Radiation Development Laboratory

The engineering assistance contract with AMF Atomics for cell layouts and equipment specifications have been completed and the drawings forwarded to Burns and Roe, the architect-engineer.

At present, work is progressing on the review of the equipment specifications and drawings by BNL and the invitation to bid for the various equipment should be forthcoming in the near future.

Work is also progressing on the building of a model (¾ in. – 1 ft-0 in.) of the cells by the BNL Carpenter Shop. This model will serve a number of purposes such as an interference check, location of conduit and piping reference during erection, and for display. G. NUGENT, D. HUSZAGH

Facility for Criticality Measurements of Slab Lattices

New control rod mechanisms and the supporting framework were designed, fabricated, and installed in Building 526 for the critical experiments on slab lattices. The 4 to 1 ratio slab lattice critical experiment will be run during the next report period. The fabrication of the 3 to 1 ratio slab lattice has been completed and is awaiting assembly. Component parts for the 2 to 1 and the 1½ to 1 ratio slab criticals are in the last stages of fabrication. F. PALLAS

UO_2 Rod Lattice Assembly

A measurement platform for the UO_2 oxide rod critical experiments was designed, fabricated, and installed. F. PALLAS

Low Mass Critical Assembly

The table drives and auxiliary equipment for the Low Mass Critical Assembly is now in fabrication. The two tables have been designed and material procurement for their fabrication is now in progress. F. PALLAS

Dry Irradiation Facility – Mark IV

The in-pile hole mockup assembly for this facility has been fabricated and installed in the basement of the Graphite Reactor Building. The final components for the furnaces are now in fabrication. The entire assembly will be tested in the mockup prior to installation in the graphite reactor during the next report period. Installation in the graphite reactor is scheduled for the month of October 1960. F. PALLAS

Nitrofluor Process

The production cost estimate of the Nitrofluor Process Reprocessing Plant, described in BNL 618, has been completed. The estimate showed that this process compares favorably with present day costs for aqueous reprocessing of highly enriched fuels. L. GREEN

Fluidized Bed Reprocessing Plant

In conjunction with the Chemical Technology Group a cost estimate and plant design was prepared for a reprocessing facility utilizing the method of halogenation and fluorination of fuel elements in a fluidized bed. In order to simplify the preparation of the estimate most of the assumptions made on the Nitrofluor Process (see above) were assumed for this estimate. In general, the results of both cost estimates were similar and compared favorably with present day plants.

Since the cost of processing equipment was a small cost when compared to the total capital investment it appears that any significant reduction in capital costs can only be realized if there is a reduction in the cost of these heavy "civil" engineering items. Other areas where cost reductions may be realized are:

1) Since both processes are non-aqueous, developing methods for economic solid waste disposal may be possible.
2) In the Fluidized Bed Plant it may be possible to decrease the cost of HCl by better process utilization.
3) It may be possible to increase production since both plant designs have a large overcapacity.

L. GREEN

Research Irradiation Project

The Irradiation Facility consists of a 12-ft high and 5-ft 9-in. wide stainless steel tank, which can be filled with water to a height of 10 ft. At the bottom of this tank are located 2 source plaques spaced 11 in. apart about the centerline of the tank. Three radiation containers straddle these two plaques providing double exposure on the inner container and one side exposure on the two outer containers. The length of exposure time can be controlled manually or automatically. A conveyor system is used to move these containers in and out of the tank.

There are three separately controlled elevators in the system. Each one consists of a motor-driven 17½-ft long stainless steel ball screw attached to one side of the radiation container with a 1-in.-diam guide rod and linear ball bushings on the other side.

The ball screw is driven by ¾ hp, 216 rpm gear motor which produces 198 inch pounds of torque. A Hilliard slip coupling (adjustable) is used to connect the motor to the ball screw which is held between two double row ball bearings, the upper one of the two is self-aligning. The travel of the container is controlled by a rotary limit switch. The bottom of the container must be stopped 2 in. above the bottom of the tank in order to avoid hitting the source plaque with the cover. Upper adjustment depends on whether the full 18 ft of guide rod are used or the last 6-ft section is removed for easier access to the containers, which is this case come up to a point approximately 8° above the working platform. The 6-ft extensions are needed, however, to install and remove the containers from the conveyor system.

The adjustable clutch should be set at minimum torque value required to operate the ball screw in or out of the water. The most severe condition is probably at the time when the container coming up leaves the water and loses the effect of buoyancy. With a payload of maximum 40 pounds the clutch should not slip, but should not be set any higher than this in order to protect the lead screw on its travel down with the container hitting the bottom stop due to limit switch failure or maladjustment.

A. OLTMANN

Reactor Evaluation and Advanced Design

W. ROBBA

During this period the review of the status of direct conversion with special emphasis on civilian nuclear power was completed and a survey report was submitted to the AEC. It is planned to issue a revised edition for standard distribution during the next period. In summary, it is found that an accurate prediction of the potential of nuclear direct conversion systems for civilian power applications cannot be made at this time due to the early stage of development of these devices. However it can be said that there is a potential, the magnitude of which is based on predictions of an expanding nuclear power economy ten years from now. The review has established that at present no direct conversion device is efficient enough to be considered for sole use in a conventional or nuclear power plant. Efficiencies are approaching the point however, where such mechanisms may be considered as topping devices in central station plants.

In the area of magnetohydrodynamics theoretical work and exploratory experiments have been initiated on a pulsed fission plasma device.

Chemonuclear evaluation work continues with the investigation of the polyethylene system. Recent work by the Russians indicate G values as high as 6500 for the polymerization of ethylene. The polymer produced was of high quality. The potential of a system based on this G value and a 2% energy deposition efficiency will be studied.

Evaluation of the suspended fuel reactor concept continues. Emphasis is now to be placed on current status, technical problems remaining to be solved and economic potential. A report entitled "Laminar Fluidized Bed Reactor" was completed and submitted to the AEC during this period. Power costs of a 300-Mw(e) plant based on current status come to 9.9 mill/kw-hr. This is compared on an equal basis to 14.7 mill/kw-hr for the current status SGR plant.

Two special projects were initiated during the period. One is concerned with a classification system for power reactor concepts, the other is a tabulation of reactor coolant properties. The results of these projects will be published upon completion.

Three evaluation studies were undertaken for the AEC and assistance was given on the PWR program in areas of spectral shift physics, bulk boiling, and core physics.

L. GREEN, J. POWELL, H. SUSSKIND, M. STEINBERG